Relating flamingo counts in Lac Goto, Bonaire, to the water balance by coupling this balance to salinity and food availability

MSc Thesis

Daniel van de Craats

Wageningen University

WAGENINGEN UNIVERSITY
WAGENINGEN UR

Figure 1.1 (previous page): Overview of the catchment of Lac Goto, with the mountain range as northern boundary. Lac Goto is visible on the right, in front of the ocean. Photograph taken towards the south east, from top of the Brandaris mountain.

This report is a partial fulfillment of the Master of Science programme Earth and Environment (MEE) at the Soil Physics and Land Management group (SLM) at the Wageningen University (WUR). This research is conducted in cooperation with and with help from STINAPA (Stichting Nationale Parken), a non-governmental organization 'dedicated to the conservation of natural and historical heritage on Bonaire'. It is not an official publication of the Wageningen University or Wageningen UR.

Relating flamingo counts in Lac Goto, Bonaire, to the water balance, by coupling this balance to salinity and food availability

A field survey and modeling study to verify whether the flamingo population of Lac Goto is influenced by the water balance, through mechanisms involving salinity and food availability

Student:	Daniël van de Craats
Student number:	930316164050
Specialization:	Soil Physics and Land Management / Hydrology and Water Resources
Period:	September 2015 – April 2016
Supervisors:	dr.ir. K Metselaar dr.ir. ETHM Peeters
Date:	14-04-2015
Location:	Wageningen University

Preface

First of all, I would like to thank STINAPA for providing the possibility to study the system of Lac Goto, both regarding legal aspects as well as housing. I enjoyed the conversations with the rangers of STINAPA in the park during daytime and also the goat stew they made was very good. I would like to thank Sabine Engel, the (at that time) marine park manager at STINAPA, as she provided me with help for acquiring the necessary equipment for setting up this project, with transportation of my bike, other equipment and myself, with advice and support and with some nice field trips.

Furthermore, I would like to thank Klaas Metselaar for providing the opportunity for this thesis as well as for the feedback given and time spent as main supervisor of this thesis project. Especially our 'brainstorm sessions' gave interesting insights and new angles of looking upon the system of Lac Goto. Also the help of Edwin Peters (as second supervisor) with the halotolerants and the help of Harm Gooren in thinking along with and preparing the evaporation pan was very much appreciated.

Finally, I would like to thank my family for providing support when needed, for celebrating 'Sinterklaas' together and for listening to the stories of my adventures.

Abstract

Introduction and background. Lac Goto is a saliña of importance for the Caribbean Flamingo (*Phoenicopterus ruber ruber*) on Bonaire due to its hydrological conditions. These conditions provide a high salinity, which is required for the sources of food for the flamingo, the halotolerant brine shrimp (*Artemia salina*) and brine fly (*Ephydra gracilis*). High salt concentrations are caused by a combination of high evaporation rates, low fresh water inflow (by precipitation, surface runoff and groundwater flow; no river) and inflow of seawater through a natural coral dam, separating Lac Goto from the ocean. Between 2010 and 2014, flamingos were absent from Lac Goto, possibly as a result of contamination by chemical agents (mainly PFOS) released in a fire or because of large amounts of precipitation influencing lake salinity and foraging area, resulting in less optimal conditions for (foraging on) halotolerants. A field survey and modeling study were performed to investigate whether large precipitation amounts could be a cause of the disappearance of flamingos.

Methodology. A two-month field survey was conducted to quantify fluxes constituting the water balance. Precipitation and evaporation were measured directly, the influence of water flow through the dam, groundwater flow and surface runoff were inferred from a combination of these direct measurements and water level measurements in Lac Goto. Bathymetric relations were determined to relate the water balance to the salt balance and to calculate residence times of water. The halotolerant abundance and distribution in the lake and their response to different salt concentrations was measured to characterize food sources for flamingos.

The water balance of the lake was modeled using a reservoir model with parameters derived in the field survey, using meteorological data (1980 – 2015) and calculated tides as input. This balance was coupled to the salt balance. Seven water level measurements and four salinity measurements were available for model validation. Parameters were optimized based on these measurements and a sensitivity analysis of the model for all parameters was carried out. Salt concentrations and foraging area were correlated to historical flamingo abundance to verify if a relation was present.

Results. Measured evaporation rates were low (2.6 mm/d) compared to calculations and literature. Precipitation amounts were small (17 – 31 mm, depending on rain gauge) during the survey period, so that no estimates of surface runoff could be made. Flow through the dam and groundwater flow were

estimated, but given the small variation in water levels (5 cm) during the measurement period, several parameter combinations gave equally good results. Survival of (large) brine shrimp was 50% after five days at a salt concentration of 60 g/l; brine fly larvae did not respond to differences in salinity.

Only minor modifications to the parameters derived in the field study were required to fit the observations. In the normal years (85% driest years), inflow of water through the dam (72%) and outflow of water via evaporation (90%) were most important. The 15% wettest years were characterized by an increased importance of inflow by terrestrial fluxes (34%) and direct precipitation (30%) and outflow through the dam (36%). Salt concentrations were lowered in these wet years, whereas salinity recovered during drier years. Modeled salt concentrations were never below 60 g/l, but after the rainy season of 2010, concentrations dropped close to this value. Modeled salt concentrations reacted most strongly on modifications in the dam conductance and correction factors for evaporation and precipitation. A threshold of 90 g/l appeared in the correlation between flamingo abundance and modeled salinity below which little flamingos foraged in Lac Goto. No correlation was found between flamingos and foraging area. The average residence time based on outflow through the dam was 15 years.

Discussion. Only limited validation of the model results was possible due to the short measurement period and little historical measurements. Despite simplifications made by representing the whole lake as one reservoir, reasonable fits (deviations in water level of maximum 3 cm, in salt concentrations of maximum 16 g/l) could be obtained with the available historical measurements. As evaporation was an important factor for salt concentrations in the lake, several causes were identified for the low observed evaporation in the field survey as compared to calculations and literature. Additionally, it was argued that inclusion of a high-intensity precipitation event within the measurement period would greatly improve the ability to estimate parameters used to determine tidal inflow and groundwater flow.

Conclusion. Based on the modeled historical salt concentrations and the observed reduction in brine shrimp with salinity, it is likely that precipitation (in 2010) was of influence on the flamingo population by reducing salinity and food availability, but it cannot be confirmed that this was the only cause. Given the residence time of water of 15 years, dilution of PFOS could have occurred as well. Therefore, the cause of the disappearance of flamingos from Lac Goto was most likely due to a combination of both contamination due to the fire and the extraordinary precipitation amounts in 2010.

Contents

List of images

Figures

Tables

List of symbols

Symbol	Unit	Description	Value [a] (if constant)	Used in equations
A_c	m^2	Extent of catchment area	13.1×10^6	5.5
A_G	m^2	Extent of Lac Goto		5.3, 5.4
$A_{G,max}$	m^2	Maximum extent of Lac Goto	2.0×10^6	5.2
BS	no.	Number of adult brine shrimp		3.7
c	$m^{-1} d^{-1}$	Conductance of dam (1-layer)	5.2×10^{-3} [b]	3.3a, 5.4
c_1	$m^{-1} d^{-1}$	Conductance of lower layer (2-layer)		3.3b
c_2	$m^{-1} d^{-1}$	Conductance of upper layer (2-layer)		3.3b
c_{min}	$m^{-1} d^{-1}$	Conductance at bottom of dam (n-layer)		3.4
c_{max}	$m^{-1} d^{-1}$	Conductance at top of dam (n-layer)		3.4
C_G	$g\ l^{-1}$	Concentration of salts in Lac Goto		5.6
C_{gw}	$g\ l^{-1}$	Concentration of salts in groundwater	0	5.6
C_s	$g\ l^{-1}$	Concentration of salts in seawater	35	5.6
d_{dam}	m +BRL	Bottom of dam w.r.t. reference level	-10	- [c]
E	$m\ d^{-1}$	Evaporation calculated with data F.A.		5.3, 5.5b
E_{cor}	-	Correction factor lake evaporation	1.0	5.3
$E_{cor,pan}$	-	Correction factor lake evaporation from pan evaporation measurements	2.0 *	3.2
$ET_{cor,ter}$	-	Correction factor terrestrial evapotranspiration	1.0	3.5b, 5.5b
g	$m\ s^{-2}$	Gravitational acceleration	9.81 *	3.1
h	m	Height of water column above diver		3.1
h_{pan}	m	Height water column in evaporation pan		3.2, 3.5b
h_{max}	m	Maximum height of dam (n-layer)	11 *	3.4
h_{trans}	m	Height (above bottom dam) of transition layers (2-layer)	10.4 *	3.3b
$\overline{H}$	m	Average of sea – and lake level (above bottom dam)		3.3, 3.4, 5.4
H_G	m +BRL	Water level of Lac Goto		3.2, 3.3, 5.4
H_s	m +BRL	Water level of sea		3.3, 5.4
p_{atmos}	Pa	Atmospheric pressure		3.1
p_{diver}	Pa	Pressure recorded by diver		3.1
P	$m\ d^{-1}$	Precipitation recorded by F.A.		5.2
P_{cor}	-	Correction factor precipitation	1.0 [b]	5.2
q_{ETter}	$m\ d^{-1}$	Evaporation flux from terrestrial reservoir		3.5b, 3.5c
q_{gw}	$m\ d^{-1}$	Groundwater flux towards Lac Goto		3.2, 3.5c
q_p	$m\ d^{-1}$	Precipitation flux on Lac Goto		3.2
q_{sea}	$m\ d^{-1}$	Flux through dam towards Lac Goto		3.2, 3.3
q_{sr}	$m\ d^{-1}$	Surface runoff flux towards Lac Goto		3.2, 3.5

Symbol	Unit	Description	Value [a] (if constant)	Used in equations
Q_E	$m^3\ d^{-1}$	Evaporation flux from Lac Goto		5.1, 5.3
$Q_{ET,ter}$	$m^3\ d^{-1}$	Evaporation flux from terrestrial reservoir		5.5b, 5.5c
Q_{gw}	$m^3\ d^{-1}$	Groundwater flux towards Lac Goto		5.1, 5.5c, 5.6
Q_P	$m^3\ d^{-1}$	Precipitation flux on Lac Goto		5.1, 5.2
Q_{si}	$m^3\ d^{-1}$	Inward flux through dam		5.1, 5.4a, 5.6
Q_{so}	$m^3\ d^{-1}$	Outward flux through dam		5.1, 5.4b, 5.6
Q_{sr}	$m^3\ d^{-1}$	Surface runoff flux towards Lac Goto		5.1, 5.5
r	$m\ d^{-1}$	Recharge on terrestrial reservoir		3.5
R	$m^3\ d^{-1}$	Recharge on terrestrial reservoir		5.5
S	kg	Total mass of salts in Lac Goto		5.6
SPr	$kg\ d^{-1}$	Precipitation of salts from Lac Goto		5.6
tr	m	Size of terrestrial reservoir		3.5
tr_{max}	m	Max. size terrestrial reservoir before surface runoff takes place	0.2 *	3.5
TR	m^3	Volume of terrestrial reservoir		5.5
TR_{max}	m^3	Max. volume of terrestrial reservoir before surface runoff takes place	2.62×10^6	5.5
V	m^3	Volume of Lac Goto		5.1
YBS	no.	Number of young brine shrimp		3.7
α	d^{-1}	Terrestrial reservoir coefficient	5×10^{-3} *b*	3.5c, 5.5c
β	-	Fraction excess water which runs off	0.01	3.5a, 5.5a
γ	m^{-1}	Shape factor conductance function	2.0 *	3.4
ρ_{water}	$kg\ m^{-3}$	Density of water	1020 sea, 1080 Goto *	3.1

[a] If applicable, the value given is for the baseline model. Values indicated with an asterisk (*) are not used in the baseline model itself, but are constants in other equations. Blank spaces indicate parameters do not have a fixed value. [b] Value is for the baseline model. Deviating values used for preliminary models can be found in table 4.2. [c] Used in the calculation of several variables, but not mentioned explicitly in a formula.

1. Introduction

1.1 Context of the study

Lac Goto is a saliña located in the northwestern part of Bonaire, in the southern Caribbean (figure 1.2). It is a legally protected wetland under the RAMSAR convention, added in 1980 as RAMSAR site no. 202 (RAMSAR, 2015). Apart from this status, the lake is partly located within Washington Slagbaai National Park. Lac Goto is an important site for foraging and nesting Caribbean flamingos (*Phoenicopterus ruber ruber*), the national bird of Bonaire. Its importance is a result of the high salinity of the lake (at least three times higher than seawater) in which only brine shrimp and brine fly (larvae) thrive (Rooth, 1965). As the flamingos of Bonaire are specialized in consuming these halotolerant species, these very specific sites where conditions for halotolerant species are favorable should be treated carefully to protect the flamingo population on Bonaire (Rooth, 1965).

At the end of 2010, a strong reduction in the amount of foraging flamingos in Lac Goto was observed (with less than 10% of the normal population present, figure 1.3). This coincided with a reduction in (or even absence of) brine shrimp and brine fly (Slijkerman *et al.*, 2013), as well as a change in color of the waters of Lac Goto from clear to green (visible in appendix IV). This situation lasted until the end of 2014, when flamingos returned. Slijkerman *et al.* (2013) posed two possible causes for the observed changes in 2010. Either (1) toxic chemical components of the fire fighting agents used to extinguish fires at the BOPEC oil terminal (location shown in figure 1.2) in 2010 caused mortality of brine shrimp and brine fly or (2) high precipitation amounts in the rainy season of 2010 resulted in the decline of the flamingo population. The latter could be of importance due to an increase in water levels (reducing foraging area for flamingos) or due to a reduction in salinity (hampering halotolerant growth) (Vargas *et al.*, 2008). The first option, suggesting that fire fighting agents were the main cause for the observed changes, has been investigated by the IMARES and RIVM institutes (Mooij *et al.,* 2011, Zwart *et al.*, 2012 and Slijkerman *et al.*, 2013) after the fire of 2010. They concluded that acute and chronic exposure to PFOS (perfluorooctane sulfonate, a persistent compound) was the most likely reason for the disappearance of the brine shrimp – and brine fly populations. According to Slijkerman *et al.* (2013), it was 'unsure whether the ecosystem of Goto can ever recover from this (polluted, red.) state, and if so, when, (…)'. In contrast to their expectations, flamingos returned to Lac Goto in 2014 (figure 1.3), which implies that either PFOS concentrations were reduced (by dilution, binding) to non-toxic levels, or there was another cause (or causes working together) for the disappearance of the brine shrimp and brine fly populations.

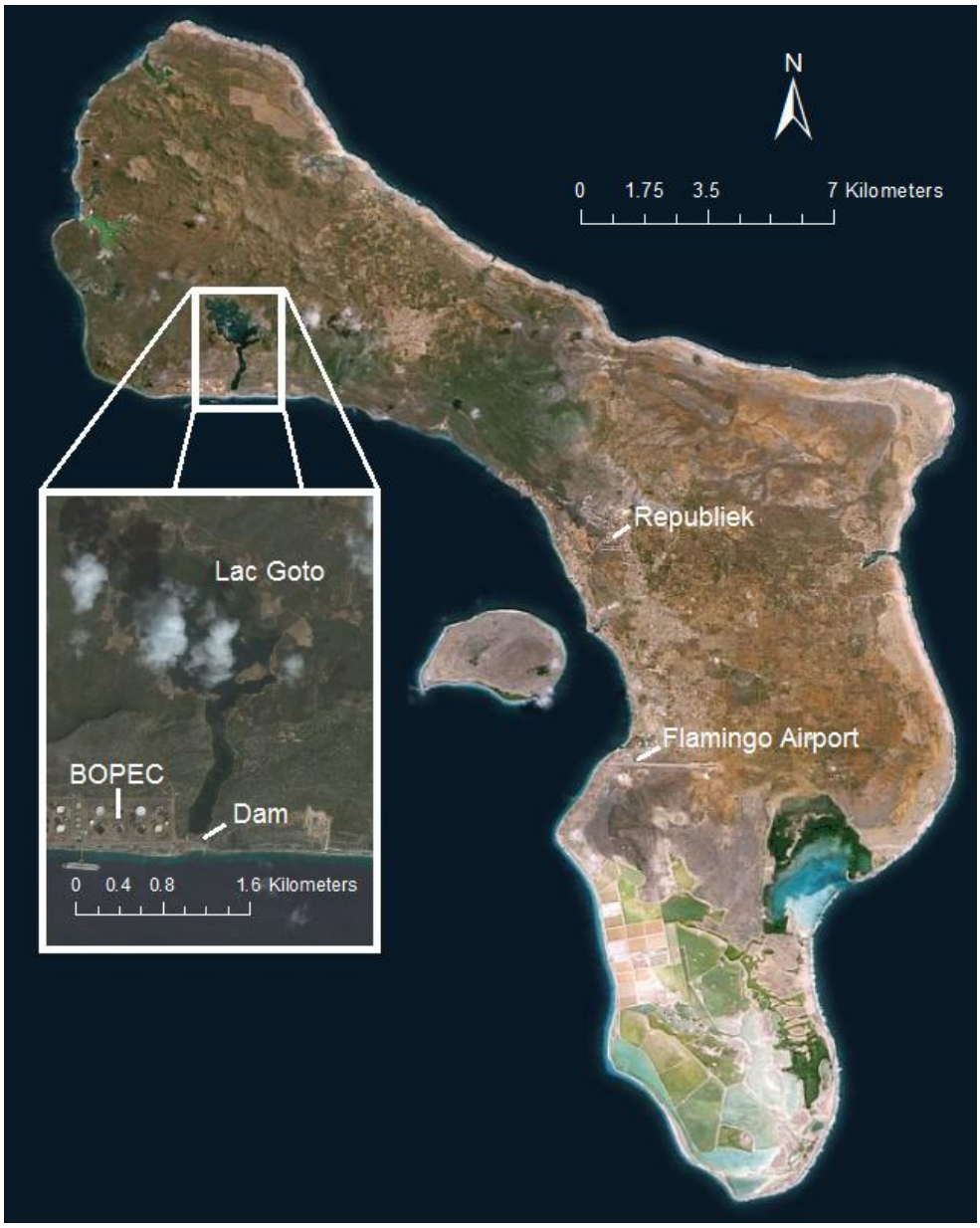

Figure 1.2: Location of Lac Goto on the island of Bonaire. A close-up of the lake is shown in the inset. A canal is present between the main area of the lake and the sea. A natural dam separates the canal from the sea in the south. Also indicated are the BOPEC oil terminal and weather stations 'Flamingo Airport' and 'Republiek'. Adapted from Google Earth (2016).

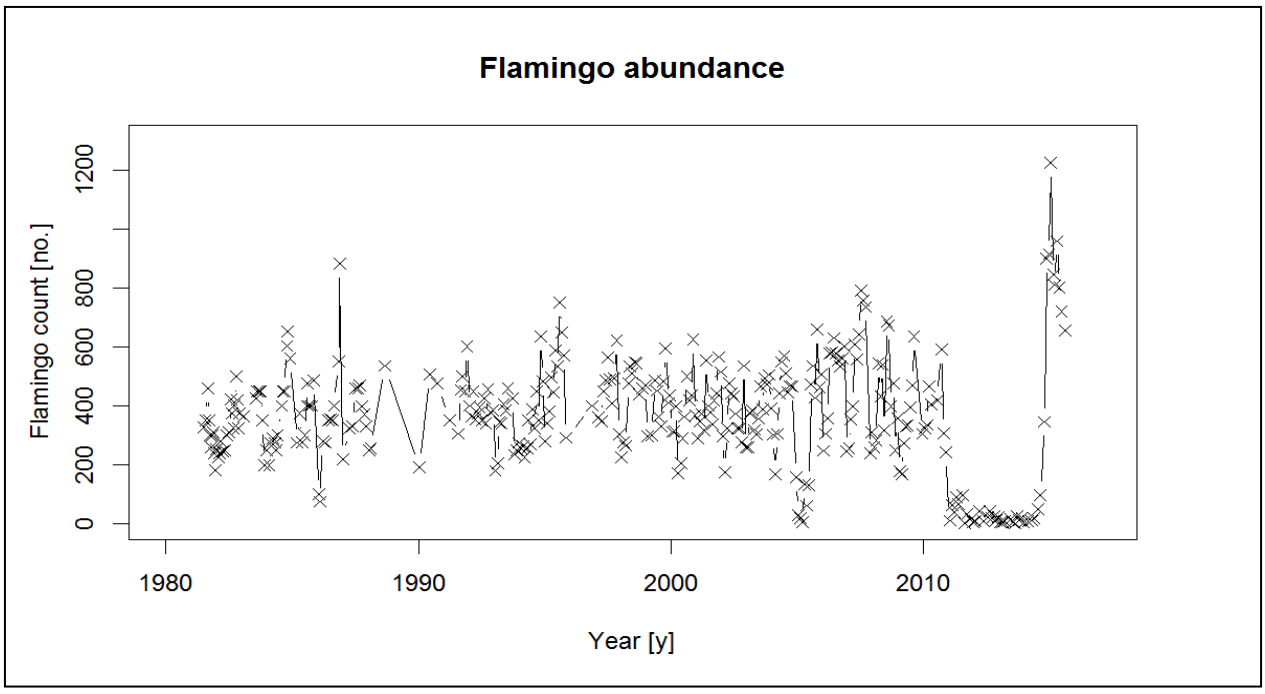

Figure 1.3: Observed flamingo abundance, from 1981 until 2015, from DCBD (2015). Yearly averages are given in appendix VI.

1.2 Hypotheses and objectives

The aim of this research was to test whether the high amounts of precipitation in 2010 could have been a cause for the observed changes in Lac Goto. This reflects the second hypothesis posed by Slijkerman *et al.* (2013). This aim required more insight into the relations between the water – and salt balance, the abundance and dynamics of brine fly larvae and brine shrimp and the flamingo counts in Lac Goto. For the present study, the hypotheses of Slijkerman *et al.* (2013) were first modified to include the return of flamingos to Lac Goto:

> *The (bio-available) concentrations of PFOS in the lake were too high for halotolerants to survive after the fires of 2010. In the years following the fire, concentrations of PFOS have been reduced (by dilution) so that they are now at an acceptable level for halotolerants to survive in Lac Goto; therefore Lac Goto is able to provide enough food resources for flamingos again.*

> *The exceptionally heavy rains of 2010 were the cause of the disappearance of flamingos from Lac Goto due to a reduction in foraging area or salinity (hampering halotolerant growth); in the relatively dry years following 2010, the area available for foraging returned to normal and salt concentrations increased. Therefore, halotolerant growth is no longer hampered so that Lac Goto can provide enough food resources for flamingos again.*

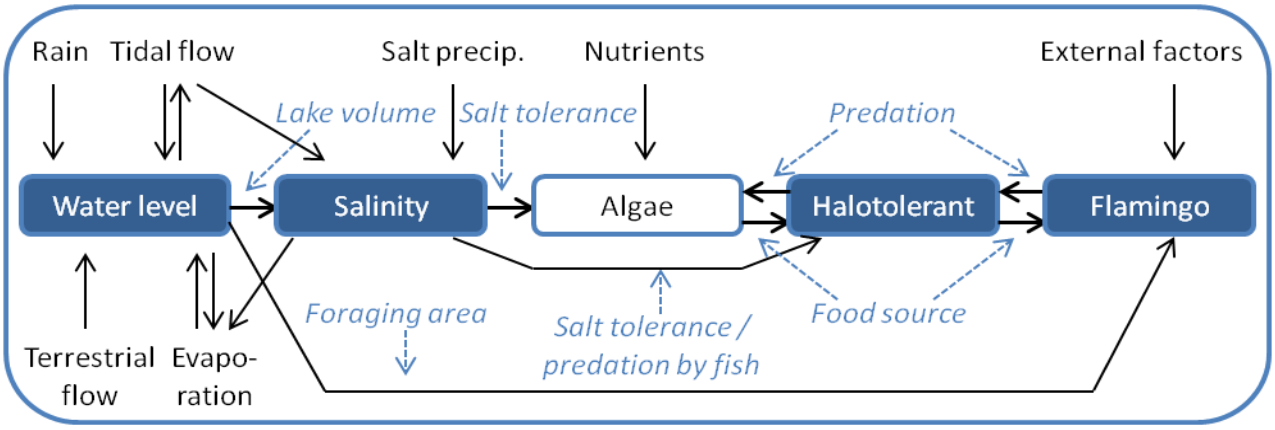

Figure 1.4: Conceptualization of relations present in Lac Goto, based on the second hypothesis. Black arrows represent a variable influencing another variable. This influence can be positive or negative. Blue dotted arrows indicate the mechanisms behind a black arrow. The filled blue boxes are incorporated in the (field) study, the empty box is not. More information on these relations and mechanisms can be found in chapter 2.

As a starting point for this study, the relations depicted in figure 1.4 were proposed as main driving mechanism of the flamingo population in Lac Goto. More detailed information on these relations can be found in chapter 2. Note that the figure simplifies relations and is therefore not complete. The figure suggests that precipitation, surface runoff, tidal flow, groundwater flow and evaporation affect water levels in Lac Goto. Water levels influence salinity by dilution and concentration of salts. Tidal flow can also transport salts in and out of the lake. Salinity affects both algae growth and halotolerant abundance. Abundance is directly influenced through an increased predation by fish and increased stresses (and mortality) at low salt concentrations, as well as indirectly through changes in food (algae) availability for halotolerants. Finally, halotolerant abundance affects the flamingo population as halotolerants are used as prey by flamingos. A direct link between flamingo abundance and the water balance (and therefore water level) is proposed in this figure as well, as flamingos have been observed (own observations) to mainly forage in shallow water (up to 60 cm in depth). Note that the flamingo population is influenced by external factors as breeding success and disease as well, which are not further discussed in this report. This driving mechanism (figure 1.4) reflects the second hypothesis; high precipitation amounts result in both a change in foraging area as well as in a decrease in salinity and therefore a change in (accessibility of) halotolerants. With the halotolerants as main source of food for flamingos, this change results in changing flamingo counts in Lac Goto due to limitations in food availability.

Given the proposed mechanism in figure 1.4, one would expect a correlation between the observed number of flamingos and water levels or the observed number of flamingos and salinity in Lac Goto to be present. If PFOS had (additional) effects as hypothesized by the first hypothesis, the correlation should be less clear. With this mechanism as starting point, the main research question for this study is:

> *How well can the abundance of flamingos in Lac Goto be explained by modeling historical water levels and salt concentrations of Lac Goto, using relations between the water balance, salt balance and food availability?*

To answer this question, several objectives were formulated. The final objective was added to analyze (with help of the water balance) to what extent PFOS could have been diluted within the years following the fire at the BOPEC oil terminal (the first hypothesis). All other objectives were used to answer the main research question. The objectives are to:

- *Quantitatively determine the water balance terms in Lac Goto;*
- *Relate the water balance to the salt balance;*
- *Derive a relation between salinity and reduction in halotolerant abundance;*
- *Investigate the population dynamics of brine shrimp and brine fly;*
- *Validate whether a relation exists between the (potential) halotolerant abundance and historical flamingo abundance in Lac Goto, by modeling historical salt concentrations;*
- *Validate whether a relation exists between water levels and flamingo abundance in Lac Goto, by modeling historical water levels;*
- *Determine the residence times of water in Lac Goto.*

2. Background information

This chapter provides background information on the study area, with a focus on the geo(morpho)logy, hydrology and salinity, as well as on the fauna present in Lac Goto, to provide the reader with more insight into the choices made regarding the objectives and hypothesis. Also a short description of the fire in 2010 and the investigations into the effects of this fire is presented in this chapter.

2.1 Study area

2.1.1 Geo(morpho)logy

Bonaire can be divided into two distinct geological deposits (Beets *et al.*, 1977). The geological core of Bonaire, the Washikemba formation, consists of volcanic material of mainly basalts, diorites and tuffs, which were deposited in a sub marine environment during the Cretaceous period. Some thin layers of cherty limestone are present in between the volcanic deposits, as well as some volcanic intrusions which show up as sills and dykes in these deposits (Beets *et al.*, 1977, Boekschoten & Westermann, 1982). The topography in this part of the study area is hilly, with stony and shallow soils (lithisols) with a reddish color. The underlying rocks are fractured and saprolitic. Some erosion gullies exist which drain the area during strong precipitation events (de Freitas *et al.*, 2005, , appendix I). The second geological deposit of Bonaire consists of limestone. Due to uplift and changes in sea level, several plateaus of limestone were formed on the side of the Washikemba formation in the last 5 Ma (Alexander, 1961), which was then the coast of the island. These plateaus consist of the remnants of coral reefs (Buisonje, 1974, Boekschoten & Westermann, 1982). The most flat positions on the younger (lowest) terraces show a developed soil with possibilities for internal drainage (de Freitas *et al.*, 2005), but other parts of the terraces are bare rock. Several saliñas are present in the northwestern part of Bonaire. These are drowned valley systems which used to drain the volcanic centre of Bonaire. Currently, the valleys are, at least during part of the year, filled with (highly) saline water (several times the salinity of the sea). Filling of the valleys was initially caused by a rise in sea level after the last glacial period (Engel *et al.*, 2012). After the valleys drowned, most valleys were cut off from the ocean by natural dams consisting of coral rubble and sands (Zonneveld, 1982). This is a dynamic and still ongoing process (Buitrago *et al.*, 2010), resulting from both gradual sand transport as well as events such as tsunamis and hurricanes (Engel *et al.*, 2012). An overview of the distribution of soils in the catchment of Lac Goto is given in appendix I (after DCBD, 2015).

Figure 2.1: (A) Seawater entering Lac Goto through the dam at the locations of the arrows. (B) Loose coral material of which the dam is build up. (C) Brine fly (grey band on the shore of Lac Goto) on the eastern shore of Lac Goto. (D) Alternating layers of sediments and salt (with salts indicated by arrows) at the outlet of a gully near Halo2. The spoon in this figure is approximately 20 cm long. Photographs taken during field survey.

Lac Goto fits the description as given above for the saliñas of Bonaire. A dam separating the lake from the sea is present here as well (figure 1.2). This dam is approximately 150 m wide and 100 m thick. The deepest parts of the valley (over 10 m in depth) are found in the south, close to the ocean where a gorge is cut through the limestone plateau. Towards the north, Lac Goto becomes wider and shallower. Here, the lake is located on the volcanic Washikemba formation (see geological map in e.g. Alexander, 1961 or appendix I). The total (topography based) catchment area without Lac Goto itself is 13.1 x 10^6 m^2; the maximum lake extent is 2.0 x 10^6 m^2. More than 80% of the catchment area of Lac Goto consists of the Washikemba formation. The rest of the catchment consists of limestone (Buitrago *et al.*, 2010).

2.1.2 Hydrology and salinity

Bonaire is situated in a semi-arid climate where (potential) evapotranspiration exceeds precipitation over the largest part of the year. On average, the potential evapotranspiration is 8.6 mm/d (de Freitas *et al.*, 2005). This is caused by the combination of a fairly constant and relatively high wind speed of 7 m/s together with the availability of solar energy due to Bonaire's position close to the equator (NOAA, 2015). It should be noted that, at least during the rainy season (lasting from mid October to mid January), cloud cover is significant (own observations), reducing the amount of energy available for evaporation. For Hato Airport (located 60 km west of Lac Goto, on Curaçao), the average sunshine duration throughout the year is 8 to 9 hours per day and cloud cover varies between 40 to 50% over the year (MDC, 2015), with the highest values during the rainy season. Apart from the presence of clouds, evaporation is also reduced by the salinity of the lake, reducing the saturation vapor pressure over the lake (Salhotra *et al.*, 1985).

During the dry season, the water balance is mostly affected by evaporation and exchange of water with the sea through the dam deposits. This exchange is visible by upwelling water at several locations along the dam (figure 2.1 A). These connections between the sea and lake can be both diffuse, through dam deposits themselves (figure 2.1 B) or through the limestone surrounding the entrance of Lac Goto, or direct, through underground cavities (Rooth, 1965). In accordance, Mackenzie *et al.* (1995) state that porosity and permeability of the surrounding bedrock determine inflow of seawater in marine lakes such as Lac Goto. Rooth (1965, p.31) suggest that for saliña Slagbaai the permeability of the wall of coral debris is likely higher in the upper parts, as lower parts of the dam contain larger amounts of sands. This results in an enhanced exchange of water at high sea – or lake water levels. This effect could also play a role in Lac Goto. The importance of the flow through the dam is illustrated by the fact that despite the large evaporation term in the water balance, Lac Goto always contains water; these fluxes through the dam can thus (partly) compensate for losses of water by evaporation.

During the wet season, the water balance is affected by additional processes next to evaporation and exchange through the dam. With trade winds on Bonaire coming from the east, showers have most time to develop over land in the northwestern part of the island (where Lac Goto is located), an effect which is enhanced by the undulating terrain here. As a result, precipitation varies over the island, with the highest values in the northern and western parts of Bonaire (Buitrago *et al.*, 2010). The climatological summaries of the Meteorological Department Curacao (MDC, 2015) indicate that yearly precipitation

sums at the BOPEC rainfall station in the northwestern part are indeed higher than precipitation in the southern part (at Flamingo Airport weather station). Monthly precipitation amounts may even exceed monthly potential evaporation in the wet season, resulting in a precipitation excess in this period (e.g. de Freitas *et al.*, 2005).

Additionally, surface runoff takes place during heavy precipitation events through erosion gullies in the catchment area (de Freitas *et al.*, 2005). During such an event, Buitrago *et al.* (2010) have observed sudden changes in water level in Lac Goto (32 mm increase in lake water level for a precipitation sum of 25 mm) coinciding with a decrease in salinity, which indicates the importance of precipitation and surface runoff in the rainy season. Hobbelt (2014) investigated surface runoff in the catchment of Lac Bay, a relatively flat catchment in the southern part of Bonaire, located mostly on limestone formations rather than the Washikemba formation. She reported minor quantities of surface runoff even for large showers (e.g. 1.3 mm of surface runoff for 24 mm of precipitation). However, it is possible that surface runoff is larger in the catchment of Lac Goto, due to a more pronounced topography. Next to surface runoff, groundwater flow through the volcanic deposits is expected to take place, as the saprolitic layer is relatively thick and the rocks underneath are folded and cracked. Water wells are present in the area, indicating that groundwater is present.

Lake salinity increases in the dry season as a result of the two major fluxes in this period. Evaporation concentrates salts and the compensating inflow of seawater transports even more salts into the lake. In the dry season of 2008, Buitrago *et al.* (2010) reported an average salinity of 160 g/l (hyper-saline conditions). In the subsequent rainy season, salinity decreased as a result of the aforementioned precipitation excess, diluting the water in the lake and increasing the outflow of water to the sea. In November, an average salinity of 100 g/l was measured (Buitrago *et al.*, 2010). It should be mentioned that salinity was much more variable in November than in the dry season, as Buitrago *et al.*, 2010 reported several measurements with a salinity of over 140 g/l in November. As it remained unclear in their report how the sampling locations were distributed, this variability might be explained by recent inflow of fresh water (Buitrago *et al.* (2010) reported 15 mm of rain around the sampling date), reducing salinity in some locations significantly, while not affecting other locations. In contrast to Buitrago *et al.* (2010), Rooth (1965) measured very little change in salinity over a year. His measurements (with salinity fluctuating around 130 g/l) were performed in a dry year. He attributed the lack of change in salinity to the large buffering capacity of the lake given its size and depth.

Salinity in Lac Goto is affected by other processes as well, such as precipitation and dry deposition of salts (Obrador *et al.*, 2008). Figure 2.1 D illustrates the occurrence of salt precipitation. A small soil pit is shown here, with alternating salty – and sandy layers. These sandy layers most likely originated from surface runoff in wet years, as this soil pit was dug close to the outlet of a gully. The salty layers were thought to be deposited in dry years.

2.1.3 Ecology

The most prominent species in Lac Goto is the Caribbean Flamingo (*Phoenicopterus ruber ruber*). It belongs to one of the four distinct populations of the Carribbean Flamingo in Central America (Wetlands International, 2015). The population of Bonaire, which individuals travel between Venezuela (located 70 kilometers to the south) and Bonaire, breeds in Pekelmeer (southern Bonaire) and (occasionally) in Lac Goto and feeds in several saliñas on Bonaire and in Venezuela (Rooth, 1965). The size of this population was estimated in 2000 at 50,000 individuals (Espinoza *et al.*, 2000). Other bird species are present in Lac Goto as well, albeit less prominent than the flamingo (own observations).

Several reports on the behavior of the Caribbean Flamingo are available for the populations in Central America. For the population on the Galapagos Islands, precipitation, lagoon water level and water temperature have been reported to affect the flamingo distribution over different saliñas (Vargas *et al.*, 2008). During an extreme precipitation event during which water levels rose more than 30 cm above normal, flamingo counts dropped to zero for the rest of the year in the two most important (and deepest) saliñas on these islands. This change was not due to mortality, but rather due to migration to more suitable locations for the flamingos (Vargas *et al.*, 2008). Two possible explanations were given: either the water became too deep for the flamingos to forage, or salinity decreased, affecting food availability. Similar behavior has been reported by Espinoza *et al.* (2000), who claim that the distribution of the population of Venezuela and Bonaire was directly affected by water levels within lakes.

According to Rooth (1965) and Casler and Esté (2000), the two most important food items for the Caribbean Flamingo population on Bonaire and Venezuela are the halotolerant brine shrimp (*Artemia salina)* and brine fly larvae and chrysalids (*Ephydra gracilis*). Arengo and Baldassarre (1995) also recognized the importance of brine fly and brine shrimp as food items for the Mexican flamingo population, but this population used other food types (such as gastropods) as well. Baldassarre and Arengo (2000) mention that flamingos initially go towards areas with highest food density, but spread out when food density decreased. Simultaneously, the time spend for collecting food increases. Similar

results have been found by Casler and Esté (2000), who reported that at least 2,000 individuals of the Venezuelan population were feeding in man-made saliñas where food density was initially high (exact numbers unknown). However, food density decreased as a result of overexploitation of food resources by flamingos so that flamingos spread out towards other areas in the region.

Esté and Casler (2000) found that after the halotolerant density in a saliña in Venezuela decreased, the populations of brine fly and brine shrimp did not recover until a dry period in which water levels were lower and salinity was higher than in a wet period. As an explanation for this, they mention that at the time salinity increased, predatory fish could no longer survive in the saline waters, so that growth of the halotolerant species was no longer hampered by predation. This hypothesis is supported by Browne and Wanigasekera (2000). Rooth (1965) mentions a similar mechanism in Lac Goto; predatory fish species (*Cyprinodon dearborni* and *Mollienesia sphenops vandepolli*) were present in areas with less saline water.

Brine shrimp and brine fly live in Lac Goto in large quantities; for instance, Rooth (1965) estimated that there were on average 67 million brine fly chrysalids in Lac Goto. The band of brine fly along the shore as shown in figure 2.1 C illustrates their abundance during the field survey period as well. Brine shrimp and brine fly live from algae and detritus (Rooth, 1965). Large densities of brine shrimp have been reported in turbid water with plenty of algae (up to 3000 individuals in a 10 liter sample, Rooth, 1965). As the water became clearer due to filtering of algae by brine shrimp, such high densities were no longer reached, probably due to an insufficient food supply for these shrimp (Rooth, 1965). These algae responded to salt concentrations; a lower salinity was thought to result in higher growth rates, even for halotolerant algae as illustrated by Henley *et al.* (2002). Figure 2.1 A also indicates this: in the present study, algae were found close to locations where seawater entered the lake, whereas they were not visible further away from these locations. However, as it is unknown which species of algae were present in the lake, the response of algae to salinity was not quantified any further in this study.

According to Zweers *et al.* (1995), Caribbean flamingos mainly use filter feeding for gathering food resources between 0.5 mm and 6 mm in size, a mechanism used to catch both brine shrimp and brine fly larvae. Rooth (1965) mentions that the flamingos on Bonaire also stamp on the sediments to loosen brine fly larvae and chrysalids from the sediments before filtering the water. Rooth (1965) calculated that, on average, one flamingo needs 270 grams (10% of its body weight) of food per day, which adds up to 40,000 brine fly larvae or 135,000 brine shrimp per flamingo per day. Also taking into account that

flamingos try to minimize time spend for feeding by going towards areas with high food densities, large numbers of brine shrimp and brine fly are required to feed the flamingo population in Lac Goto.

A study by Browne and Wanigasekera (2000) showed the effect of temperature and salinity on *Artemia salina*. The brine shrimp population they used (from the Mediterranean) thrived best under conditions of 24°C (sampled for 15, 24 and 30°C) and a salinity of 180 g/l (sampled for 60, 120 and 180 g/l), for which 79% of brine shrimp (n=50) survived after 21 days. For salt concentrations of 120 and 60 g/l (and a temperature of 24 °C) survival was 51% and 0%, respectively. Under the best conditions, the life span of the remaining male individuals was on average 132 days (99, where the number in brackets denotes the corresponding value for the treatment with salt concentrations of 120g/l). Females lived on average 71 (39) days and started producing eggs after 30 (20) days. The time between broods was 4.3 (4.5) days and their total offspring was on average 260 (131) small brine shrimp per female over the course of their life. Summarizing, reproduction rates in general were high, but lower salt concentrations resulted in lower survival and reproduction rates. If the brine shrimp population of Lac Goto reacts similarly, this gives an indication that their abundance might decrease when fresh water dilutes the salt waters of Lac Goto. Note that Naceur *et al.* (2013) demonstrate that these figures largely depend on which population of brine shrimp is used because of large variations between populations. Similar figures are not available for brine fly larvae or chysalids.

2.2 Timeline of events in Lac Goto

In September 2010, a fire took place at the BOPEC (Bonaire Petroleum Cooperation) oil refinery, which is located on the shore of Bonaire next to the connection of Lac Goto with the ocean (figure 1.2). While extinguishing the fires, potentially toxic and persistent chemical compounds used in the oil industry, such as dioxins, PCBs (polychlorinated biphenyls), PFCs (perfluorinated compounds), PAHs (polycyclic aromatic hydrocarbons) and heavy metals, came into the environment and washed into Lac Goto (Mooij *et al.,* 2011). A few weeks after the fire, concentrations of these compounds in sediment – and water samples were measured (Mooij *et al.*, 2011). No indications were found that dioxins, PCBs, PAHs and heavy metals were present in (acute) harmful concentrations. However, acute risks regarding elevated concentrations of PFCs were found. Of this group of substances, PFOS (perfluorooctane sulfonate) was the most prominent substance. This compound was present in the fire fighting agents used to extinguish the fire in 2010. PFOS hardly evaporates, does not bind strongly to organic matter and does not degrade (Stevens and Coryell, 2007), so that outflow of water through the dam is relevant for removal of this

compound from the lake. A follow up study by de Zwart *et al.* (2012), for which samples were taken at five locations across Lac Goto, showed that concentrations of PFOS in water and sediment decreased within the two years following the fire by 17% and 65%, respectively. Concentrations were highest in water samples; concentrations in sediments were lower, but they were all within the 'possible risk' category as defined in de Zwart *et al.* (2012). Concentrations of PFOS in reference samples from other saliñas were in the 'no risk' category. De Zwart *et al.* (2012) and Slijkerman *et al.* (2013) mention that the risk of harmful effects could have been larger by multi-stresses due to the presence of several (albeit in lower concentrations) toxic chemical compounds and the long exposure time to (the persistent) PFOS. This could induce chronic effects, which were not taken into account when defining the risk categories.

The follow up study by de Zwart *et al.* (2012) was initiated because the population of flamingos, which usually fluctuates around 400 individuals, had left Lac Goto. A decrease in flamingo counts was observed starting after approximately four months after the fire (figure 1.3 and de Zwart *et al.*, 2012). The color of the lake changed from blue to green in this period as well. This change in color is visible when comparing satellite images of 2013 and 2014 to those of 2002, 2003 and 2011 (appendix IV). In cooperation with de Zwart *et al.* (2012), Slijkerman *et al.* (2013) investigated the dynamics of the flamingo population. They suggested that the reason for the absence of flamingos in Lac Goto was the absence of adequate food items (the halotolerant brine shrimp and brine fly larvae), probably related to the elevated PFOS concentrations found in Lac Goto. The change in color of the lake was likely related to the absence of brine shrimp, as e.g. Rooth (1965) mentions their capacity to filter algae out of the water in large quantities. The change in flamingo counts was not due to mortality of the flamingo population, as they were reported to forage in other areas (mainly in the south) of Bonaire (DCBD, 2015).

Despite the initial estimate of Slijkerman *et al*. (2013) that ecological recovery was not likely to happen soon, the halotolerants, as well as the flamingo population, have returned to Lac Goto (figure 1.3). In addition, the water of Lac Goto is clear again (visibility of three meters, own observations). The recovery of the flamingo population in Lac Goto occurred over a four month period (between August and November 2014), in which flamingo counts increased from 50 to 900 individuals (figure 1.3). The speed and moment of recovery of the halotolerants is unknown, but must have occurred somewhere between November 2012 (when Slijkerman *et al.* (2013) reported the absence of halotolerants) and October 2015 (when they were present again according to own observations). According to the park rangers at Washington Slagbaai National Park, the color transition occurred within one month, in January 2015.

3. Field survey: methodology

This section describes the methodology as followed for the field survey. The setup of the field study is discussed first, followed by an outline of how the acquired data was analyzed, including the additionally required datasets. The methodology of the model study is not outlined in this chapter (but in chapter 5), as results of the field survey were required for the methodology followed in the model study.

3.1 Setup

A map of all measurement locations (excluding bathymetric measurements) with their coordinates is shown in appendix I. This map also shows the (topography based) catchment area of Lac Goto.

3.1.1 Bathymetric relations

Bathymetric relations in Lac Goto were determined (in order to quantify the salt balance and residence times) on the 11th and 20th of November by taking depth measurements by boat in transects across the lake, using a sounding line. The actual measurement locations are shown in figure 4.1 B. Some measurements were done on foot for locations with a depth up to 70 cm. GPS coordinates (determined with an accuracy of three meters) were written down while measuring. If necessary, the influence of water level changes between measurements was accounted for. Accuracy was estimated at ±10% as a result of e.g. wind moving the boat during measurements.

Apart from manual measurements, flamingos were used as depth indicators. As flamingos have a leg length between 60 and 80 cm, observations of a flock of flamingos were used to approximate water depth for those locations. This way of measuring depth was introduced to avoid any disturbance of the flamingos at locations where they regularly feed.

3.1.2 Water balance

Input of water in Lac Goto originated from precipitation, tidal inflow, surface runoff and groundwater flow. Of these, precipitation was the only term which could be measured directly. Other terms were deduced from water level measurements. Outflow of water from Lac Goto occurred due to evaporation and tidal outflow. Evaporation was measured directly, whilst tidal outflow was deduced from recorded water levels as well.

Precipitation

Precipitation was gauged manually at least once every three days (and always on the day after a precipitation event was observed) on four locations (see appendix I) within the catchment of Lac Goto. Three gauges (PR2, PR3 and PR 4) were placed in the vicinity of Lac Goto, the other gauge (PR1) in a more upstream part towards the north. The gauges were placed in a relatively open environment to reduce wind effects of obstacles (Mekonnen *et al.*, 2015); possible obstacles were at least four times their height away from the rain gauge. The gauges were made of PET bottles (figure 3.1 C). The top of the bottle was removed at a height of approximately 20 cm and placed upside down in the bottom part, forming a funnel. The top of the rain gauge had a diameter of 10.3 cm. To reduce evaporation from the gauge, a light-weight (table tennis) ball was placed in the opening so water could flow into the bottle, whilst limiting evaporation. The bottles were placed approximately 10 cm into the ground (so that the top was 10 cm above the ground) to provide stability, to reduce the influence of solar radiation on evaporation of collected water and to reduce wind effects (Mekonnen *et al.*, 2015). The measurements were performed by transporting all collected water to a measuring cylinder with a diameter of 4.3 cm and a scale with measurement lines every 2.0 mm.

Evaporation

Lake evaporation was determined using an evaporation pan. Lowe *et al.* (2009) summarize several sources of uncertainty when estimating reservoir evaporation rates from pan evaporation rates. Of these sources, differences in wind speed above the pan and lake and differences between temperature of the pan – and lake water are the most important. Research by Tanny *et al.* (2008) illustrates the importance of minimizing the difference in temperature; they compared eddy covariance measurements with pan evaporation measurements and found that evaporation derived from a pan, situated on the shore of a lake in a semi-arid warm climate, was mostly fifty percent higher than suggested by eddy covariance measurements. The difference was caused by large temperature differences between lake – and pan water. Masoner *et al.* (2008) used a floating pan and compared the results to a normal pan. Floating pan evaporation was smaller and resembled the actual conditions better than a pan on land.

In this study, pan evaporation was determined with a pan with diameter of 65 cm and height of 40 cm (figure 3.1 A and B). This pan is smaller and deeper than the standard class A pan (diameter 120 cm, depth of 25 cm). This choice was necessary because of the limited capacity to transport large items to the field study site. Since wind blows generally from east to west on Bonaire, the pan was situated on the western shore to ensure a large fetch length (1 km), so air passing the pan has come into equilibrium

with the water surface. This location was thought to be more representative for the lake as a whole than the eastern shore, where winds were coming from a dry land surface (Weisman and Brutsaert, 1973). Water levels in the pan were measured automatically in a five-minute interval by a pressure sensor with a resolution of 0.1 mm. This sensor measured the difference in pressure between the atmosphere and a location 2.0 cm above the bottom of the evaporation pan (figure 3.1 B), thus measuring the pressure exerted by the overlying water column. Temperature of pan water was measured in the same frequency. A rain gauge (PR2) was placed in the vicinity of the pan to be able to account for changes in water levels due to precipitation. Manual measurements of water levels with respect to the top and bottom of the evaporation pan were performed using a tape-measure at least once every three days, to calibrate measured (changes in) pressure with actual observed (changes in) water level.

It was tried to limit the mentioned sources of uncertainty originating from the use of pan evaporation as representation of lake evaporation; temperature differences between lake and pan water were reduced by placing the pan in Lac Goto. It was placed on the bottom of the lake, in water with a depth of approximately 25 cm, so that excess solar energy captured by the (black) pan could be transported towards the surrounding water. The pan was filled with water from Lac Goto itself up to approximately 5 cm below the edge of the pan to reduce the effects of the walls of the pan on wind speed over the water surface in the pan. Water was partially refreshed once every ten days to maintain a similar salinity and water height. The effect of spatters entering the pan originating from waves was limited by constructing a dam of wood two meters in front of the pan towards the east.

Water levels

Sea water levels were measured during the first two weeks of the field survey (starting at the 31st of October), at a time interval of fifteen minutes. Both a salt water diver (hereafter named SeaSalt) and a fresh water diver (SeaFresh), of which the latter was protected from salt water by a rubber balloon partially filled with fresh water, were used for this purpose. The salt water diver (Reefnet Sensus Ultra) had a resolution of 1 hPa and accuracy of 30 hPa, whereas the fresh water diver (Eijkelkamp micro diver) had a resolution of 0.067 hPa and an accuracy of 1 hPa. They were installed in a piezometer made of a PVC tube, which had several holes a few centimeters above the sediments to allow for exchange of water. The divers were installed at a depth less than 50 cm below the water surface.

Figure 3.1: (A) Evaporation pan, with wooden dam (indicated by arrow on the left) two meters upstream to reduce wave effects. Also visible is the piezometer of GotoFr, indicated by the second arrow. Picture taken towards the north. (B) Close up of evaporation pan. Data logger is located in the yellow casket. The white tube going out of the water is the air pressure tube, which is connected to the pressure sensor (located at the position of the left arrow) attached on the side of the cross at the bottom of the pan. The water pressure tube is attached to this cross as well (right arrow), to ensure a fixed measurement height. (C) Rain gauge (PR4), placed 10 cm into the soil. The funnel, which is closed off with a table tennis ball, is clearly visible. (D) Piezometer containing salt water diver on location GotoSalt1. All photographs taken during field campaign.

Water levels in Lac Goto were measured by a salt water diver (GotoSalt1) starting the 3rd of November, installed in a similar way as the divers in the ocean at the transition from the canal to the lake itself. The piezometer used here is shown in figure 3.1 D. The divers used to measure sea water levels were moved to Lac Goto after two weeks (the 14th of November), to determine whether wind effects were of importance for the water level measurements. These divers (GotoSalt2 and GotoFresh) were placed in a piezometer at the western side of Lac Goto, close to the evaporation pan (figure 3.1 A).

3.1.3 Salt balance

Salinity was measured using an electrical conductivity (EC) sensor (YSI Professional Plus) which automatically compensated for temperature. Measurements were performed approximately once every one or two weeks at those locations where halotolerants were sampled to observe salinity changes over time. Vertical profiles of temperature and salinity were measured simultaneously with depth measurements for bathymetric relations to observe whether stratifications in temperature or salinity were present in the lake. Salinity of seawater and precipitation water was measured as well.

Apart from these measurements, a rough estimate of the amounts of salt precipitating in the lake was made by digging a soil pit on the shore of Lac Goto and determining the thickness of salt layers. It was assumed that any layer with terrestrial sediments which was located the highest in the soil profile was caused by the precipitation events of 2010, as this caused surface runoff towards Lac Goto. Any salt layer on top would thus have formed in the five years following this event.

3.1.4 Halotolerants

Abundance and distribution

Esté and Casler (2000) measured the abundance of benthic macro-invertebrates in a shallow salt concentrator (used in the production of salt) in western Venezuela by inserting a cylinder with a diameter of 10 cm into the water. Rooth (1965) measured brine shrimp abundance in several saliñas on Bonaire by taking a 10 l sample and sieving this sample. Brine fly chrysalids were sampled by counting the number of chrysalids and percentage of occupation on stones. Slijkerman *et al.* (2013) on the other hand sampled only the freely moving brine fly larvae in Lac Goto using a net.

In the present study, three locations close to the shore of Lac Goto were chosen for sampling of fauna. The first location (Halo1) was on the western, windy side of the lake with sandy sediments, approximately 40 cm deep and with a flat bottom. The second location (Halo2), on the northern side, had shallow waters (15 cm deep, flat bottom) with muddy sediments and the third location (Halo3) was located close to the canal to the sea. The sediments were sandy and partly covered by algae. The sampling location was 40 cm deep, but depth increased rapidly moving away from the shoreline. Halo1 and Halo2 were frequently visited by flamingos, whereas the latter was not.

Abundance of brine shrimp was determined by dragging a circular net with a surface area of 150 cm^2 and mesh size of 1 mm approximately 1 m through the water column, with the middle of the net at a depth of approximately 10 cm, thereby sampling a volume of roughly 15 liters. In each catch, brine shrimp larger than 2 mm were counted. The amount of brine shrimp smaller than 2 mm was estimated in one of the following classes: 0-5 individuals (class 1), 5-20 individuals (class 2), 20-50 (3), 50-200 (4) and more than 200 (5). Also, it was noted how many brine fly larvae appeared in the catch. This procedure was followed five times per location per observation and the results were averaged. Observations were done approximately twice every week, at dates indicated in figure III.7 (appendix III). Apart from these regular sampling points, brine shrimp were sampled while crossing the lake for depth measurements for bathymetric relations on the 11th and 20th of November in a similar way to estimate the abundance in other locations. No samples were taken at depths other than 10 cm below the water surface.

Contrary to brine shrimp, brine fly larvae were not sampled regularly, due to the difficulty of sampling a representative volume of sediment and finding suitable locations at Halo1 and Halo3. Brine fly larvae were sampled more intensively near Halo2 on the 10th of December. Three locations were chosen which appeared to be similar, for which a 1 x 1 m area was marked with wooden sticks. The upper centimeter of sediments in this area was stirred by hand to disperse brine fly larvae into the water column. Only a quarter of the area (0.5 x 0.5 m) was stirred at a time to allow for collection of the dispersed larvae in between. After the total 1 x 1 m area was stirred, the area was stirred again to determine if this improved the catch. The larvae were collected with the same net as used for collection of brine shrimp. This procedure was not followed at Halo1 and Halo3, due to high wind action or large depth, limiting the possibility to apply this procedure.

Salinity tolerance

Two experiments were carried out to give an initial estimate of the relation between salinity and survival of halotolerants for the populations found in Lac Goto. Note that for both experiments the amount of replicates was small compared to other studies (e.g. Browne and Wanigasekera, 2000 and Naceur *et al.*, 2013), which makes it (statistically) impossible to draw conclusions.

In a first experiment, four water samples of 150 ml were prepared with total salt concentrations of <1 g/l, 35 g/l, 77 g/l and 115 g/l. These samples were made with tap water (first sample) or with (a combination of) sea – and Goto water. For each sample, two large brine shrimp (>5 mm), two small brine shrimp (<5 mm), two large brine fly larvae (>8 mm) and two small brine fly larvae (<4 mm) were used.

This experiment was carried out in duplo. Survival was observed every twelve hours, for five days in a row. The samples were kept in a location without direct sunlight or climate control, so temperatures followed a daily pattern.

A second experiment was conducted using nine water samples of 150 ml with different salt concentrations, after the results of the first experiment indicated that brine shrimp appeared to be less tolerant to lower salt concentrations. Salinity ranged from <1 g/l (8 parts tap water, 0 parts Goto water) to 115 g/l (0 parts tap water, 8 parts Goto water). In this experiment two small and one large brine shrimp were added to each treatment. This experiment was carried out in duplo. Other conditions were identical to those in the first experiment.

3.2 Data analysis

3.2.1 External data

Weather

Weather data (precipitation, temperature (minimum, maximum, mean and dewpoint), wind speed and pressure) was available at a daily basis for Flamingo Airport (F.A.) from 1973 until present date (NOAA, 2015). A summary of this data set can be found in appendix VI. The weather station is located on the leeward side of Bonaire near Kralendijk, approximately 20 km southeast of Lac Goto (figure 1.2). It should be noted that yearly precipitation sums as given by NOAA (2015) did not entirely match precipitation sums given by MDC (2015), as illustrated in appendix VI. A correction factor was determined to translate precipitation from F.A. to precipitation in the northwest of Bonaire by correlating yearly precipitation sums reported by F.A. and the BOPEC weather station (MDC, 2015). It was assumed that no differences existed between F.A. and the catchment of Lac Goto regarding weather data other than precipitation, as their spatial variability is smaller than for precipitation. Gaps in data were identified and filled with zero (in case of precipitation) or interpolated. Years with large gaps were identified (appendix VI). From 2014 onwards, F.A. did not report precipitation. Due to this discontinuity, it was impossible to relate measured precipitation amounts during the field study to precipitation measured at F.A.. Furthermore, Koster (2013) also mentioned that during his measurement period (in 2012), this weather station sometimes recorded precipitation which was not observed (by the author himself), and vice versa. Also reports of the local newspaper (Bonaire, 2016) suggest that precipitation recorded in the rainy season of 2010 did not always fall on the days it was recorded on.

For some of the calculations performed in this study (outlined later), data from Republiek weather station was used in addition to data from F.A. (figure 1.2, Wunderground, 2015). This station was not operated by an official meteorological institute, so the quality of measurements was unknown. This station reported data in a five-minute interval. Data also included direct solar radiation. As this station was located in a less open environment than F.A. and Lac Goto, wind speed was corrected by multiplying wind speeds of weather station Republiek with a factor 2.7, determined after correlating daily averaged wind speeds for the two weather stations.

Tides

Data describing the tides of the sea was used to determine water flow through the dam between Lac Goto and the sea, as this flux was driven by the difference in water level these water bodies. Modeled tidal data is available from Flater (2015). Data span a timeframe of 1970 to 2037. These tides were modeled for Kralendijk, which is located on the same side of the island as Lac Goto. This dataset only provides minimum and maximum water levels at the time of occurrence of a minimum and maximum. Therefore, spline interpolation was used (RStudio Team, 2015) to calculate sea levels between high – and low tide.

3.2.2 Bathymetric relations

Apart from actual measurements of depth, satellite imagery was used for interpolation. Satellite images of 2002, 2003 and 2011 (see arrows on satellite images in appendix IV) revealed an underwater ridge in Lac Goto and the canal towards the sea. This ridge was observed (with depth measurements) to be present as well. Transects in the field study were chosen such that this ridge was crossed several times (figure 4.1 B) to extrapolate depths over this ridge. Satellite imagery was also used to delineate the maximum extent of Lac Goto. For those locations where there was a difference between the maximum extent and the extent during the field study, the height of the outer margin was set 10 cm above the water level at time of measurements, as no height measurements were possible for these locations.

All data points were combined in RStudio (‘akima’ package, RStudio Team, 2015) to construct a digital elevation model (DEM) of the lake by linear interpolation between depths. Resolution of the DEM was set at 4 x 4 m. It should be noted that the accuracy was not as high as the resolution might suggest, as it was constructed with irregularly spaced point measurements. Using the DEM, relations between water level, volume and area were calculated. A DEM was constructed for the standard situation, as well as for depths plus or minus 10% to yield an estimate of the effects of uncertainty.

No reference could be made to the Bonairian Reference Level (BRL) during the field survey. Therefore, the height of the water was approximated using the findings by Rooth (1965), who measured the water level development over a year (1959-1960). He found that the water level was mostly between 10 and 20 cm below the average sea level. The conditions during and two years before his measurement campaign were relatively dry. As the time prior to the current field study was also dry, it was assumed that water levels were similar to his water levels. The water level at the time of the current field survey was set at 10 cm below the average sea water level. According to the tidal data from Flater (2015), this average level was 0.41 m +BRL.

3.2.3 Water balance

Precipitation

Given the general direction in which showers move over Bonaire, it was expected that the three rain gauges close to Lac Goto (PR2, PR3 and PR4) roughly represented one third of the area of Goto. Therefore, the amount of precipitation falling on the water surface of Lac Goto was approximated by averaging precipitation amounts measured by these three gauges.

Evaporation

Measured time series of water levels in the evaporation pan were corrected for abrupt changes in level which were a result of inflow of lake water (spatters) or refilling of the pan. Days with precipitation were omitted from the analysis. Daily evaporation sums were determined and evaporation over the day was calculated by determining the cumulative change in water level in the pan (after calculating a moving average of eight hours to remove noise) from the start of the day until a certain time, for each five-minute interval. An average daily evaporation curve was constructed by averaging evaporation over the day from each individual day and normalizing it from zero to one. The average daily evaporation curve was used to calculate evaporation on a five minute timescale for days for which the pressure sensor was not working correctly, by multiplying this curve with manually measured daily evaporation sums. By doing so, the evaporation dataset was extended to cover the whole study period instead of only the period for which the sensor was working. This extended dataset is referred to in the text as artificial evaporation series. The water level change in the evaporation pan was correlated with radiation, wind speed, air temperature, water temperature and the difference between water - and air temperature on both a five-minute and daily scale, to analyze the most important factors influencing evaporation. Daily correlations were examined for data from both meteorological stations.

Apart from direct measurements, evaporation was calculated using measurements of minimum, maximum and dewpoint temperature, wind speed and pressure at weather station F.A. (at a daily resolution) and from measurements of temperature, dewpoint temperature, wind speed and direct radiation at weather station Republiek (at a five-minute resolution). Calculation was done using a modified Penman equation, as described by Calder and Neal (1984). The exact equations used are outlined in appendix II. This method was chosen after comparison with the reference Penman-Monteith equation (Allen *et al.*, 1998) and the Penman equation for open water (Penman, 1948). The equation proposed by Calder and Neal (1984) accounts for a reduction in evaporation due to high salt concentrations by inclusion of the activity of water. This factor was fixed at 0.9, as estimated from reported values by Salhotra *et al.* (1985). Although it is known that activity varies with ionic composition, salt concentration and temperature, this coefficient was assumed to be constant. Other fixed factors in these calculations were sunshine hours, set at eight hours per day (for calculation of radiation following methods described by Allen *et al*. (1998)) and albedo, set at 0.05. The discrepancy between calculated and measured evaporation was determined by correlating these two. A correction factor to convert measured evaporation to calculated evaporation (and vice versa) was determined.

Water levels

Pressure recordings of the divers were corrected for inconsistencies originating from changing depths at which a diver was placed after reading data from the logger. Recorded pressure was converted to meters water column by correcting for atmospheric pressure by applying equation 3.1, using atmospheric pressure recordings from Republiek weather station (Wunderground, 2015).

$$\text{Eq. 3.1} \quad : \quad h = \frac{p_{diver} - p_{atmos}}{\rho_{water} * g} \quad [m]$$

where: h is the height of the water column [m]
p_{diver} is the pressure recorded by the diver [Pa]
p_{atmos} is the pressure recorded by the weather station [Pa]
ρ_{water} is the density of water, fixed at 1080 for water in Goto (temperature of 30 °C, salinity of 110 g/l) and 1020 for sea water (temperature of 30 °C, salinity of 35 g/l) [kg m^{-3}]
g is the gravity acceleration, set at 9.81 [m s^{-2}].

Calculated heights of water column were translated to meters above Bonairian Reference Level similarly as described for the bathymetric relations.

Surface runoff

All outlets of gullies located between PR2 and PR4 on the northern side of Lac Goto (see appendix I) were examined after a rainfall event, to see whether a gully might have contributed to surface runoff. This was visible by the presence of e.g. transported sediments or organic material or by ponds. Direct runoff was estimated for those precipitation events where these effects of direct runoff were observed. The water level eight hours prior to such an event was subtracted from the water level eight hours after an event ended. Precipitation from the three rain gauges close to Lac Goto was averaged and subtracted from this value as well. The resulting water level increase was attributed to surface runoff.

Tidal – and groundwater flow

As both tidal – and groundwater flow were not measured, these fluxes were determined as residuals of the water balance. To do so, a time series was constructed which resembled the net flow of water into the lake by three fluxes; flow through the dam, groundwater flow and surface runoff (of which the latter was very small during the measurement period). This time series was called the residual time series and was constructed for the water level measurements of all divers in Lac Goto separately, with the aid of evaporation – and precipitation measurements. The residual time series was constructed as follows: firstly, the first water level measurement of a diver was taken as reference; the corresponding value was subtracted from all water level measurements. Secondly, cumulative evaporation was computed using the artificial evaporation time series. For each time interval of fifteen minutes, the sum of evaporation between the time of the first measurement and that specific time step was calculated. For each time step, this value was subtracted from the water level measurement at the same time step. Thirdly, precipitation was subtracted from the water level measurements as well when precipitation fell during the reconstructed (so not measured) part of the artificial evaporation time series.

It was expected that both groundwater flow and flow through the dam took place in the catchment of Lac Goto, but it was not known whether one flux dominated the other or that they were comparable in magnitude. Several procedures were tested to determine this.

In a first approach, cross correlations were determined. For each diver, two additional time series were calculated from both the measured water level in Lac Goto and from the residual time series. These were a moving average of four hours over the original time series and de-trended time series (using a moving average of five days to de-trend), resulting in six time series. The derivative of these series was calculated as well. The time series were correlated with modeled tidal data from Flater (2015) (or with

the derivative of the modeled tidal data when the derivative of the time series was used), yielding twelve possible cross correlations for each diver. A table summarizing these cross correlations is given in table III.2 (appendix III) for two divers. Finding a good correlation with the inflow time series (where -1 and +1 are perfect correlations and 0 means no correlation) with this analysis would imply that flow through the dam dominated over groundwater flow, as the inflow time series would be driven mainly by differences in sea water level. Finding a poor correlation would however not necessarily imply that groundwater flow dominated, as other aspects (e.g. measurement errors or a very small variation in lake water levels) could have resulted in a poor correlation as well.

In a second approach, daily trends in water levels were calculated (for all divers separately) by taking, for each dry day with measured evaporation data, the first water level measurement of that day as reference and subtracting this reference water level from all measurements of that day. This procedure was followed for both the measured water level data, as well as for the residual time series (where the development over the day was only due to flow through the dam, groundwater flow and surface runoff). By averaging these daily trends, two curves were constructed, showing the average daily water level development and the average daily residual flow development. Depending on the shape of these curves, information could be deduced on the source of inflow. If inflow would mainly have occurred during the time that water levels in the sea were high, flow through the dam could be identified as important source. If inflow was more regular throughout the day, groundwater flow would be of more importance.

A third approach involved fitting several water balance models to the water level measurements; as evaporation and precipitation were measured, the remaining terms in the water balance could be estimated by fitting modeled water levels to observed water levels by optimizing parameters. These models were calculated using fluxes in m/d and states in m, using a general structure as shown in equation 3.2. The time step used in this equation was fifteen minutes, the same as the measurement frequency. For each time step, the initial water level at that time was calculated based on the water level in the previous time step and the in- and outgoing fluxes within this time step. Salt amounts (in kg/m^2 surface area) and concentrations could be calculated using the average depth of Lac Goto (calculated with the bathymetric relations).

Eq. 3.2 : $$H_{G,t+1} = H_{G,t} + q_{p,t} - E_{cor,pan} * \left(h_{pan,t-1} - h_{pan,t}\right) + q_{sea,t} + q_{sr,t} + q_{gw,t} \quad [m]$$

where: t denotes at which time a variable is evaluated
H_G is the level in Lac Goto [m +BRL]
q_p is the measured precipitation flux within one time step [m]
$E_{cor,pan}$ is a correction factor for translating pan evaporation to actual evaporation [-]
h_{pan} is the height of the water column above the pressure sensor in the evaporation pan [m]
q_{sea} is the in- or outflow (positive inward) of water through the dam within one time step (eq. 3.3a, b or c) [m]
q_{sr} is the surface runoff amount within one time step (eq. 3.6a) [m]
q_{gw} is the ground water flow towards Lac Goto within one time step (eq. 3.6c) [m].

The flux through the dam (q_{sea}) in equation 3.2 was modeled using one of the variations on the Darcy equation, which describes flow through porous media. These variations included a 1-layer model, which used one conductance throughout the dam (eq. 3.3a), a 2-layer model, which consisted of two layers with a different conductance (eq. 3.3b) and an n-layer model, where conductance was a continuous function of height (eq. 3.3c). A sketch of these situations including a more thorough explanation of the equations is given in appendix II.

Eq. 3.3a : $$q_{sea,t} = \frac{c}{96} * \bar{H}_t * (H_{s,t} - H_{G,t}) \quad [\frac{m}{15\ min}]$$

Eq. 3.3b : $$q_{sea,t} = \begin{cases} if\ \bar{H}_t > h_{trans} & : \frac{c_1}{96} * h_{trans} * \left(H_{s,t} - H_{G,t}\right) + \frac{c_2}{96} * (\bar{H}_t - h_{trans}) * (H_{s,t} - H_{G,t}) \\ if\ \bar{H}_t \leq h_{trans} & : \frac{c_1}{96} * \bar{H}_t * \left(H_{s,t} - H_{G,t}\right) \end{cases} \quad [\frac{m}{15\ min}]$$

Eq. 3.3c : $$q_{sea,t} = \frac{c(\bar{H})_t}{96} * \bar{H}_t * (H_{s,t} - H_{G,t}) \quad [\frac{m}{15\ min}]$$

where: c is the conductance of the dam per meter height [$m^{-1}\ d^{-1}$]. c_1, c_2 are the conductance for the lower layer and upper layer and $c(\bar{H})$ is an average conductance, depending on the water level (eq. 3.4)
H_s is the sea level [m +BRL]
$\bar{H}$ is the average water level of the sea and Lac Goto, calculated as $(H_s+H_G)/2 + d_{dam}$ [m]
h_{trans} is the height (above the bottom of dam) of transition between the two layers [m].

In these equations, the flux through the dam (q_{sea}) was defined positive towards Lac Goto. The depth of the bottom of the dam (d_{dam}) was fixed at 10 m below Bonairian Reference Level (BRL), as depths in the canal close to the dam were also approximately ten meters. The division by 96 was included in the equations to account for the time step of fifteen minutes. Also, note that these equations assumed that both the width and thickness of the dam did not change with dam height. The conductance of the dam

(*c*) could be translated to the regular permeability (in m/d) as used in the Darcy equation as explained in appendix II. $c(\bar{H})$ in equation 3.3c was described by equation 3.4. In this equation, the shape factor was used to describe how gradual the transition from low to high conductance takes place. With a lower factor, the transition becomes more gradual.

$$\text{Eq. 3.4} \quad : \quad c(\bar{H})_t = c_{min} + \frac{(c_{max} - c_{min})}{\bar{H}_t * \gamma} * (e^{\gamma * (\bar{H}_t - h_{max})} - e^{-\gamma * h_{max}}) \quad [\frac{1}{md}]$$

where: $c(\bar{H})$ is the average conductance of the dam [$m^{-1}\,d^{-1}$]
c_{min} is the conductance at the bottom of the dam [$m^{-1}\,d^{-1}$]
c_{max} is the conductance at the top of the dam [$m^{-1}\,d^{-1}$]
h_{max} is the maximum height for which the function is defined, fixed at 11 (which equals 1 m +BRL) [m]
γ is the shape factor determining the shape of the conductance curve (>0), fixed at 2 [m^{-1}].

Groundwater flow and surface runoff were described with the aid of a terrestrial (linear) reservoir model, which included simplified equations for a fast component (surface runoff), evapotranspiration and a slow component (groundwater flow). Recharge on the terrestrial reservoir was calculated by multiplying measured precipitation by 6.65, as the catchment area of Lac Goto is 6.65 times larger than the lake area. The terrestrial reservoir itself was described by equation 3.5:

$$\text{Eq. 3.5} \quad : \quad tr_{t+1} = tr_t + r_t - q_{sr,t} - q_{ETter,t} - q_{gw,t} \quad [m]$$

where: tr is the water level in the terrestrial reservoir [m]
r is the recharge on the terrestrial reservoir within one time step [m]
q_{ETter} is the terrestrial evapotranspiration flux within one time step (eq. 3.6b) [m].

The fluxes out of the terrestrial reservoir were given by equations 3.6a, b and c. For each time step, these equations were evaluated in the order given. The fluxes calculated with equations 3.6a and c were input for the water balance model of Lac Goto (equation 3.2). Surface runoff from the terrestrial reservoir occurred only when the reservoir was full, with water levels in the terrestrial reservoir above a certain height (tr_{max}). Evapotranspiration was dependent on the potential evaporation and a reduction in times of soil moisture stress. This reduction which was defined as a simple linear relation, with actual evaporation equal to potential evaporation when the terrestrial reservoir was full and actual evaporation equal to zero when the terrestrial reservoir was empty. Groundwater flow was calculated after precipitation, surface runoff and evaporation were accounted for and was dependent on a reservoir coefficient α.

Eq. 3.6a : $$q_{sr,t} = \begin{cases} if\ tr_t + r_t < tr_{max} & : 0 \\ if\ tr_t + r_t > tr_{max} & : (tr_t + r_t - tr_{max}) * \frac{\beta}{96} \end{cases} \quad [\frac{m}{15\ min}]$$

Eq. 3.6b : $$q_{ETter,t} = \min\left(\frac{tr_t + r_t - q_{sr,t}}{tr_{max}}, 1\right) * ET_{cor,ter} * \frac{-\Delta h_{Epan,t}}{\Delta t} * 6.55 \quad [\frac{m}{15\ min}]$$

Eq. 3.6c : $$q_{gw,t} = q_{gw,t-1} * e^{-\frac{\alpha}{96} * \Delta t} + (r_t - q_{sr,t} - q_{ETter,t}) * (1 - e^{-\frac{\alpha}{96} * \Delta t}) \quad [\frac{m}{15\ min}]$$

where: tr_{max} is the maximum amount of water stored before surface runoff starts, fixed at 0.2 [m]
β is the runoff fraction, fixed at 0.01 [d^{-1}]
$ET_{cor,ter}$ is the terrestrial evapotranspiration correction factor [-]
α is the reservoir coefficient [d^{-1}]
Δt is the time step, fixed at 1 times its unit [15 min].

The reservoir coefficient (α) determined the speed in which water flowed from the terrestrial reservoir to the lake. A smaller coefficient resulted in longer residence times in the terrestrial reservoir, allowing for a longer period with evapotranspiration resulting in a lower fraction of recharge reaching Lac Goto. The runoff fraction was defined between zero and one, as it was not expected that the total catchment would respond immediately after exceeding the maximum size of this reservoir. This implied that surface runoff could also occur in a subsequent time step without recharge if the terrestrial reservoir was still above its maximum. This maximum amount of water in the terrestrial reservoir was set at 0.2 m/m^2 catchment area, which is low for the type of soil found in the catchment. However, the presence of rock outcrops was expected to reduce the average storage of the catchment. It should be noted that the maximum reservoir size in these equations had to be sufficiently large (larger than the maximum evapotranspiration flux in one time step) to avoid negative groundwater flow.

With these equations, seven cases of equation 3.2 were constructed. All of these cases included measured precipitation and evaporation, but the calculation procedure of the other terms (flow through the dam and terrestrial flow) varied. In three cases only flow through the dam and surface runoff were allowed (represented by either eq. 3.3a, eq. 3.3b or eq. 3.3c, without eq. 3.6c), in one case only terrestrial flow occurred (represented by equations 3.5 and 3.6a, b and c) and in three cases both flow through the dam and terrestrial flow were allowed (represented by either eq. 3.3a, eq. 3.3b or eq. 3.3c and equations 3.5 and 3.6a, b and c). The options with influence from both the sea and land were expected to resemble reality the best, as inflow of seawater was observed to occur (Rooth, 1965, Buitrago *et al.*, 2010 and own observations) and some groundwater flow towards Lac Goto must be

present to drain excess water from the catchment. Note that the effect of a change in area of Lac Goto with increasing water levels was omitted in this water balance model. This choice was made to simplify the calculation – and fitting procedure. A water balance model including the effect of a change in surface area is described in chapter 5.

All models were initialized by setting the water level to the level of the first measurement (0.335 and 0.330 meters above BRL for GotoSalt1 and GotoFresh, respectively) and applying 6 and 4 mm of precipitation for GotoSalt1 and GotoFresh, respectively, in the second time step. The latter was done to provide an initial water level in the terrestrial reservoir. The difference between the initialization of GotoSalt1 and GotoFresh regarding the terrestrial reservoir was present because precipitation occurred a few days prior to the start of measurements for GotoSalt1 (on the 27th of October, start measurements at 3rd of November), whereas it had been dry prior to the start of measurements for GotoFresh.

Parameters in these equations which were not fixed (the conductance of the dam (c, c_1, c_2, c_{min} and/or c_{max}) and the reservoir coefficient (α)) were fitted by minimizing the sums of squared differences between modeled and observed lake levels. The resulting modeled water level development for parameter combinations with the lowest sum of squared differences were also analyzed visually to ensure that trends in water levels were correct, as a lower sum of squared differences does not always imply a better representation of reality. The cumulative deviation of modeled water levels from measured water levels was computed by summation of all deviations from the start of the measurements until a given time. A negative trend thus meant an underestimation by models, a positive trend an overestimation and the steepness of the cumulative deviation was a measure of how large the deviation at a given time was. A horizontal line represented a perfect fit. Additionally, the Nash-Sutcliffe efficiency was computed, where values between 0 and 1 indicate that a model performs better than using the observed average as model, and values below zero indicate that this average is better (Nash and Sutcliffe, 1970).

A Monte Carlo simulation was performed to determine whether problems in parameter identifiability were present. 2,000 randomly chosen parameter value combinations were used; the value of the reservoir coefficient was chosen between 0 and 0.5 d^{-1}, the lower conductance (c, c_1 and c_{min}) between 1×10^{-3} and 1×10^{-2} $m^{-1}d^{-1}$ and the higher conductance (c_2 and c_{max}) between 1×10^{-2} and 1×10^{-1} $m^{-1}d^{-1}$.

3.2.4 Salt balance

Measured salt concentrations were analyzed by checking for changes in time (for measurement locations Halo1, Halo2 and Halo3) and space (for Halo1, Halo2 and Halo3 as well as for salinity measurements performed during the depth measurements). Observed salt deposits were used to calculate average daily deposition rates, assuming these deposits consisted of gypsum (with a density of 2308 kg m^{-3}) and calcium carbonate (with a density of 2930 kg m^{-3}) (Schreiber and Tabakh, 2000) and formed over the whole area of Lac Goto.

3.2.5 Halotolerants

Halotolerant abundance

Field data collected on halotolerants was analyzed by checking for changes in space and time. Correlations between measurements at Halo1, Halo2 and Halo3 and daily average – and maximum air temperature, daily average lake temperature and salinity on the corresponding locations were made and the significance of these relations (p-value) was determined.

The total amount of brine shrimp in Lac Goto was estimated using an average of the observed brine shrimp density at Halo1, Halo2 and Halo3 and the average area and depth of the lake at the time of the field survey. The amount of brine fly larvae available as food source for flamingos was estimated using the average observed density at Halo2 and the surface area of the lake where flamingos could reach brine fly larvae (the area with depths <60 cm). This choice was made as the mobility of brine fly larvae was low, so that brine fly larvae at a depth larger than 60 cm were presumed to always be inaccessible for flamingos.

A simple model was set up, described by equations 3.7a and b, to estimate whether the numbers of (large) brine shrimp where high enough to avoid over-predation by 500 flamingos, using data on brine shrimp population dynamics presented in chapter 2 (after Browne and Wanigasekera, 2000). A distinction was made between young brine shrimp and adult brine shrimp.

$$\text{Eq. 3.7a} \quad : \quad YBS_{t+1} = YBS_t - \frac{1}{30} * YBS_t + \frac{260}{41} * 0.5 * BS_t - \frac{1}{5} * 500 * 135{,}000 - \frac{0.21}{21} * YBS_t \; [no.]$$

$$\text{Eq. 3.7b} \quad : \quad BS_{t+1} = BS_t + \frac{1}{30} * YBS_t - \frac{4}{5} * 500 * 135{,}000 - \frac{1}{41} * BS_t \quad [no.]$$

where: *YBS* is the amount of Young Brine Shrimp [no.]
BS is the amount of adult Brine Shrimp [no.]
t denotes the time step [day]

The second term (on the right hand side) in equation 3.7a represented the amount of young brine shrimp (YBS) growing up to adults (BS) within one time step, as it took on average 30 days before a female started producing offspring. The third term in this equation were the newly hatched brine shrimp, as a female produced 260 young brine shrimp in a period of 41 days. Hereby the assumption was made that half of the adult brine shrimp population was female. The fourth term was mortality due to foraging flamingos, where it was assumed that 1/5th of the individuals caught by 500 foraging flamingos were young brine shrimp. The last term in this equation was the natural mortality of the young brine shrimp, where it was reported that 79% of the small brine shrimp survived until the 21st day.

In equation 3.7b, the last term was the natural mortality of adult brine shrimp, where females lived on average 41 days after maturing. Note that these equations do not take into account limitation by food shortage; therefore they can only indicate whether a given amount of individuals was sustainable at a given flamingo population assuming no limitation in halotolerant growth by food.

Salinity tolerance

The results of the salt tolerance experiment were used to determine the probability of survival as function of salinity. This was calculated using a (binomial) logistic regression model. This relation was determined for four exposure times (1, 2, 3 and 5 days), for small – and large brine shrimp as well as for small – and large brine fly larvae, using the combined results of experiments one and two.

4. Field survey: results

This chapter describes the results of the field survey, starting with an outline of the state of Lac Goto during the study period, followed by the results of the field study, in the same order as seen in chapter 3. A discussion of these results can be found in chapter 7.

4.1 General observations and state of Lac Goto

Precipitation events were limited during this wet season (in 2015), possibly related to the effects of a strong El Niño event occurring during the field study. Surface runoff on a large scale did not occur; only small scale runoff was observed. Cloudiness was significant during most days and mostly higher over the area of Lac Goto than further north and south on the island. The water of Lac Goto was clear (in contrast to 2010 to 2014), with a visibility of at least three meters as observed during the measurements for the bathymetric relations. Water levels were neither extremely low nor high (compared to historical satellite imagery, appendix IV) and showed little fluctuations during the study period. In contrast to earlier reports by Buitrago *et al.* (2010), no clear tidal movement was present in the lake.

Variations in salinity were small in space; salinity was at most 2 g/l lower on one location than on another, and salinity was slightly higher (2 g/l) at the end of the measurement period than at the start. No large differences in salinity and temperature were found with depth, indicating a well-mixed system (at least at the time of measurement), possibly caused by high wave action and low fresh water input. An exception was found in the southern part of the canal. Water with a similar salinity as sea water entered Lac Goto at the southern tip of the canal (figure 2.1 A), at least during high tides, which resulted in a shallow layer of less saline water floating on top of more saline water in the southern part of the canal.

Brine shrimp were observed almost everywhere, except for the less saline top layer in the canal of Lac Goto. In this top layer, some small fish (unknown species) were observed, at salt concentrations of up to 75 g/l. Brine fly were mainly present on the eastern shore (figure 2.1 C), where winds were not as strong as on the western shore. Brine fly larvae and chrysalids were also observed, mainly in muddy sediments (larvae) and on salt crusts (chrysalids). Flamingos were present at an average of 300 to 500 individuals. They were found to forage mainly in shallow parts (less than 60 cm deep) of Lac Goto, where they could stand rather than swim. Some smaller water birds were observed in Lac Goto as well. No aquatic plants were observed. Some algae were present, mainly as a layer on the bottom of the lake.

4.2 Results of measurements

4.2.1 Bathymetric relations

The DEM which was made for constructing the bathymetric relations is shown in figure 4.1. Largest depths were found in the canal and southern part of Lac Goto, with depths up to 12 meters. The northwestern area, which is furthest from the sea, showed a gentle increase in depth towards the southeast, whereas steep gradients were found both near the south(west)ern and (north)eastern shores of the lake, reflecting the old drainage patterns as described in chapter 2. The dark green spots in figure 4.1 A indicate islands. The average depth of the lake was 3.0 meters.

Based on this DEM, bathymetric relations shown in figure 4.2 were constructed. The dotted lines show the results calculated with depth plus and minus ten percent, reflecting the effect of uncertainty in the measurements. The percentage of area with depths between 0 and 60 cm as function of water level is shown as well, as these were locations at which flamingos mainly searched for food. This foraging area showed a maximum extent when water levels were around the normal level. For extremely low – and high water levels (below 0 m +BRL and above 0.7 m +BRL), this area decreased.

4.2.2 Water balance

Precipitation

Precipitation was highly variable over the area, as illustrated by the differences in precipitation intercepted during the measurement period by the different rain gauges (table III.1). Comparison of yearly precipitation sums of Flamingo Airport (F.A.) with available sums at the BOPEC rainfall station between 1999 and 2008 (appendix VI) revealed that precipitation over the catchment of Lac Goto was on average 1.5 times higher than over F.A.. The difference was most pronounced during years with little precipitation. This factor (1.5) was used as (initial) precipitation correction factor in the model study.

Evaporation

Evaporation was measured automatically in the period of 21st of November until the 12th of December. The pressure sensor was not working correctly outside this period. Manual measurements were performed throughout the whole field survey period. Comparison of the water temperature in the pan and the water temperature in the lake (figure III.2, appendix III) indicated that temperatures in the pan showed a bit more extreme values, with both lower and higher temperatures than the surrounding lake water. This difference was at most 1 °C, but did not exceed 0.1 °C most of the time.

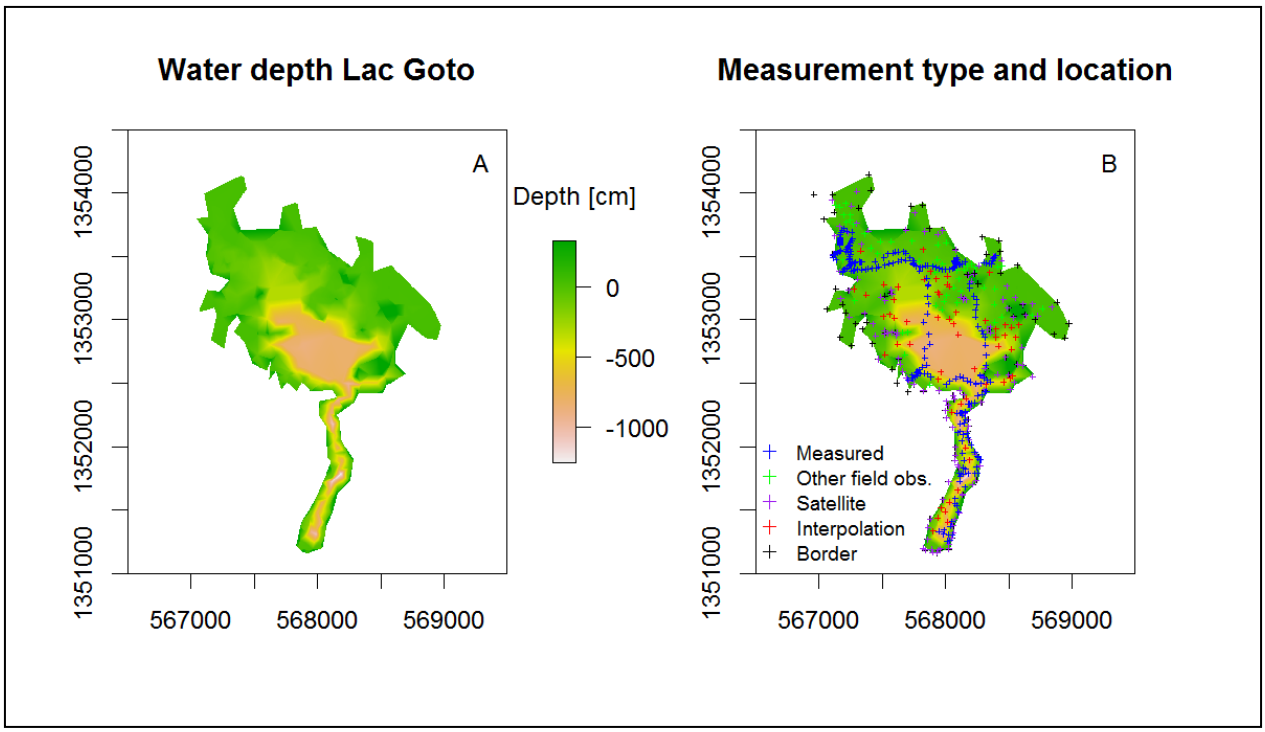

Figure 4.1: Water depth of Lac Goto in centimeters without (panel A) and with (B) measurement type and location of measurements. The horizontal (easting) and vertical (northing) display coordinates in WGS84/UTM 19N.

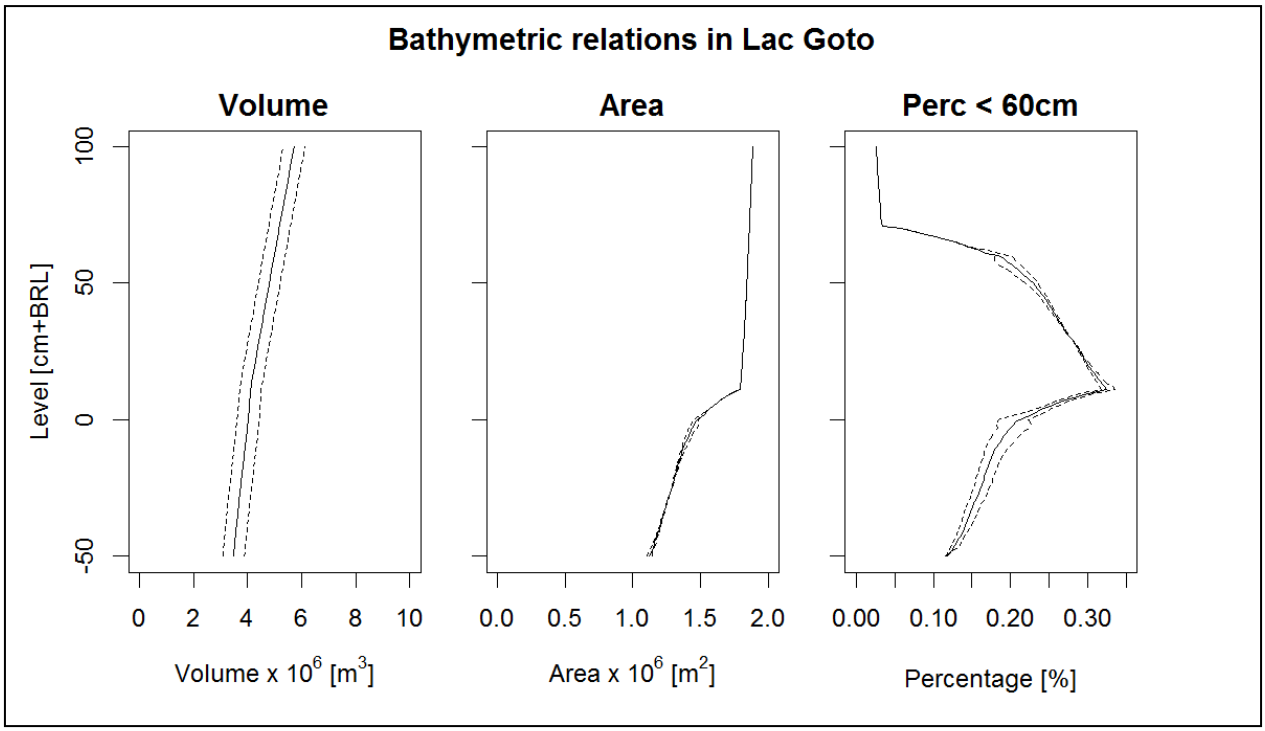

Figure 4.2: Bathymetric relations as determined for Lac Goto. The left panel shows the level-volume relation, the middle panel the level-area relation and the right panel shows the relation between water level and the fraction of area with depths less than 60 cm. Solid lines indicate relations using measured and interpolated depths. Dashed lines indicate the relations when for each depth measurement 10% is added or subtracted, indicating measurement uncertainty. Note that the dependent variable is located on the x-axis rather than the y-axis, for convenience in plotting.

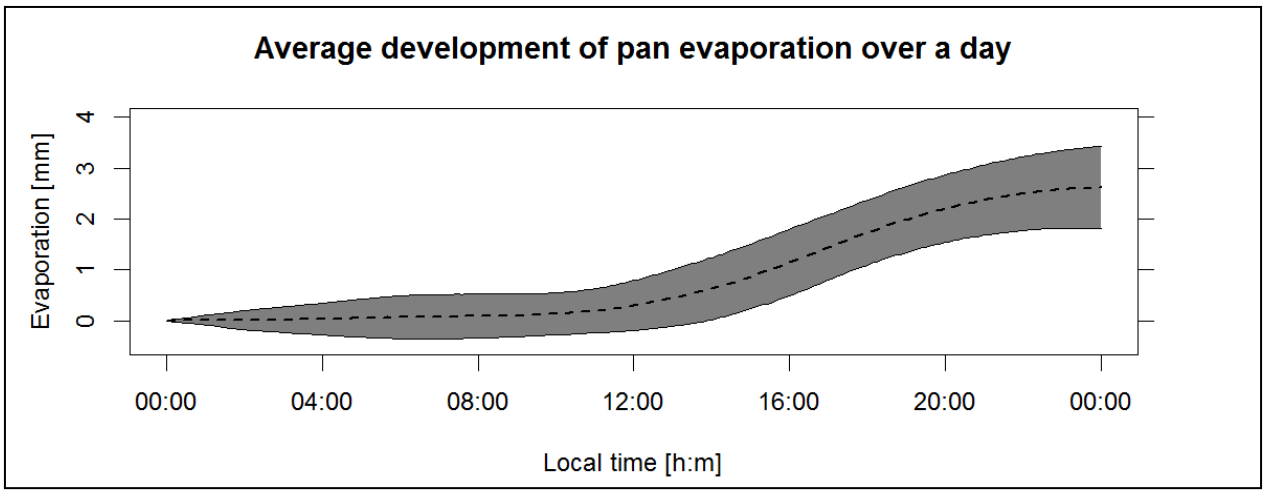

Figure 4.3: The dashed line indicates the development of average evaporation over a dry day (n=19 days), as measured by the pressure sensor. The grey shaded area delineates average evaporation plus and minus one standard deviation, indicating day to day variability in evaporation. The average evaporation at the end of a day is 2.61 ± 0.81 mm.

Evaporation over the day as measured by the pressure sensor followed a similar pattern for each day, as shown in figure 4.3. Evaporation lagged behind solar radiation; the majority of evaporation took place between 1 and 11 PM. During this time, water temperatures exceeded air temperatures. Correlation of the change in level in the evaporation pan over five minutes with possible explaining factors for evaporation showed that the difference in water – and air temperature correlated best with evaporation (r^2 = 0.357, n ≈ 6000 five-minute interval samples, shown in figure III.3), with higher evaporation rates coinciding with larger (and positive) differences between water – and air temperatures. Correlation was also good with absolute water temperature (r^2 = 0.336). A weaker association between relative humidity and evaporation was also present (r^2 = 0.163). Wind speed or incoming shortwave radiation did not show correlations on this timescale. On a daily scale, no clear relations were found between measured evaporation and wind speed, or minimum, mean and maximum temperature. A relation was found for daily radiation and daily evaporation (r^2 = 0.448, n=21 days, for Republiek), which could be attributed to higher water temperatures resulting from an increased warming by solar radiation. Measured daily averaged lake temperature correlated with daily evaporation (r^2 = 0.214, for Republiek), but a stronger correlation was found after computing the difference between daily averaged lake – and air temperature (r^2 = 0.386, for Republiek), with more evaporation coinciding with higher lake – than air temperatures.

Daily evaporation sums as measured or calculated (using meteorological data on a five-minute interval (Republiek) or at a daily basis (Flamingo Airport)) during the period for which the pressure sensor of the evaporation pan was working are shown in figure 4.4. Measured (with pressure sensor) evaporation sums showed best agreement with the five-minute interval calculations. The 24-hour calculation showed

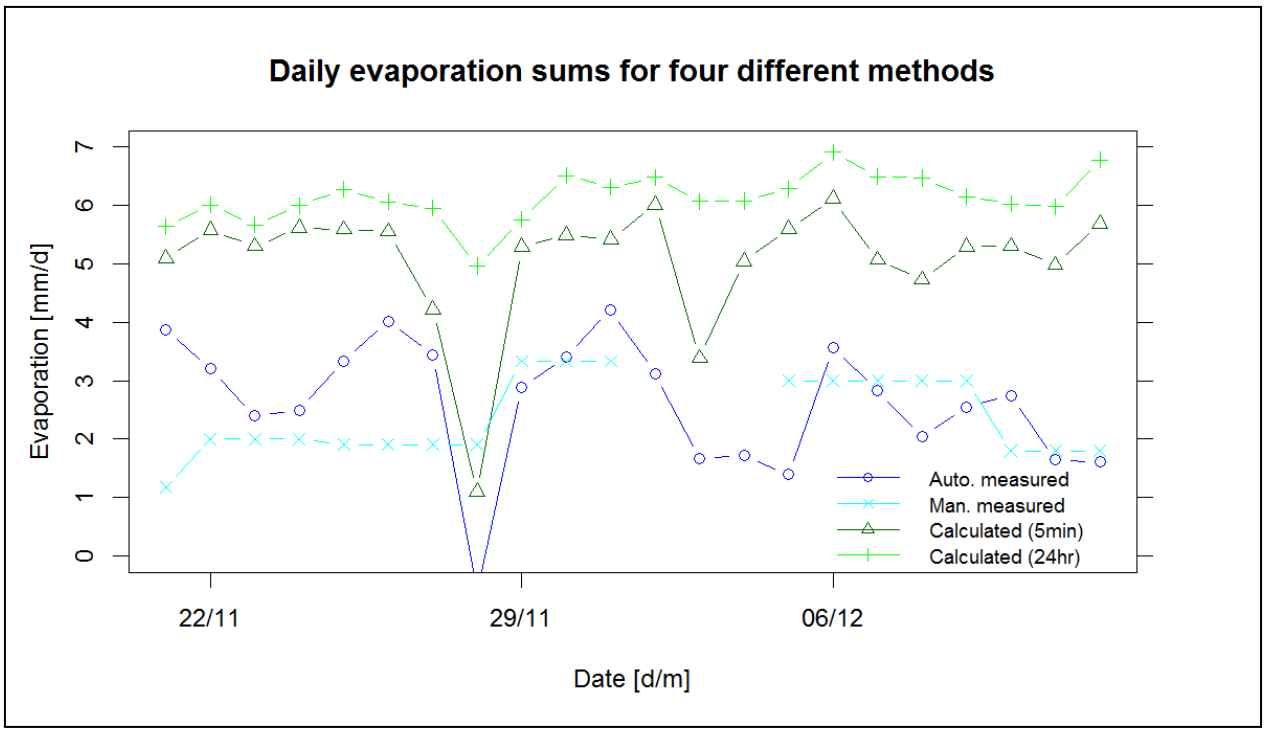

Figure 4.4: Daily evaporation sums over a course of three weeks during the field study, determined using four methods; blue shows results of two measurement methods (automatic and manual), green shows results of two calculation methods (five-minute interval data from Republiek and 24-hour interval data from Flamingo Airport weather stations).

less variation in estimated evaporation amounts than was observed or calculated with data from Republiek. This is clearly visible on the 28th of November, which was a completely cloudy (and rainy) day. The decrease in the 24-hour estimate for this day was caused by a low difference in minimum and maximum temperature, whereas the decrease in the 5-minute estimation was caused by the absence of direct solar radiation. Both calculation methods suggested evaporation to be approximately twice as high as measured values, but were still lower than the potential evaporation mentioned by De Freitas *et al.* (2005). Based on these data, a correction coefficient of 2 was needed to match measured evaporation rates to calculated evaporation rates. This coefficient is discussed more extensively in the section on tidal – and groundwater flow (page 41).

Water levels

The water levels as measured in the sea by SeaSalt and SeaFresh for a two week period were similar in signal as modeled tides by Flater (2015), both in magnitude and timing of ebb and flood (figure III.1). Effects of wind action were not recognized within this measurement period.

Water levels recorded by GotoSalt2 were discarded, as this diver showed sharp water level fluctuations, which were not present in reality. An interesting feature in the water level recordings was found when

comparing measurements on December 2nd by GotoSalt1 with measurements by GotoFresh (figure III.5). A peak in water level was present at GotoFresh, whereas a decrease was visible in the recordings of GotoSalt1. This increase at GotoFresh was noted in the field as well and was most likely caused by high wind speeds during that day (own observations, wind speed measurements Republiek).

Surface runoff

Surface runoff did not occur often. It was observed to occur only two times, and only from dense soil patches such as dirt roads and dried up land areas of Lac Goto (which were dense due to salt crusts (figure 2.1 D)). Due to high spatial variability in and the local nature of precipitation, only minor parts of the catchment responded to precipitation.

Based on data availability, three precipitation events were selected for surface runoff analysis. For one event, no surface runoff was observed; for the other two events minor occurrences of surface runoff were observed. Measured precipitation amounts and observed water level changes for these events are shown in table 4.1. Also included in this table is an event reported by Buitrago *et al.* (2010). Water level changes for all measured events (including the one without observed surface runoff) were roughly two times as large as measured precipitation amounts. Assuming surface runoff originated from the whole catchment, this would imply that 15% of the precipitation falling on the total catchment would have reached Lac Goto within eight hours, given their extent of 13.1 x 10^6 m^2 and 2.0 x 10^6 m^2, respectively. Stated differently, this required an area the size of Lac Goto from which all precipitation was transported to Lac Goto within eight hours. Given the field observations of runoff (very minor and local surface runoff events), this seemed unlikely. The surface runoff amount calculated for the event reported by Buitrago *et al.* (2010) required only 4% of the precipitation falling on the total catchment to reach Lac Goto within one hour (as this change was reported to be within one hour by Buitrago *et al.* (2010)).

Table 4.1: Measured amounts of precipitation and water level change during selected precipitation events. Average precipitation was calculated as average of rain recorded by PR2, PR3 and PR4. Surface runoff was calculated as average level change minus average precipitation. The last column shows where (if any) runoff was observed. A dot means no data.

Date [d-m-y]	PR2/PR3/ PR4/ET [mm]	Average precipitation [mm]	GotoSalt1/ GotoFresh [mm]	Average level change [mm]	Surface runoff [mm]	Runoff observed [-]
19-11-15	5.4/7.0/10.3/ .	7.6	16.7/13.4	15.0	7.4	PR4
28-11-15	6.6/13.6/4.7/9.6	8.3	15.2/12.9	14.0	5.7	PR3
15-12-15	3.1/4.0/5.8/ .	4.3	7.9/7.8	7.8	3.5	-
01-02-09[a]	.	24.9	.	32	7.1	.

[a] *Event from Buitrago et al. (2010), with measurements at unknown locations.*

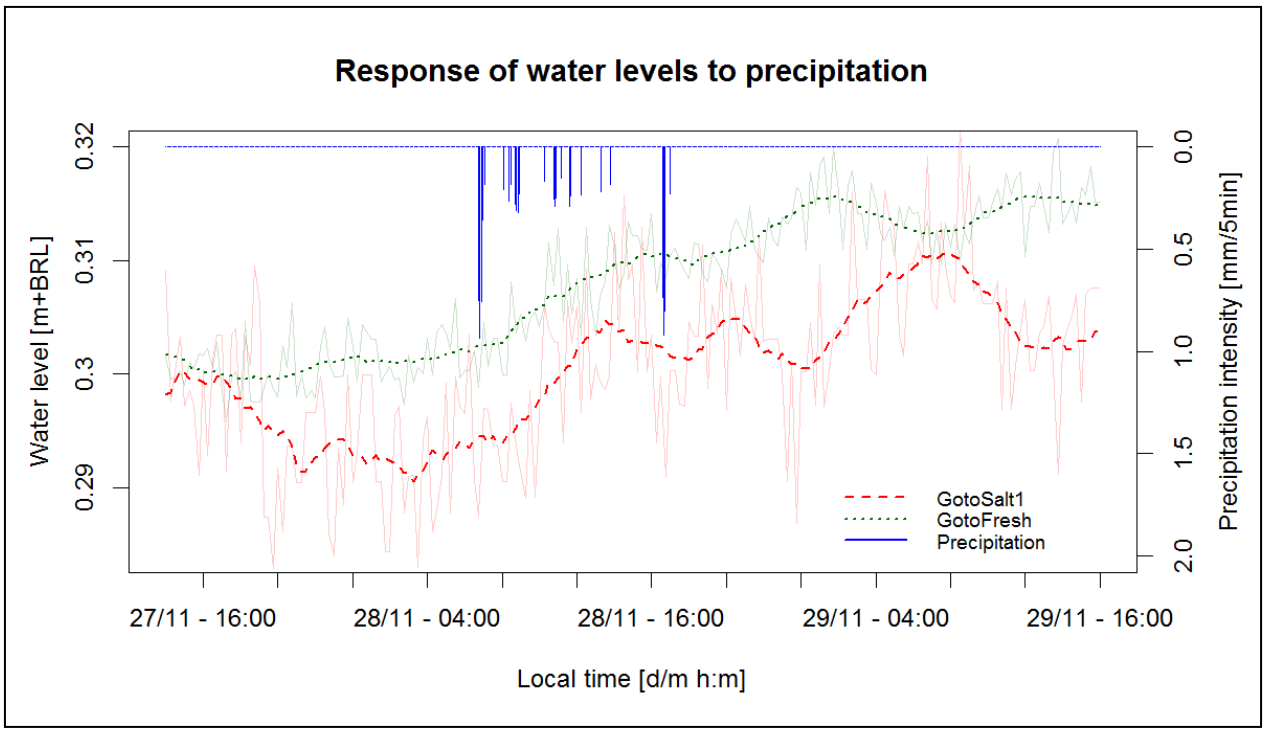

Figure 4.5: Response of the water levels as measured by GotoSalt1 (red dashed) and GotoFresh (green dotted) to the precipitation event on the 28th of November. Precipitation intensity is indicated by the blue bars. Intensity was determined using the change in level over five minutes measured by the pressure sensor in the evaporation pan. Due to the precision of this sensor, intensities must be interpreted as indication for when precipitation has occurred rather than as exact sums.

The response of the water level to the precipitation event of the 28th of November is shown in figure 4.5. This event was characterized by two periods with high intensity precipitation, with a period of rather constant, low intensity precipitation in between. The sky was completely overcast during the day, so evaporation of water from the lake would have been low; fluctuations were therefore mostly determined by precipitation, surface runoff, groundwater flow and exchange through the dam. Water levels reacted to the input of precipitation by showing an increase in level. This reaction did not take place instantly; there was a delay of one hour between the first precipitation peak and the onset of the water level increase. Also note the large fluctuation in individual water level measurements, especially for GotoSalt1 (which has a coarser resolution).

Due to both the absence of events with a large precipitation intensity and – total and the fact that calculated surface runoff amounts did not seem to fit observations of surface runoff occurrences, it was impossible to determine a proper relation between precipitation and surface runoff. Based on observations of surface runoff in the current study, it can only be concluded that showers with less than 10 mm of rain do not result in surface runoff. Showers with totals larger than 10 mm give rise to small scale surface runoff.

Tidal – and groundwater flow

In the first approach, for which cross correlations were examined, most correlations were poor as shown in table III.2 (appendix III). Generally, correlations where higher for GotoFresh than for GotoSalt1, probably related to the better measurement resolution of this diver. The best relation was found between the derivative of the moving average of the measured time series (recorded by GotoFresh) and the derivative of the sea level development. This cross correlation is shown in figure III.4. The time lag for this correlation was -24 hours for the maximum correlation and -11.25 hours for the minimum correlation. Water levels in Lac Goto thus increased 11.25 hours after seawater levels decreased, and 24 hours after seawater levels increased. Given the fact that a tidal cycle takes approximately 24 hours, lake levels thus responded instantly to changes in sea levels; therefore, tidal inflow did indeed play a role in Lac Goto. The correlation was not very high, indicating that either tidal flow was not the only factor of importance, or that there was a large measurement uncertainty.

The second approach, in which the average daily trend in water level was calculated, resulted in figure 4.6. The average daily development of the water level (blue dashed line) and the residual time series (red dashed line) is shown here, for GotoFresh. The results for GotoSalt1 are not shown, as the coarser resolution of this diver gave a larger uncertainty. The red line must be interpreted as the in – or outflow, which has occurred from the start of the day until a given time, originating solely from tidal – and groundwater flow (not surface runoff and precipitation, as line was constructed using only dry days). Water levels were on average declining with 1.7 mm/d (± 2.4, using one standard deviation, determined at the end of blue line), but there was a net inflow of ground- and seawater of 3.6 mm/d (± 3.6). It should be noted that the blue – and red shaded areas, showing measurements plus and minus one standard deviation, indicate that uncertainty was so large compared to the actual change in water level, that average daily fluctuations were not significantly different from zero.

The results presented in figure 4.6 (when disregarding the significance of the results) indicate that net inflow (through tidal – and groundwater interaction) mostly took place during high tides, when the average water level (of the lake and sea) exceeded 0.4 m +BRL. During the rest of the period, inflow of groundwater seemed to balance outflow through the dam. Note that the line indicating seawater level is an average as well; variations in height of high and low tide existed, but the timing of high and low tide was rather constant during this measurement period (figure III.1, appendix III).

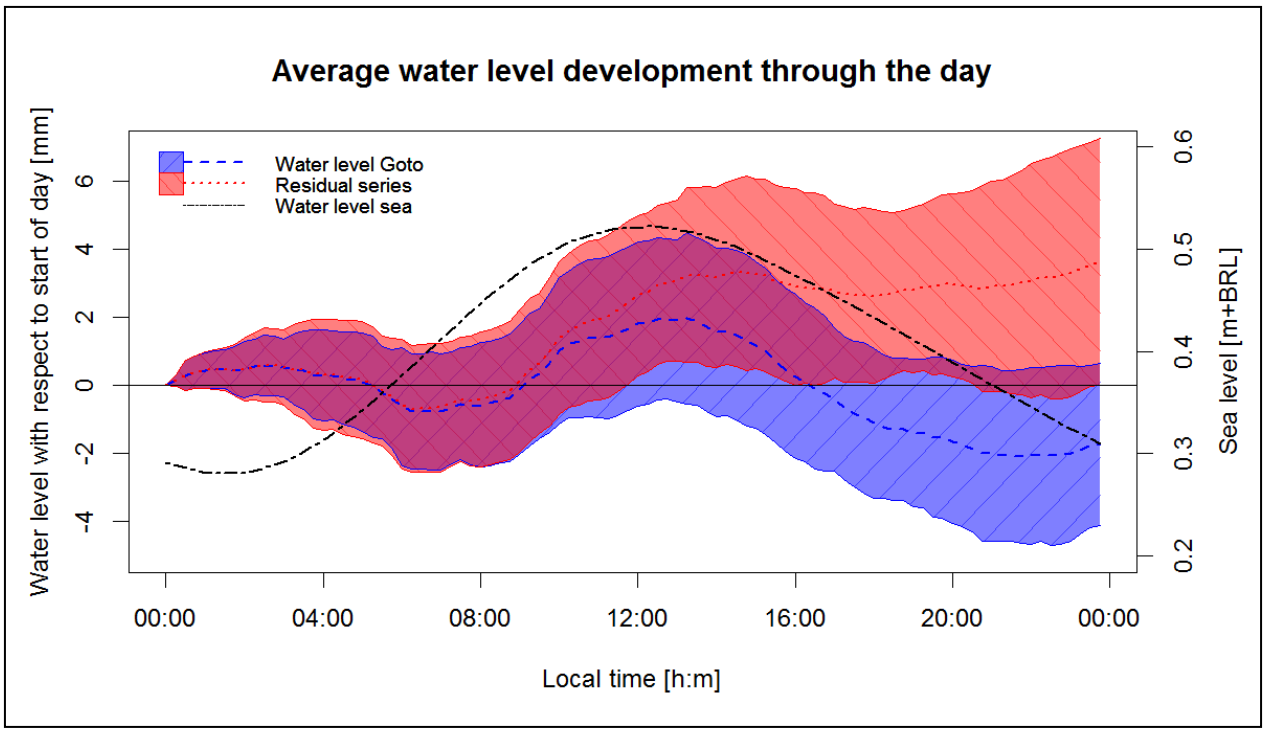

Figure 4.6: Average water level development over the day (for GotoFresh). The blue dashed line shows the average water level as measured by the diver, the red dashed line shows the residual time series, which is the average net in- or outflow over the day originating from tidal – and groundwater flow. Shaded areas delineate one standard deviation above and under the average line. The average sea level (black dotted line) is indicated on the right axis. Included data is from 22nd of November to 12th of December, excluding rainy days and the 2nd of December (total number of days is 19).

For construction of the red line in figure 4.6, measured evaporation was compensated by multiplying with the evaporation correction factor (which was determined to be 2). It was chosen to increase measured evaporation to the level of calculated evaporation rather than vice versa. If one would have assumed measured evaporation rates to be correct, the red line would show a decrease in the afternoon, similar (but less steep) as the blue line. This would imply that, over this period, net outflow would take place which cannot be the result of evaporation, as this was accounted for. However, no other explaining mechanisms for outflow in this period were found, as outflow through the dam was not possible given the high sea water level during this period of decline.

A summary of the results of the third approach, in which seven water balances were constructed and parameters were fitted, is given in table 4.2. Best fits of the water balance models with measured water levels for the 1-layer and n-layer dam models with and without groundwater influence as well as for the model without flow through the dam are listed here. The 2-layer model was not shown here, as during the optimization of parameters for this model (with fixed transition height at 0.4 meters +BRL, as figure 4.6 indicated that most tidal inflow took place when the average level of the sea and lake was above 0.4

meter +BRL), best parameter fits were found when c_1 and c_2 were both equal, and the same as the best conductance for the 1-layer model. It should be noted that the values given in this table were as determined over the whole measurement period. Using half of the measurement period as calibration and half of the period as validation yielded comparable values. A feature which was visible for all models, is that at the end of the period (starting December 12th) all models estimated water levels to be higher than measured. This was attributed to a low manually measured daily evaporation sum and therefore low artificial evaporation sums over this period. Evaporation sums were multiplied by 1.5 for this period (so that daily measured evaporation sums in this period were similar to the rest of the period), which resulted in a better fit than could otherwise be obtained. In general, best fits (with a lower sum of squared differences) were obtained for measurements of diver GotoFresh, which was explained by both a smaller number of observations for which the sum of squared differences was determined, as well as by a higher resolution of this diver. In terms of Nash-Sutcliffe efficiency, GotoFresh showed the best performance as well.

For GotoFresh best results were obtained for dam models with groundwater flow (with a positive Nash-Sutcliffe efficiency, table 4.2). The 1-layer and n-layer models performed equally well. The dam conductance was 60% lower for the models with groundwater flow as compared to those without. Performance of the model without flow through the dam was poor. The optimum value found for the reservoir coefficient (using the 1-layer model with groundwater flow) implied that the groundwater reservoir would lose 15% of its volume within one day for any given precipitation event, which equals a volume equivalent to all precipitation which fell on Lac Goto itself in such an event. After ten days, the groundwater reservoir would only have 20% of its volume left.

Contrary to GotoFresh, best results for GotoSalt1 were obtained with the models without groundwater flow. Models with groundwater flow performed best when the reservoir coefficient (α) was zero; the values listed for these models in table 4.2 are therefore not the optimum but a combination of well-performing parameters. All four models with flow through the dam performed approximately equally well. Similar as for GotoFresh, performance of the model without flow through the dam was poor. The Nash-Sutcliffe efficiency was negative for all models, indicating that using the mean of observations as model would yield better results than the model itself. The value obtained for α for the models with groundwater flow implied that ten days after a rain event, approximately 10% of the reservoir would be emptied. It would take 180 days to drain 80% of the reservoir.

According to the water balance given in table 4.2, the contribution of seawater inflow to the total inflow was less than 50% for GotoFresh with groundwater flow, whereas for GotoSalt1 the contribution of seawater to the total inflow was only slightly reduced when adding groundwater flow. This difference was both a direct consequence of the lower reservoir coefficient found for GotoSalt1 (resulting in more evapotranspiration and less groundwater flow from the terrestrial reservoir), as well as caused by the presence of a relatively long dry period in the measurement period of GotoSalt1, which was not included for GotoFresh. It is interesting to note that 95% of outflow was due to evaporation; outflow to sea accounted for only 5% of outflow (or even 2.5% for GotoFresh with groundwater flow).

The salt balance (table 4.2, calculated with an average depth of Lac Goto of 3.0 m and excluding salt precipitation) responded to the relative importance of the different water balance terms; the lower dam conductance for GotoFresh with groundwater flow resulted in a reduced inflow of seawater and salt and therefore a lower increase of salinity over the measurement period as compared to other models.

Table 4.2: Sum of squared differences and Nash-Sutcliffe efficiency, parameter values (x 10^3) and resulting water – and salt balance for the best model fits for five water balance model combinations and two divers. Best fits are displayed in italic for both GotoSalt1 (calibration period: 2/11 – 20/12) and GotoFresh (calibration period: 14/11 – 20/12). The addition +gw indicates that groundwater flow was incorporated in the water balance model. Note that the sum of squared differences was always smaller for GotoFresh due to differences in number of measurement samples and a better diver resolution.

Diver		GotoSalt1					GotoFresh				
Dam model		1-layer		n-layer		No dam flow	1-layer		n-layer		No dam flow
Groundwater flow		.	+gw	.	+gw	+gw	.	+gw	.	+gw	+gw
Sum of squared differences	[m^2]	*0.616*	0.622	0.619	0.629	13.0	0.303	0.117	0.297	*0.117*	0.639
Nash-Sutcliffe	[-]	*-0.091*	-0.102	-0.097	-0.114	-22.0	-0.138	0.560	-0.115	*0.561*	-1.40
c or c_{min} (x 10^3)	[1/md]	*5.27*	5.08	5.06	4.68	.	4.24	1.97	1.92	*1.90*	.
c_{max} (x 10^3)	[1/md]	.	.	18.6	33.2	.	.	.	159	*6.61*	.
α (x 10^3)	[1/d]	.	9.02	.	8.40	1000	.	150	.	*150*	900
Water inflow	[m]	*0.323*	0.322	0.323	0.322	0.210	0.204	0.187	0.202	*0.187*	0.162
q_P	[%]	*9.97*	9.99	9.98	10.0	15.3	12.9	14.0	13.0	*14.0*	16.2
q_{si}	[%]	*90.0*	87.3	90.0	87.5	.	87.1	43.7	87.0	*43.7*	.
q_{gw}	[%]	.	2.74	.	2.55	84.7	.	42.4	.	*42.3*	83.8
Water outflow	[m]	*0.312*	0.311	0.311	0.311	0.297	0.202	0.197	0.201	*0.197*	0.193
q_E	[%]	*95.4*	95.6	95.5	95.7	100	95.2	97.7	95.8	*97.7*	100
q_{so}	[%]	*4.57*	4.37	4.52	4.31	.	4.77	2.27	4.23	*2.26*	.
Salt inflow	[kg]	*10.2*	9.84	10.2	9.86	0	6.21	2.86	6.16	*2.86*	0
Salt outflow	[kg]	*1.54*	1.47	1.52	1.45	0	1.04	0.483	0.919	*0.480*	0
Salinity change	[g/l]	*2.88*	2.79	2.88	2.80	0	1.72	0.793	1.75	*0.794*	0

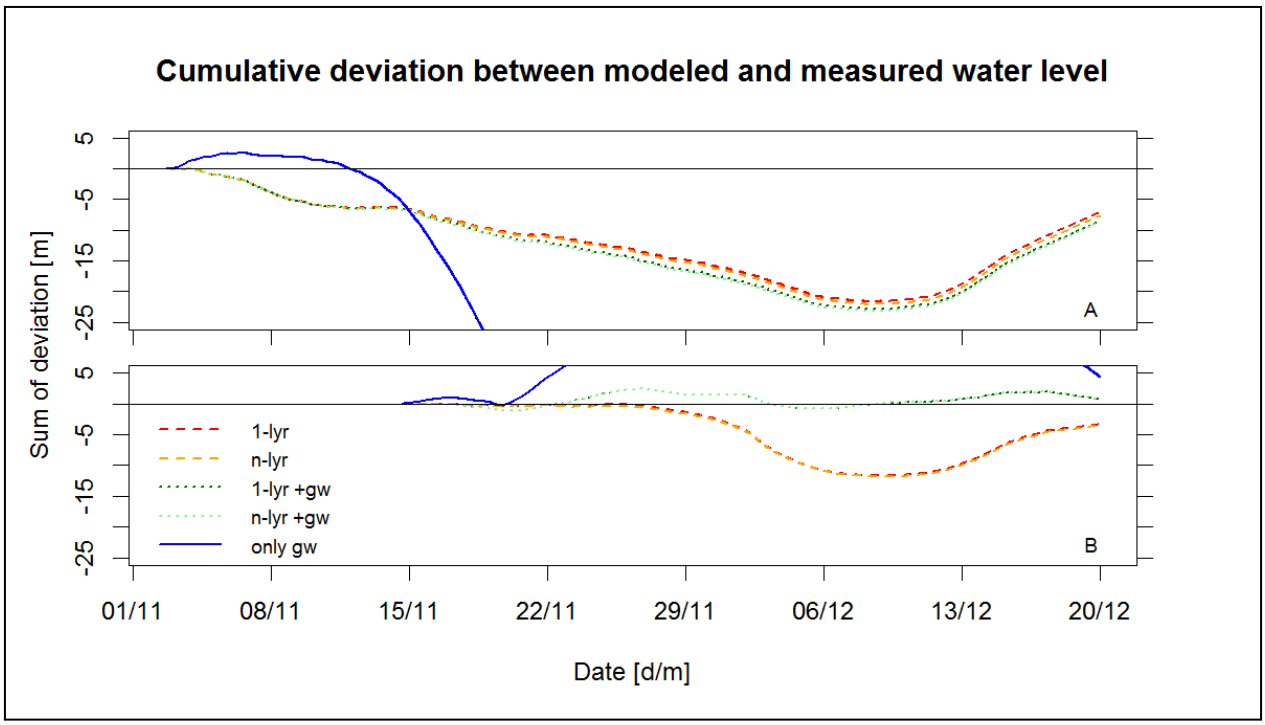

Figure 4.7: Development of cumulative deviation (in m) between modeled and measured water levels for all models listed in table 4.2, for GotoSalt1 (panel A) and GotoFresh (B). A negative trend means an underestimation, a positive trend an overestimation of observations and the steepness is an indication for the size of the deviation. A horizontal line means a perfect fit. For the models without flow through the dam, deviations were too large to fit in the panels. Note that 1-layer and n-layer models performed mostly equally well, so that lines can be plotted over each other. Note that measurements for GotoFresh only started the 14th of November, which contributes to the smaller cumulative deviations.

The cumulative deviation between modeled and measured water levels for all models presented in table 4.2 from the start of measurements until a given time is shown in figure 4.7 A (GotoSalt1) and figure 4.7 B (GotoFresh). Figures III.6 and III.5 (appendix III) show the development of the non-cumulative deviation from measured levels and the absolute modeled and measured water levels, respectively. Differences between models were small for GotoSalt1. All models predicted water level development too low for the majority of the period (negative trend), but followed the trend in signal well (constant decrease of the line). Performance was not good for the last period (steep increase). For GotoFresh, performance of the models with groundwater flow was better than for models without, mostly due to two periods in which performance of the models without was poor (steep line for periods between 30/11 to 4/12 and 11/12 to 16/12). In the first period (until 30/11), the models without groundwater flow performed better.

Calculation of the average daily water level development (similar as in the second approach) for modeled time series (results not shown), yielded a graph similar as figure 4.6 in terms of both shape and magnitude for the modeled water levels of GotoSalt1. For GotoFresh with groundwater flow, a lower peak during the day and a larger increase during the night were visible as compared to figure 4.6.

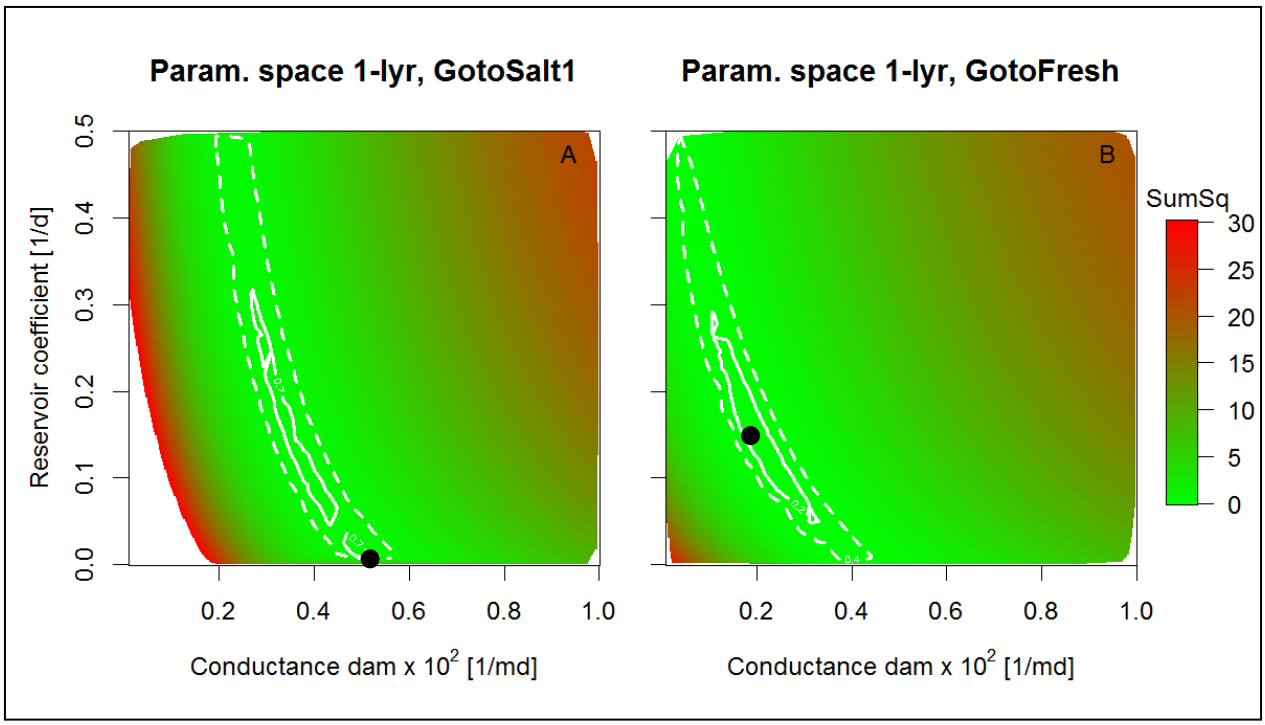

Figure 4.8: Parameter space with two varying parameters for the 1-layer models with groundwater flow, for GotoSalt1 (panel A) and GotoFresh (B). The x-axis displays the conductance of the dam (times 100, in $m^{-1}d^{-1}$), the y-axis shows the reservoir coefficient (in d^{-1}). Green colors indicate parameter combinations which fitted observations relatively well. The contour lines in panel A show regions where the sums of squared differences were lower than 0.7 and 1 m^2 (solid and dashed line, respectively). The contour lines in panel B show regions where the sums of squared differences were lower than 0.2 and 0.5 m^2 (solid and dashed line, respectively). The dots show the best parameter combinations (table 4.2).

The results of the Monte Carlo simulation for the 1-layer dam model with groundwater flow are shown in figure 4.8 A and B for GotoSalt1 and GotoFresh, respectively. A band appeared in the parameter space which displays the two varied parameters, for which the given parameter combinations produced reasonable results. Bands were similar in shape for both models, but the location of the band within the parameter space was slightly different. For GotoSalt1, best results were found for a slowly responding terrestrial reservoir, although good values could also be obtained with a slightly lower dam conductance and higher reservoir coefficient, as indicated by the contour lines. For GotoFresh best values were found with a faster responding reservoir (compare with table 4.2), but good results could also be obtained with a somewhat lower reservoir coefficient and higher dam conductance. The bands with well-performing parameter combinations indicated that parameter identifiability was an issue for both divers and that the model was not very sensitive for the reservoir coefficient (as revealed by the nearly vertical contour lines at higher values). This was likely due to the low amount of precipitation during the field survey. An attempt was made to narrow down the region with well-performing parameter combinations by taking into account the salinity development. However, variations in (measured and modelled) salinity were too small to be used for this purpose (table 4.2 and figure III.8).

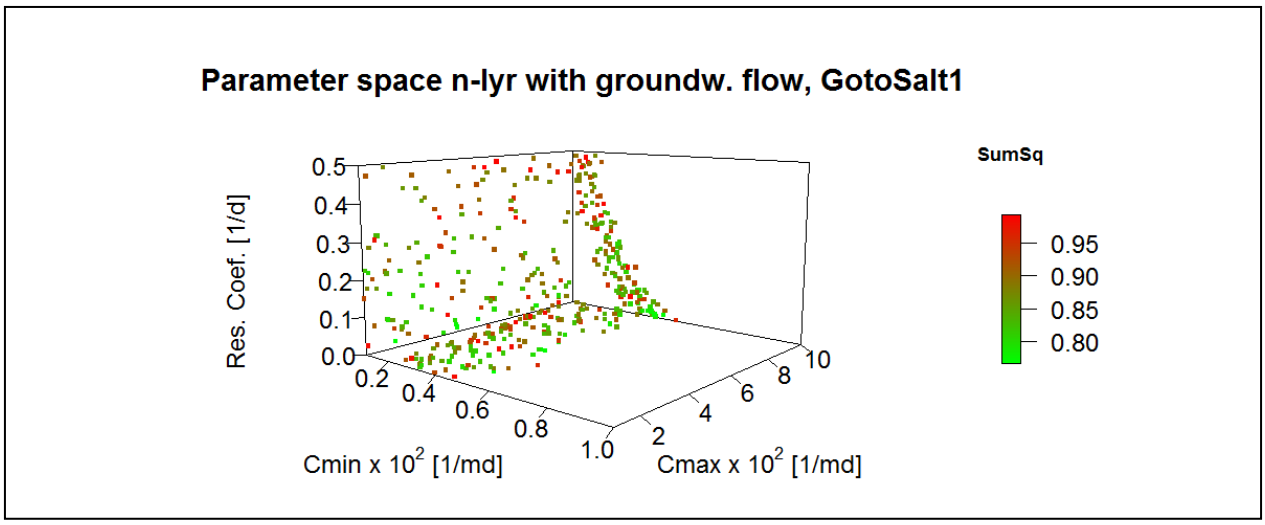

Figure 4.9: Parameter space for the n-layer model with groundwater flow, with three varying parameters. The bottom plane shows all combinations of c_{min} and c_{max}, the left vertical plane shows the relation between c_{max} and the terrestrial reservoir coefficient, the right vertical plane shows the relation between c_{min} and the terrestrial reservoir coefficient. Each point is displayed three times; once on every plane. Points represent combinations of parameters for which the sum of squared differences between modeled and measured water levels for GotoSalt1 was smaller than 1 m^2.

The problem of parameter identifiability was also examined for the n-layer dam models with groundwater flow. The result for GotoSalt1 is shown in figure 4.9. All three panels in this figure represent a two dimensional parameter space similar as figure 4.8, showing a combination of two of the three varied parameters (minimum – and maximum conductance and reservoir coefficient). Displayed points are parameter combinations for which the sum of squared differences was lower than 1 m^2. Each point is displayed three times; once on each panel. Well performing parameter combinations of c_{min} and the reservoir coefficient were found in a band similar as for the 1-layer dam models. Low sums of squared differences were found for values all over the sampled domain for the maximum conductance, indicating that the model was insensitive for this parameter. As with the 1-layer model for GotoSalt1, best fits (green dots) were obtained for a high value for c_{min} and a low reservoir coefficient. The results for GotoFresh are not shown, as these are similar, albeit with the band of well-performing parameter combinations shifted towards lower conductance values, similar as in figure 4.8 B.

In conclusion, both tidal – and terrestrial influence should be included in the water balance model as this was a good representation of the actual system and performed equally well (GotoSalt1) or much better (GotoFresh) than models without groundwater flow. A choice between the 1-layer and n-layer dam models could not yet be made; therefore the most simple model (1-layer with groundwater flow) is proposed as the best model.

4.2.3 Salt balance

Salinity measurements are given in figure III.8 (appendix III). A small decrease in salinity of 1 to 2 g/l was observed after rain events and a gradual (but slow) increase in salinity was present during dry periods. Salt crusts were found on some areas of the bottom of Lac Goto. Layers of precipitated salts were found when digging into the sediments, as illustrated in figure 2.1 B. This particular location was near the outlet of a creek where salt layers and sediment deposits alternated. Presuming that the thick sedimentary layer (second layer from the top in this figure) was deposited by the last extreme rain event in the area (at the end of 2010), the salt layer on top must have formed in the five years following this event. Assuming the salt deposit consisted of gypsum and calcium carbonate and formed all over Lac Goto (with an average area of 1.5 x 10^6 m^2) at the same rate, the thickness of approximately one centimeter of salt deposit as present in figure 2.1 B would imply salt precipitated with a rate of roughly 18 x 10^3 kg/d, or 12 g/m^2 per day. This value for salt precipitation rate was used in the model study.

4.2.4 Halotolerants

Abundance and distribution

Abundance of large – and small brine shrimp varied in both time and space (figures III.7 and III.8, respectively). Trends in abundance were not similar for the three sampling locations. Variations in time did not correlate with salinity, wind speed or water – and air temperature (table III.4). The variation between samples taken at one location at the same day was in general small and there was no decreasing trend in catch with sample number (table III.3). At Halo1 and Halo2, densities of small brine shrimp were recorded to be mostly between 5 and 50 individuals (per 15 l), whereas at Halo3, densities were mostly higher than 200 individuals (figure III.8). Sampling of brine shrimp across the lake at locations with a depth larger than 1 m (sampled on the 11th and 20th of November, on locations distributed over the blue sample sites in figure 4.1 B) revealed that no small brine shrimp were present on those locations. On average, 18.1 (±16.6, n = 13 samples) large brine shrimp were present, as opposed to 28.7 (±15.9, n = 8 samples) large brine shrimp close to shore around the same dates (samples taken between the 10th and 20th of November at Halo1, Halo2 and Halo3).

Densities of brine fly larvae (at Halo2) ranged between 32 and 50 individuals per m^2 sediment for the first measurements. The additional measurements on the same locations resulted in an extra catch of 4 to 13 larvae. Larvae were occasionally found in the water column when sampling for brine shrimp as well, but at most one larva was found per sample.

Estimates of the total numbers of brine shrimp in the lake were made, assuming an average brine shrimp density of 20 individuals per 15 l. Extrapolation over the whole area of Lac Goto (1.5×10^6 m^2) and the average depth (3.0 m) resulted in an estimated amount of 6×10^9 brine shrimp individuals. Using the estimate of Rooth (1965) that approximately 135×10^3 brine shrimp individuals were required as food item for one flamingo for one day (if only brine shrimp are consumed), a reserve of 45×10^3 eating days was present in Lac Goto. This equals a food supply of 90 days for 500 foraging flamingos. Using equations 3.7a and b, the amount of brine shrimp present was sufficient to prevent over predation by 500 flamingos. Based on these equations (and assumptions made therein), a brine shrimp population of less than 2×10^8 individuals would be insufficient to support this number of flamingos.

Assuming a brine fly larvae density of 40 individuals per m^2, over the area with a depth up to 60 cm (as this is the only accessible part for flamingos), yielded an estimated available amount of 11×10^6 brine fly larvae individuals. Using the estimate of Rooth (1965) that approximately 50×10^3 individuals are necessary as food item for one flamingo for one day (if only brine fly larvae are consumed), the reserve of Lac Goto with respect to brine fly larvae was only 225 eating days. For 500 foraging flamingos this is a food supply of 0.5 days. No estimate of the brine fly chrysalids was made. Also no estimate of sustainable amounts could be given as no information was present on population dynamics of the brine fly.

Salinity tolerance

The combined results of the first and second salinity tolerance experiment are shown in figure 4.10. For brine shrimp, the probability of survival was higher at higher salt concentrations, but decreased with increasing exposure time. Only a few small brine shrimp survived to the fifth day (even in water with the same salinity as found in Lac Goto). At a salt concentration of 60 g/l, the probability of survival for large brine shrimp was only 50% after an exposure duration of five days. Brine fly larvae hardly responded to low salt concentrations. Only at salt concentrations below 1 g/l (made with tap water), mortality was observed after five days (for large fly only).

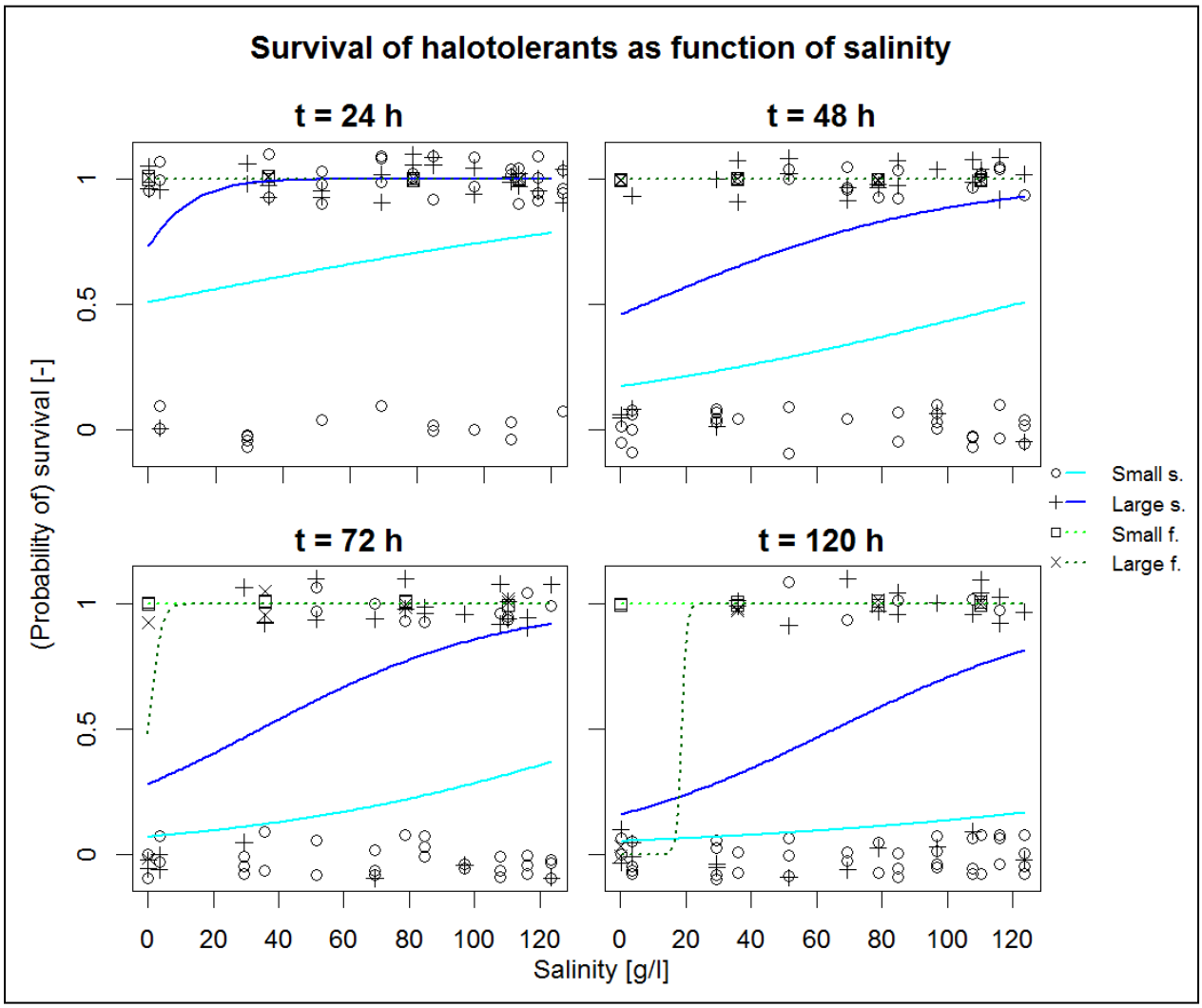

Figure 4.10: (Probability of) survival of halotolerants (both small (s) and large (l) individuals) as function of salinity, for four exposure durations (1, 2, 3 and 5 days). Each symbol represents one individual; the value of 1 is given when an individual survived until the given time, a value of 0 if not. Note that symbols are scattered around 0 and 1, for better readability. Lines indicate the calculated probability of survival at a given salt concentration and time. Results of experiment 1 and 2 are combined in these plots.

5. Model study: methodology

This chapter first describes the methodology as followed to construct the water – and salt balance models for Lac Goto. Next, the modeling procedure and analyses on and validation of the resulting water levels and salt concentrations are discussed. Finally, some information is given on how the sensitivity of the model to its parameters was tested.

5.1 Model setup

Based on the low spatial variability in salt concentrations as found in the field study, it was decided that Lac Goto could be represented as one single reservoir to calculate water volume and salinity. This reservoir model was constructed in RStudio (RStudio Team, 2015), using meteorological data of Flamingo Airport (NOAA, 2015), including precipitation, wind speed, minimum – maximum – and dewpoint temperature as well as tidal data (Flater, 2015) from Kralendijk to calculate the state variables water volume (m^3) and salt (kg). The model used a daily time step, except for calculation of the flux through the dam, which were done on an hourly scale. The model was run with data from 1980 until 2015. The basic equation for the water balance of Lac Goto is given by equation 5.1, which shows similarities with equation 3.2. Fluxes in equation 5.1 are given by equations 5.2 to 5.5.

$$\text{Eq. 5.1} \quad : \quad V_{t+1} = V_t + Q_{P,t} - Q_{E,t} + Q_{si,t} - Q_{so,t} + Q_{sr,t} + Q_{gw,t} \quad [m^3]$$

where:
- V is the volume of Lac Goto at a certain moment in time [m^3]
- t denotes at which time a variable is evaluated
- Q_P is the precipitation within one time step (eq. 5.2) [m^3]
- Q_E is the evaporation within one time step (eq. 5.3) [m^3]
- Q_{si} is inflow of sea water within one time step (eq. 5.4a) [m^3]
- Q_{so} is outflow of sea water within one time step (eq. 5.4b) [m^3]
- Q_{sr} is surface runoff towards Lac Goto within one time step (eq. 5.5a) [m^3]
- Q_{gw} is groundwater flow towards Lac Goto within one time step (eq. 5.5c) [m^3].

For each time step, lake volume was translated to an area and water level using the bathymetric relations presented in figure 4.2. The precipitation flux in equation 5.1 was calculated using equation 5.2. Precipitation was assumed not to depend on the current lake area, as precipitation hardly infiltrated on the dense dried up lake bottom (own observations). Therefore, all precipitation falling on the maximum area of Lac Goto directly contributed to the water balance of the lake. Furthermore, precipitation as measured at Flamingo Airport was multiplied with a correction factor to account for the difference between Flamingo Airport and Lac Goto.

Eq. 5.2 : $Q_{P,t} = P_t * P_{cor} * A_{G,max} \quad [m^3/d]$

where: P is precipitation as recorded by Flamingo Airport [m d^{-1}]
P_{cor} is the correction factor to translate measured precipitation by Flamingo Airport to actual precipitation [-]
$A_{G,max}$ is the maximum extent of Lac Goto, set at 2.0 x 10^6 [m^2].

Reference lake evaporation was calculated using meteorological data from Flamingo Airport with equations described in Calder and Neal (1984) and Allen *et al.* (1998). These equations are given in appendix II. Evaporation from the lake was calculated by multiplication of the evaporation with the correction factor (determined to be 1.0 in chapter 4). In contrast to precipitation, evaporation was multiplied with the actual area of Lac Goto at a given time (equation 5.3).

Eq. 5.3 : $Q_{E,t} = E_t * E_{cor} * A_{G,t} \quad [m^3/d]$

where: E is evaporation as calculated using data from Flamingo Airport [m d^{-1}]
E_{cor} is the correction factor to translated calculated evaporation to actual lake evaporation, fixed at 1.0 [-]
A_G is the extent of Lac Goto at a certain moment in time [m^2].

Based on results presented in chapter 4, it was decided that the best model to describe in- and outflow of water due to tidal exchange and terrestrial interaction was the 1-layer dam model with groundwater flow. For that purpose, equation 3.3a was rewritten into equations 5.4a and 5.4b to account for both changes in lake area with changing lake levels and for the different time step. The n-layer dam model was converted as well for the purpose of comparison between results of these different dam models. This equation is not shown here, as this conversion is similar as for the 1-layer dam model. Calculations of in – and outflow of water through the dam were done at an hourly timescale. The lake level was kept constant during a day (using the lake level as calculated at the end of the previous day) whereas sea level was calculated for each hour using the (interpolated) tides from Flater (2015). This calculation procedure was chosen as the time scale of sea level fluctuations was smaller than the time scale of lake level fluctuations.

Eq. 5.4a : $$Q_{si,t} = \sum_{\hat{t}=0}^{\hat{t}=24} \begin{cases} if\ H_{G,t} < H_{s,\hat{t}} & : \frac{c}{24} * \overline{H}_{\hat{t}} * \left(H_{s,\hat{t}} - H_{G,t} \right) * A_{G,t} \\ if\ H_{G,t} > H_{s,\hat{t}} & : 0 \end{cases} \quad [\frac{m^3}{d}]$$

Eq. 5.4b : $$Q_{so,t} = \sum_{\hat{t}=0}^{\hat{t}=24} \begin{cases} if\ H_{G,t} < H_{s,\hat{t}} & : 0 \\ if\ H_{G,t} > H_{s,\hat{t}} & : \frac{c}{24} * \overline{H}_{\hat{t}} * \left(H_{G,t} - H_{s,\hat{t}} \right) * A_{G,t} \end{cases} \quad [\frac{m^3}{d}]$$

where: c is the conductance of the dam per meter height [$m^{-1}\ d^{-1}$]
H_G is the level in Lac Goto [m +BRL]
H_s is the sea level [m +BRL]
$\hat{t}$ denotes the hourly time step at which a variable is evaluated
t denotes the daily time step at which a variable is evaluated, similar as used in the general water balance model (eq. 5.1).

Surface runoff and groundwater flow were calculated with a terrestrial reservoir similar as used in equation 3.5. Slight modifications were made to equations 3.6 to calculate fluxes on a daily time scale and to explicitly incorporate the area of the terrestrial reservoir, as shown in equations 5.5a, b and c.

Eq. 5.5a : $$Q_{sr,t} = \begin{cases} if\ TR_{t-1} + R_t < TR_{max} & : 0 \\ if\ TR_{t-1} + R_t > TR_{max} & : (TR_{t-1} + R_t - TR_{max}) * \beta \end{cases} \quad [\frac{m^3}{d}]$$

Eq. 5.5b : $$Q_{ETter,t} = \min\left(\frac{TR_{t-1} + R_t - Q_{sr,t}}{TR_{max}}, 1 \right) * ET_{cor,ter} * E_t * A_c \quad [\frac{m^3}{d}]$$

Eq. 5.5c : $$Q_{gw,t} = Q_{gw,t-1} * e^{-\alpha * \Delta t} + (R_t - Q_{sr,t} - Q_{ETter,t}) * (1 - e^{-\alpha * \Delta t}) \quad [\frac{m^3}{d}]$$

where: TR is the total volume in the terrestrial reservoir [m^3]
TR_{max} is the maximum water volume which can be stored before surface runoff starts, fixed at 0.2 meters per m^2 of catchment area, equaling 2.62 x 10^6 [m^3]
A_c is the catchment area, fixed at 13.1 x 10^6 [m^3]
R is the recharge on the terrestrial reservoir, calculated by multiplying precipitation P with the catchment area A_c [m^3]
β is the runoff fraction, fixed at 0.01 [d^{-1}]
α is the reservoir coefficient [d^{-1}]
Δt is the time step, fixed at 1 times its unit [d].

The salt balance was computed based on the results of the water balance. Salt content (kg) of Lac Goto was calculated for each day using equation 5.6. Using the volume of Lac Goto, salt content was converted to salinity. Note that g/l equals kg/m^3.

Eq. 5.6 : $S_{t+1} = S_t + Q_{si,t} * C_s - Q_{so,t} * C_{G,t} + Q_{gw,t} * C_{gw} - SPr \quad [kg]$

where: S is the total mass of salt in Lac Goto [kg]
C_s is the concentration of salt in sea water [g l^{-1}]
C_G is the concentration of salt in Lac Goto [g l^{-1}]
C_{gw} is the concentration of salt in groundwater, fixed at 0 [g l^{-1}]
SPr is the precipitation of salts from Lac Goto, fixed at 18.000 [kg d^{-1}].

The model was initialized with a lake level of 0.3 m +BRL, a salinity of 150 g/l and an initial volume of the terrestrial reservoir of 0 m^3.

5.2 Data analysis

Six preliminary water balance models were set up, using the model – and parameter combinations as given in table 4.2. The 1-layer dam model with groundwater flow was used as the main model (as determined in chapter 4), either using parameters as determined for GotoFresh (high terrestrial reservoir coefficient, low dam conductance) or for GotoSalt1 (low terrestrial reservoir coefficient, high dam conductance) and a precipitation correction factor of 1.5 (as determined in chapter 4). The model was run with the n-layer dam model and the 1-layer model without groundwater flow (with the reservoir coefficient in equation 5.5c set to zero, but still allowing surface runoff to occur) as well, for comparison. Based on the results of these preliminary models (with results compared to historical data, as explained below), other combinations parameter combinations were used which were expected to yield better results than the preliminary models. Also several combinations of conductances and reservoir coefficients (with values given in section 6.1.2) were taken from the band with equally well performing parameter combinations (figure 4.8). The model which showed best agreement with historical data was adopted as baseline model.

Historical data for validation of model results within the modeling period was scarce. Only a few water level – and salinity observations were available, all from recent times. Water level estimates were obtained from satellite images (seven images), which are shown in appendix IV. No actual water level measurements were available. Salinity was available from Buitrago *et al.* (2010) (three measurements) and de Zwart *et al.* (2012) (one measurement). Furthermore, the general behavior of the water level and salinity was compared to findings of Rooth (1965), who measured water level and salinity throughout one year, in a more qualitative way.

Balances of in- and outflow of water and salt were constructed for all models for each hydrological year. Such a year was defined as all days between the 1st of April to the 31st of March of the following year, as these dates were in the middle of the dry season. It was assumed that hydrological conditions were similar from year to year around this time, as any excess water in the terrestrial reservoir from the previous wet season should normally be drained to Lac Goto or evaporated and the lake volume should have decreased to normal values due to water flow through the dam and little fresh water inflow. The 15% wettest hydrological years (1984, 1985, 1988, 2004 and 2010) were defined as wet years. All other years were defined as normal years.

Apart from descriptive analyses of the modeled water – and salt balance, modeled salinity and flamingo abundance were correlated to determine whether there was a difference between observed flamingo abundance for days with low and high salinity. Data on flamingo abundance was obtained from DCBD (2015) (figure 1.3). This dataset contains data from 1981 to present date, partly on a monthly basis. Yearly averages and numbers of observations per year are presented in appendix VI. For each date with available flamingo counts, modeled salinity was determined and a correlation between these two was made. A similar exercise was performed for the percentage of area with depths smaller than 60 cm.

5.3 Sensitivity analysis

Parameters from the baseline model were adapted to test the model sensitivity to all parameters. Some parameters were increased by 50%: the conductance of the dam (c), the terrestrial reservoir coefficient (α), the correction factor for precipitation (P_{cor}) and for evaporation from both lake and land (E_{cor} and $ET_{cor,ter}$), the maximum size of the terrestrial reservoir (TR_{max}) and the surface runoff fraction (β). A model run was also performed with an increased depth of Lac Goto of 10% (using the dotted lines in figure 4.2). Furthermore, the reaction of the model to omitting precipitation of salts (SPr) was tested, as well as the reaction when groundwater flow was given a salinity of 10 g/l rather than 0 g/l (C_{gw}) and when initial salinity was set at 200 g/l (instead of 150 g/l). The results were used to describe which parameters in the estimation of the water balance give rise to most uncertainty and should therefore receive more attention in future research.

6. Model study: results

The first section of this chapter describes the results of the models which used parameters obtained in the field study. After this, the baseline model is presented, which followed from optimization of a selection of parameters after examination of the results of the preliminary models. The results of the sensitivity analysis on this baseline model are shown in the last section.

6.1 Parameter optimization for baseline model

6.1.1 Preliminary models

A part of the modeled water level – and salinity development for all six preliminary models is shown in figure 6.1 A and B, respectively, for 2008 to 2013. The total modeled time series is given in appendix V, together with the yearly contribution of different fluxes to the total in – and outflow for all six models. The general behavior of the modeled water levels was as expected based on the information on the study area provided in chapter 2, with elevated levels during wet seasons and lower levels in dry seasons. The lake did not run dry or flow over. Also, salinity decreased during the rainy season and increased during periods with little precipitation. Looking more into detail, highest water level fluctuations were present for the two models with groundwater flow using parameters of GotoFresh (GF 1-lyr +gw and GF n-lyr +gw in figure 6.1, with a high reservoir coefficient and low dam conductance). Water levels were very high during the wet seasons (values up to 1.5 m +BRL occurred frequently, appendix V) and low in the dry season (even below 0.2 m +BRL). This coincided with salt concentrations below 35 g/l (so below those found in the ocean), indicating that lake dynamics were mostly driven by fresh water flow. The figure depicting contributions of all water sources to the total yearly inflow (figure V.2, appendix V) shows that for these two models most inflow of water originated from (fresh) groundwater flow. The water levels in the models with groundwater flow and parameters of GotoSalt1 (GS 1-lyr +gw and GS n-lyr +gw in figure 6.1) fluctuated less and had a higher salinity than models using parameters of GotoFresh. Peaks in water levels during wet seasons were even lower for the models without groundwater flow (GF 1-lyr and GS 1-lyr in figure 6.1). For the latter models, highest salt concentrations were modeled by the model with a lower dam conductance (GF 1-lyr). It is evident from figure 6.1 that the n-layer models with groundwater flow behaved similarly as the 1-layer models with groundwater flow, similar as was seen in chapter 4. Only at high water levels a difference was present, as water levels decreased more rapidly for the n-layer models due to the higher conductance in the upper parts of the dam.

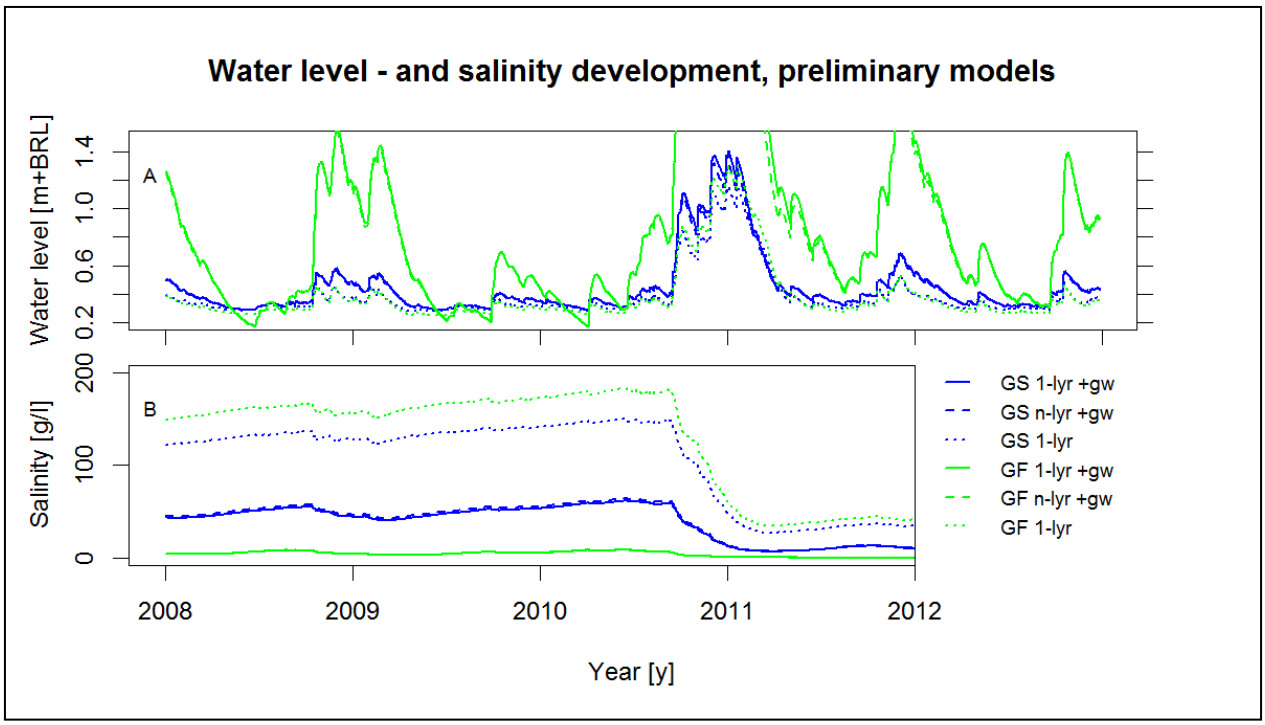

Figure 6.1: Water level (panel A) and salinity (B) development between 2008 and 2013 for preliminary models, using the optimal parameters for GotoSalt1 (GS) and GotoFresh (GF) as listed in table 4.2 and a precipitation correction factor of 1.5. The peak in water level at the start of 2011 is approximately 3 m +BRL for both models with GotoFresh parameters and groundwater flow. A time series of the total modeled period (1980 – 2015) is given in appendix V. Note that the results of the 1-layer and n-layer models are nearly identical, so that lines overlap for the largest part of the period.

Table 6.1: Comparison of modeled water levels and salinity for the six preliminary models with historical data. Small, colored values indicate how much the overestimation (red) or underestimation (green) by the models was. Historical water levels were estimated from satellite images, shown in appendix IV.

	Date [d-m-y]	Estimated	Modeled GotoSalt1			Modeled GotoFresh		
			1-layer +gw	n-layer +gw	1-layer .	1-layer +gw	n-layer +gw	1-layer .
Estimated water level [m +BRL]	19-09-2002	0.26	0.29 +0.03	0.29 +0.03	0.28 +0.02	0.28 +0.02	0.28 +0.02	0.25 -0.01
	16-05-2003	0.27	0.30 +0.03	0.30 +0.03	0.29 +0.02	0.32 +0.05	0.32 +0.05	0.26 -0.01
	14-10-2003	0.30	0.31 +0.01	0.31 +0.01	0.29 -0.01	0.36 +0.06	0.36 +0.06	0.26 -0.04
	18-01-2011	0.70	1.25 +0.55	1.17 +0.47	1.04 +0.34	3.11 +2.41	2.58 +1.88	1.18 +0.48
	21-01-2012	0.40	0.49 +0.09	0.48 +0.08	0.36 -0.04	1.25 +0.85	1.19 +0.79	0.36 -0.04
	23-08-2013	0.31	0.36 +0.05	0.36 +0.05	0.31 0.00	0.57 +0.26	0.56 +0.25	0.29 -0.02
	14-10-2014 [a]	0.30	0.28 -0.02	0.28 -0.02	0.28 -0.02	0.09 -0.21	0.09 -0.21	0.25 -0.05
Salinity [g/l]	15-06-2008	155 [b]	50.4 -105	52.6 -102	133 -22	6.06 -149	6.20 -149	162 +7
	15-11-2008	140 [b]	49.6 -90	51.9 -88	132 -8	5.21 -135	5.30 -135	161 +21
	15-01-2009	129 [b]	44.2 -85	46.5 -82	128 -1	3.61 -125	3.67 -125	157 +28
	30-10-2012	77 [c]	18.1 -59	18.9 -58	47.8 -29	0.35 -77	0.37 -77	54.0 -23

[a] Due to incomplete precipitation data for F.A. in 2014, water levels are not correctly modeled for this date. [b] Historical data from Buitrago *et al.* (2010). Exact measurement date is unknown. [c] Historical data from de Zwart *et al.* (2012).

Historical lake levels and salt concentrations are shown in table 6.1, together with modeled lake levels and salt concentrations for the same dates for all preliminary models. Performance of parameter combinations as found for GotoFresh with groundwater flow was poor for both water level and salinity, with large deviations from historical observations (water levels up to 2 m too high, salinity constantly too low). Parameter combinations found for GotoSalt1 performed better; water levels were modeled quite well during drier periods, but peaks after large rain events were too high (+ 0.5 m in 2011). Salinity was too low in this model as well. The models without groundwater flow showed best results for both water level development and salinity, but peaks in water levels were still too high. Salt concentrations were too high prior to the rainy season of 2010, but were too low after this season. Based on these findings, it was concluded that too much fresh water entered the system, at least in the rainy season of 2010, for all models. Both too high precipitation amounts and too much surface runoff could have been a cause.

6.1.2 Optimization of parameters

As the models discussed above were not able to adequately describe the dynamics as observed in Lac Goto, it was decided to lower the precipitation correction factor from 1.5 to 1.0 to resolve the strong reduction in salinity as observed for all models (including those without groundwater flow) in the rainy season of 2010. Furthermore, several sets of parameters were chosen from the lower part of the band with well performing parameters (from the parameter space shown in figure 4.8) to determine whether other parameter combinations would yield better results when validating with historical observations. Parameters were chosen with a conductance ranging between 4 x 10^{-3} $m^{-1}d^{-1}$ (best fit for GotoFresh) and 5.2 x 10^{-3} $m^{-1}d^{-1}$ (best fit for GotoSalt1) and reservoir coefficients of 5 x 10^{-3} d^{-1} and 10 x 10^{-3} d^{-1}, as combinations of a relatively high dam conductance and low reservoir coefficient yielded better results than combinations of a low dam conductance and high reservoir coefficient (section 6.1.1).

Validation results for some of the model runs are shown in table 6.2. Results were better after adjustment of the precipitation correction factor, which was evident from a comparison of the results of the 1-layer terrestrial model with parameters of GotoSalt (table 6.1, where P_{cor} = 1.5, $\alpha = 9 \times 10^{-3}$ d^{-1} and c = 5.08×10^{-3} $m^{-1}d^{-1}$) with the results of the model with a precipitation correction factor of 1.0 and similar values for the dam conductance and reservoir coefficient (table 6.2). Peaks in water level were lower and salinity was higher for the model with a precipitation correction factor of 1.0.

6.1.3 Baseline model

Best fits with historical observations were obtained using a precipitation correction factor of 1.0, reservoir coefficient of 0.005 d^{-1} and dam conductance of 0.0052 $m^{-1}d^{-1}$, of which the validation results are indicated in italic in table 6.2. These values deviate only slightly from those found for GotoSalt1 (table 4.2: 0.00902 d^{-1} and 0.00508 $m^{-1}d^{-1}$, respectively). Deviations in modeled water level from estimated levels did not exceed 3 cm for this model. Deviations in salinity were also small (max. 16 g/l) and the decrease in salinity between 2009 and 2012 was represented well. This model was therefore chosen as baseline model. Note that all fixed parameter values used in the baseline model are given in the list of symbols.

Table 6.2: Comparison of modeled water levels and salinity with historical data. Results of the baseline model are indicated in italic. All models used the 1-layer dam model with groundwater flow, with parameters given in the column headers. The reservoir coefficient (α) is given times 10^{-3} d^{-1}, the dam conductance (c) is given times 10^{-3} $m^{-1}d^{-1}$. For all parameter sets, the sum of squared differences (SSD) between modeled water levels and observations of GotoSalt1 is given in the last row. For comparison: the lowest possible value for the SSD with this model was 0.616 m^2 (table 4.2).

	Date [d-m-y]	Estimated	P_{cor} = 1.0 / α = 5				P_{cor} = 1.0 / α = 10				P_{cor} = 1.5 / α = 5			
			c = 4.4		c = 5.2		c = 4.4		c = 5.2		c = 4.4		c = 5.2	
Estimated water level [m +BRL]	19-09-2002	0.26	0.25	-0.01	*0.28*	+0.02	0.26	0.00	0.28	+0.02	0.27	+0.01	0.29	+0.03
	16-05-2003	0.27	0.26	-0.01	*0.28*	+0.01	0.27	0.00	0.29	+0.02	0.28	+0.01	0.30	+0.03
	14-10-2003	0.30	0.27	-0.03	*0.30*	0.00	0.28	-0.02	0.30	0.00	0.29	-0.01	0.31	+0.01
	18-01-2011	0.70	0.79	+0.09	*0.73*	+0.03	0.86	+0.16	0.78	+0.08	1.31	+0.61	1.17	+0.47
	21-01-2012	0.40	0.40	0.00	*0.40*	0.00	0.45	+0.05	0.44	+0.04	0.46	+0.06	0.44	+0.04
	23-08-2013	0.31	0.31	0.00	*0.32*	+0.01	0.33	+0.02	0.34	+0.03	0.33	+0.02	0.34	+0.03
	14-10-2014 [a]	0.30	0.26	-0.04	*0.28*	-0.02	0.26	-0.04	0.28	-0.02	0.26	-0.04	0.28	-0.02
Salinity [g/l]	15-06-2008	155 [b]	188	+33	*155*	0	116	-39	101	-54	75.8	-79	69.7	-85
	15-11-2008	140 [b]	183	+43	*152*	+12	112	-28	98.2	-42	74.9	-65	69.3	-71
	15-01-2009	129 [b]	176	+47	*145*	+16	105	-24	91.5	-37	69.7	-59	64.3	-65
	30-10-2012	77 [c]	90.8	+14	*76.6*	0	49	-28	45.1	-32	24.8	-52	25.1	-52
SSD [m^2]	-	-	1.31		*0.619*		1.31		0.619		1.16		0.635	

[a] Due to incomplete precipitation data for F.A. in 2014, water levels are not correctly modeled for this date. [b] Historical data from Buitrago *et al.* (2010). Exact measurement date and locations are unknown. [c] Historical data from de Zwart *et al.* (2012).

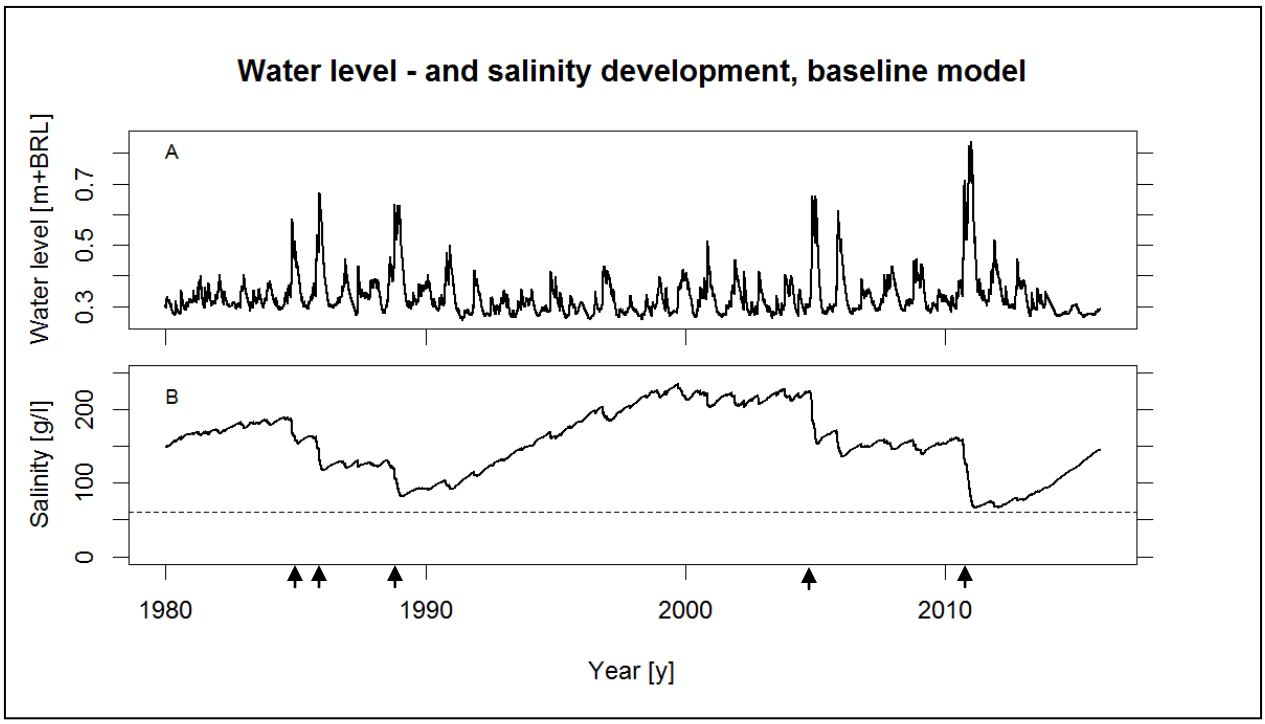

Figure 6.2: Water level (panel A) and salinity (B) development for the baseline model. The dotted line in panel B is plotted at 60 g/l and indicates where the probability of (large) brine shrimp survival was 50% after five days (figure 4.10). Note that the last period (2014 onwards) was not modeled correctly due to the absence of precipitation in the meteorological data. The 15% wettest years are indicated by arrows on the x-axis.

Water levels and salinity as modeled for 1980 to 2015 for the baseline model are given in figure 6.2. Water levels had a rather constant minimum level during the dry seasons (0.28 m +BRL) and showed elevated levels (mostly around 10 cm higher) during wet seasons, which fits the description of Lac Goto given in chapter 2 well. Peaks in water levels in the 15% wettest years (indicated with arrows) were higher than in other years. In these years salt concentrations decreased substantially. During other years salt concentrations increased up to a maximum (steady state), which seemed to depend on the multi-year average precipitation. In the period with highest modeled salinity (220 g/l, 1997-2004), yearly precipitation sums were between 200 and 300 mm (appendix VI). In the period between 2005 and 2010, salt concentrations were stable at a concentration of 150 g/l, with a yearly averaged precipitation sum of 400 mm.

The highest modeled water level (0.8 m+BRL) over the period of 1980 – 2015 occurred in the wet season of 2010. Despite this high level, water levels returned to normal heights within the subsequent dry season. The foraging area for flamingos could therefore only have been affected for a few months. The lowest modeled salt concentrations occurred after the wet season of 2010 as well. Concentrations were close to a value of 60 g/l, where the probability of survival of (large) brine shrimp growth was 50% after

five days (figure 4.10). Fish were observed at salt concentrations below 75 g/l; salinity dropped below this value early 2011 and recovered to higher values at the end of the dry season of 2012.

Yearly averages of the water balance and its components calculated with the baseline model are shown in table 6.3, for all years combined as well as for the 15% wettest years and the remaining 85% of the years. Fluxes for each year separately are given in figure V.3, appendix V. In- and outgoing water fluxes were on average equal in magnitude during a hydrological year, indicating that the water balance was closed and that indeed conditions were similar at the end of most hydrological years; only for wet years, inflow was higher than outflow indicating that lake levels were not at a normal level at the end of the hydrological year. In normal years, the majority of inflow originated from the sea (72%), whereas most outflow occurred due to evaporation (90%). In the 15% wettest years, sea water inflow was substantially lower, both relatively and absolute (-37% and -1.0 x 10^6 m^3 y^{-1}). This damped the effects of increased fresh water inflow from direct precipitation, surface runoff and groundwater flow on the total yearly inflow. Evaporation was still the main outflow mechanism for these wet years (64%), but outflow of water to the sea had an important contribution as well (36%). Note that the absolute size of the evaporation term hardly changed (even for these wet years), due to the relatively constant meteorological conditions, a constant activity of water and the fact that solar radiation was calculated. As a result of the reduced inflow and increased outflow of water through the dam in wet years, the total salt inflow was 30% lower and the total salt outflow was even four times larger than in the normal years.

Table 6.3: Average yearly contribution to in- or outflow of water for all fluxes (in m^3 y^{-1}) and the total in- and outflow of water (in m^3 y^{-1}) or salts (in kg y^{-1}) as calculated with the baseline model. Wet years were those hydrological years for which measured precipitation was in the top 15% of all years (1984, 1985, 1988, 2004 and 2010). Normal years were all other hydrological years. Flux sizes are indicated by average ± one standard deviation. The percentage is given as percentage of total yearly in- or outflow.

Component	Average all years		Wet years		Normal years	
	x 10^{6} [a]	%	x 10^{6} m^3	%	x 10^{6} [a]	%
Precipitation	0.822 ± 0.576	17.1	1.904 ± 0.674	30.3	0.642 ± 0.301	14.9
Seawater inflow	2.864 ± 0.483	66.8	2.047 ± 0.439	35.5	3.000 ± 0.336	72.0
Surface runoff	0.047 ± 0.189	0.65	0.324 ± 0.437	4.40	0.001 ± 0.008	0.0
Groundwater flow	0.753 ± 0.585	15.5	1.878 ± 0.719	29.8	0.566 ± 0.275	13.1
Total yearly inflow	4.487 ± 0.893	100	6.153 ± 1.403	100	4.209 ± 0.324	100
Evaporation	3.773 ± 0.183	86.1	3.769 ± 0.194	63.6	3.774 ± 0.185	89.8
Outflow to sea	0.714 ± 0.846	13.9	2.346 ± 1.300	36.4	0.442 ± 0.264	10.2
Total yearly outflow	4.487 ± 0.868	100	6.116 ± 1.348	100	4.216 ± 0.316	100
Total salt inflow	100.2 ± 16.9	100	71.6 ± 15.4	100	105.0 ± 11.8	100
Total salt outflow	103.9 ± 93.5	100	294.7 ± 101.8	100	72.1 ± 38.7	100

[a] *unit is m^3y^{-1} for water flux (upper 8 rows) and kg y^{-1} for salt flux (lower 2 rows).*

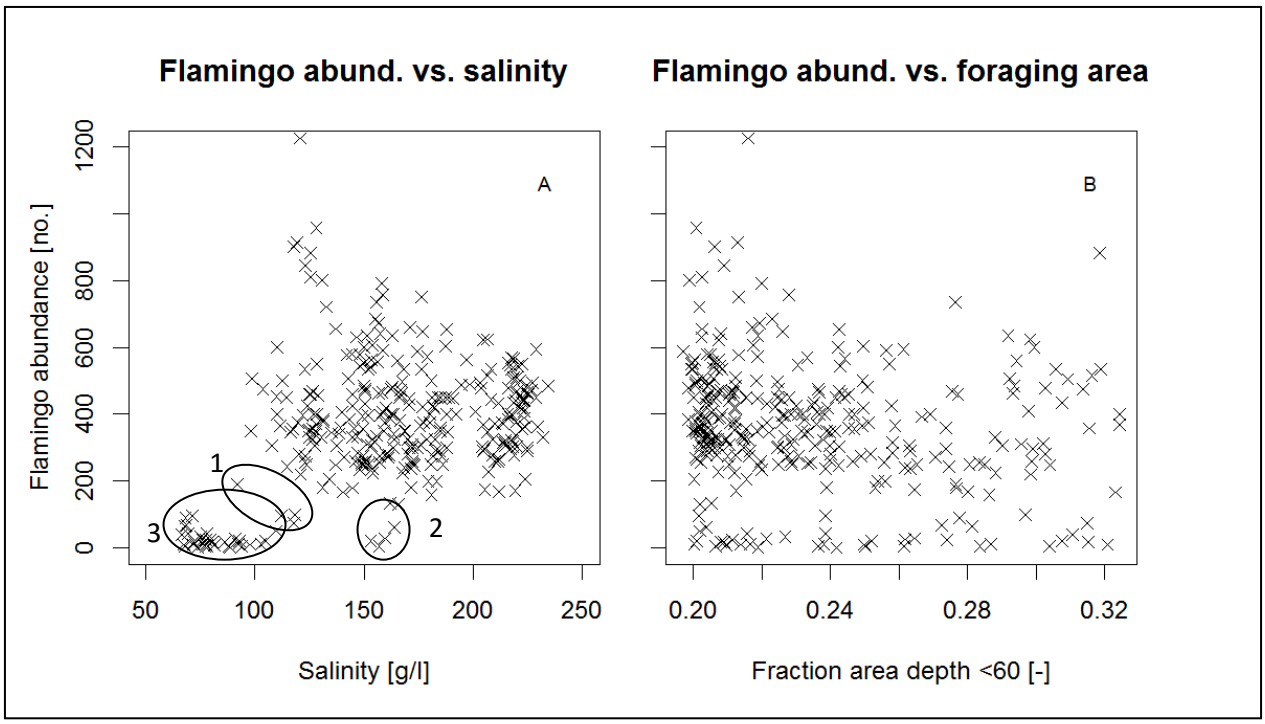

Figure 6.3: Flamingo abundance plotted against salinity (panel A) and the fraction of area with depths less than 60 cm (defined as foraging area) (B) using flamingo observations from 1981 to 2015. The numbered ovals indicate in which wet season the encircled points were measured, with 1: 1985, 2: 2004 and 3: 2010.

Based on the average yearly inflow of 4.487 x 10^6 m^3 y^{-1} (table 6.3), the average residence time of water in Lac Goto over the modeling period was 1.0 year. The residence time based on outflow of water to the sea only (with on average 0.714 x 10^6 m^3 y^{-1}) was nearly 15 years. Note that the latter figure is most relevant for dilution of PFOS (chapter 2).

The observed flamingo abundance versus modeled salt concentrations (at the same dates as flamingo observations) is shown in figure 6.3 A. Flamingo abundance was lowest during the period for which lowest salt concentrations were modeled, in 2010 (encircled with number 3 in figure 6.3 A). Flamingo abundance was also low in 1985 and 2004 (encircled with numbers 1 and 2, respectively). Note that these occurrences of low abundance can be found in figure 1.3. In 2004, modeled salt concentrations were much higher than in 1985 and 2010, but salinity did show a sharp decrease prior to the absence of flamingos (from 220 to 160 g/l, figure 6.2). No flamingo observations were available for 1989, for which modeled salt concentrations were low as well (figure 1.3 and figure 6.2). There was no linear correlation between flamingo abundance and salinity. However, a threshold seemed to be present at a salinity of approximately 90 g/l below which no flamingos foraged in Lac Goto. This threshold would however not explain the reduction in flamingos as observed in the rainy season of 2004.

The observed flamingo abundance versus modeled foraging area (at the same dates as flamingo observations) are shown in figure 6.3 B. There appeared to be no correlation between these factors. The fraction of area for which observed amounts of flamingos were small ranged between 0.2 and 0.32, which was similar as the total range over which the foraging area varied. This supports the observation that lake level returned to normal values within one year after a wet season.

6.2 Sensitivity analysis

The deviation from the baseline model for (some of the) models with adjusted parameters is shown in figure 6.4. Some statistics and the other models are shown in appendix V. Only two parameters could alter water levels during dry periods, being the conductance of the dam (c) and the evaporation correction factor (E_{cor}). An increase in dam conductance resulted in a damping of lake level fluctuations. During wet periods, a higher dam conductance resulted in lower lake levels (well visible in the rainy season of 2010, with a decrease of 12 cm as compared to baseline), whereas in dry periods a higher lake level was maintained (3.5 cm higher). The evaporation correction factor had an even larger influence on the lake level in the dry period, as it was the major component of outflow from Lac Goto (table 6.3). The yellow line (E_{cor} -50%) showed that, if evaporation rates as measured in the field study would have been adopted as true values, modeled water levels would have been 6 cm higher (throughout the year). If one was to compensate this water level (using the dam conductance, as this is the only other factor influencing lake levels in the dry season), the dam conductance would need to be multiplied by 2.5, which would have resulted in salinities below 100 g/l for the total modeling period.

The precipitation correction factor (P_{cor}) was the main factor influencing lake levels in the wet season, with deviations between the baseline model and this model of at most 50 cm (in 2010). This influence was mainly visible in the wet years (indicated with arrows) and was already discussed in section 6.1.1. The terrestrial evapotranspiration correction factor ($ET_{ter,cor}$) also influenced lake levels in the wet season. At times of a large groundwater flux (mainly in the wet years), the increase in this factor resulted in a decrease in modeled water levels (-16 cm in 2010, even larger than for a higher dam conductance), due to a lower availability of water for groundwater flow. Finally a larger terrestrial reservoir coefficient (α) and a larger maximum size of the terrestrial reservoir (TR_{max}, shown in figure V.4, appendix V) resulted in slightly higher water levels (+5 and +4 cm in 2010, but most of the time small), due to a decrease in evapotranspiration (for TR_{max}) and (therefore) an increased groundwater flow (for both TR_{max} and α). The bathymetric relations and runoff fraction (β) hardly influenced water level estimates (table V.1).

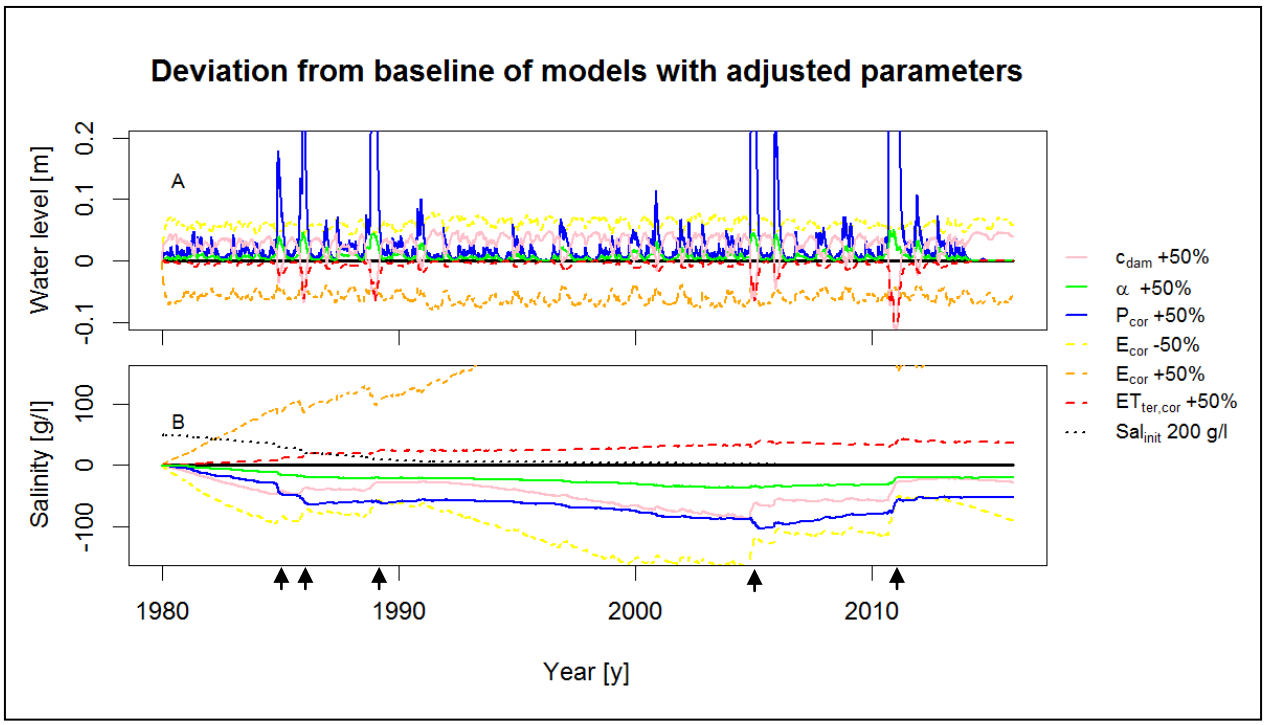

Figure 6.4: Deviation in water level (panel A) and salinity (B) from baseline model for model runs with adapted parameters. Parameter values were increased by 50% (except E_{cor} -50% and Sal_{init}). Some parameters (bathymetric relations, *β*, TR_{max}, C_{gw} and *SPr*) were omitted from this figure as their influence on results was small. For the effect of all parameters, see figure X, appendix X. The 15% wettest years are indicated by arrows on the x-axis.

The evaporation correction factor had a large influence on salt concentrations as well. A lower evaporation factor (50% lower) resulted in less saline conditions (approximately 75% lower, for years between 2000 and 2010, table V.1, appendix V), as a result of a combination of two factors. Firstly, there was less inflow and more outflow of water (and thus salts) through the dam due to the higher lake level. Secondly, as the process of evaporation leaves salts behind in the lake, a lower rate of evaporation resulted in less condensation of salts in the lake. The opposite was found for an increased evaporation correction factor (50% higher), where salinity increased by more than 200% (table V.1, appendix V).

The dam conductance influenced salt concentrations as well, but its effect was non-linear: a conductance of zero would result in a fresh water body as the lake would be driven by terrestrial processes only, without inflow of salt. A somewhat higher conductance would result in a highly saline lake, as salts would be transported into the lake but would be left behind. An even higher conductance would result in salinities similar as found in the sea, as a result of the combination of a large transport of salts into and out of the lake. For the baseline value of dam conductance, an increase by 50% resulted in a lowering of salinity by 30% due to the larger outflow of water and salts through the dam.

The other factor with a large influence on the salt balance was the precipitation correction factor (P_{cor}) (lowering of salt concentrations by 50%), resulting from both more fresh water inflow and more outflow of salts through the dam. A larger terrestrial evapotranspiration correction factor ($ET_{ter,cor}$) resulted in higher salt concentrations (+25 g/l). The increase in reservoir coefficient (α) resulted in a decrease in salinity of 25 g/l due to the increased groundwater flow. A similar value was found for the increase in the maximum size of the terrestrial reservoir (TR_{max}). The change in surface runoff fraction (β) only had a minor effect, due to the small size of this factor and the minor contribution of surface runoff to the total inflow (table 6.3). Finally, the bathymetric relations hardly influenced salinity either. Changes in salinity were a bit more damped with a larger volume, as observed when comparing salinity in 2001 and salinity in 2010 to the baseline model; salinity was a few grams lower in 2001 and a few grams higher in 2010, but differences were small.

Three model runs were performed for which only changes in salt concentrations of fluxes or initial conditions were made, which did therefore not influence the water level development. The effect of the initial salt concentration quickly diminished after a wet year (1984 and 1985). The exclusion of salt precipitation raised salt concentrations with 15 g/l and the inclusion of salt in the groundwater flux resulted in an increase of salinity of a similar magnitude (figure V.4).

7. Discussion

This section starts with a discussion on the chosen methodology and results of the field survey, with most attention to factors which were found to have a large influence on the modeled results in chapter 6. Thereafter, a discussion of the model setup and assumptions and results is given.

7.1 Methodology and results of field survey

Bathymetric relations

Bathymetric relations have been determined. The bathymetric relations showed that the foraging area for flamingos (lake area with a depth of less than 60 cm) was only significantly reduced during extremely high or – low water levels (above 0.7 meters +BRL or below 0 meters +BRL, respectively). The measurement uncertainty of 10% of the depth which was estimated did not have a large influence on the derived bathymetric relations (figure 4.2) or on the modeled water balance (table V.1, appendix V). These relations can therefore be used in future research, although a correction in height might be required due to the unknown reference height.

Precipitation

In general, uncertainty in rainfall estimates originates from (small scale) spatial variation in precipitation, which complicates the computation of (for the present study: lake and catchment) average precipitation from averages of rain gauges (Krajewski *et al.*, 2003). Interpolation by use of radar imagery (calibrated with manual measurements) can improve estimates (e.g. Krajewski *et al.*, 2003 and Pedersen *et al.*, 2010), but this data was not available in this research. Additional uncertainty arises from rain gauges themselves. Underestimation of precipitation (undercatch) by rain gauges is a known problem (e.g. Krajewski *et al.*, 2003 and Mekonnen *et al.*, 2015) and is enlarged when obstacles are present, when evaporation from rain gauges takes place and when high wind speeds occur (e.g. Duchon and Essenberg, 2001, and Mekonnen *et al.*, 2015). The latter effect is present when the rim of a rain gauge is somewhat elevated above the soil surface. For instance, Mekonnen *et al.* (2015) report 46% undercatch (on average, for a period of nearly a year) for a gauge with its rim 5 cm above the soil surface as compared to a gauge with its rim at the soil surface.

Proper rainfall estimates were important in the water balance model, as shown by the dependence of the model results on the precipitation correction factor. The field survey indicated that variability in precipitation was present; some rain gauges received more precipitation than other gauges during most

of the precipitation events (table III.1, appendix III). This could have been a coincidence, a trend due to orography triggering formation of precipitation (e.g. Yang and Chen, 2008), or it could have been caused by (systematic and random) measurement errors (e.g. Mekonnen *et al.*, 2015). Confirmation on what the most dominant cause was in the present study might only be given after longer precipitation measurements (a few years).

In the present study, the accuracy of the rain gauges was unknown. However, a difference in measured precipitation of 3 mm between PR2 and the evaporation pan, located approximately 15 m apart, was observed on the 28th of November (6.6 vs. 9.6 mm, table 4.1), indicating that accuracy of the rain gauges (or the pressure sensor in the evaporation pan) might have been low. Undercatch due to high wind speeds in combination with the gauges' rim above the soil surface could have played a role, especially for this rain gauge (PR2), as the winds at this rain gauge had a long fetch over the lake without obstructions reducing wind speed (see also appendix I). For the other rain gauges (PR1, PR3 and PR4), a reduction in measured precipitation could have occurred as well, caused by obstacles in the vicinity of the gauges. Despite careful selection of measurement locations, some obstacles were present, as large open areas were not available (or easily accessible) within the catchment of Lac Goto. The aspect of evaporation of water from the rain gauges was not expected to be a large source of uncertainty, as this was limited in the setup of the rain gauges. The influence of these uncertainties on other aspects of the field survey was present for the determination of all parameters except evaporation, as it was of influence on the water balance used for estimating the dam conductance and reservoir coefficient.

Evaporation

Measurements of evaporation have shown there was a regular pattern of evaporation over the day, with the strongest evaporation not occurring with the sun at its highest position, but in the afternoon. An explanation was found in the stability of air. This factor is of importance for lake evaporation, as illustrated by e.g. Verburg and Antenucci (2010) for a tropical lake and by Granger and Hedstrom (2011) for a temperate lake. In general, air masses over water are unstable when lake temperatures exceed air temperatures, which is even enhanced when the air is relatively dry (Verburg and Antenucci, 2010), as is the case for Bonaire. In the present study, air temperatures exceeded lake temperatures in the morning, resulting in a stable layer of air over the lake and little evaporation. During the afternoon and into the evening, water temperatures were higher than air temperatures (figure III.2), resulting in unstable conditions over the lake and higher evaporation rates. The good correlation found between measured evaporation and the contrast in water – and air temperature (figure III.3) supports this hypothesis.

In the present study, evaporation and solar radiation on a five-minute timescale did not correlate well. An earlier study by Granger and Hedstrom (2011) showed similar results on an hourly scale, for three lakes in a temperate region. They attribute this to the absorbance and release of heat by the lake. They also found that correlation between evaporation and net radiation on a daily scale is better for a shallow lake (3 – 4 meters in depth) than for a deep lake (20 meters in depth). The present study found relatively good correlations between solar radiation and evaporation on a daily timescale as well, which is therefore in accordance with Granger and Hestrom (2011). However, in contrast to the present research, they found wind speed to be even more important on an hourly timescale than the contrast between water – and air temperature. This difference might be related to how correlation was established in the present study, as it was computed on a five minute scale, with data collected at a weather station a few kilometers away of the lake instead of in its proximity. Therefore, correlations between wind speed and evaporation might have been present over Lac Goto as well. Another remarkable difference between the study by Granger and Hedstrom (2011) and the present study was the good correlation found for absolute water temperature and evaporation. This correlation was not mentioned by Granger and Hedstrom (2011), which might be related to a difference in climate. In the present study, absolute water – and air temperatures were similar for most days and maxima in water temperature always occurred when evaporation was highest. This was in contrast with the study by Granger and Hedstrom (2011), as their study was performed in a temperate region with larger temperature differences over the year.

The correlation found in the present study between evaporation and the difference in air – and water temperature might be used in future water balance studies in the catchment of Lac Goto, as it is more efficient (less maintenance) to set up only an air – and water temperature sensor (of which the latter is likely already contained in a diver which would be necessary in such a study as well) than an evaporation pan. It should be noted that this correlation will depend on the time of year, salinity and wind speed. Therefore, a longer calibration period should be considered, spanning at least a part of both the wet – and dry season. Furthermore, the magnitude of daily evaporation should be determined with more precision, as illustrated below.

As there are no reports of evaporation from a shallow, saline lake in a semi-arid environment with constant high temperatures and relatively high wind speeds, no direct comparisons could be made between literature and the present study regarding cumulative evaporation over the day. However, studies for which several of these factors were similar mainly showed evaporation rates between 4 and 7

mm/d: Vallet-Coulomb *et al.* (2001) estimate evaporation from a shallow lake in Ethiopia to be on average 5 mm/d based on 20 years of lake level measurements and the chloride balance. Two studies (Tanny *et al.*, 2008 and Tanny *et al.*, 2011) measured and calculated evaporation rates from a fresh reservoir lake in a comparable climate (Israel, during the summer). They found an average evaporation of 5 to 7 mm/d. Alazard *et al.* (2015) estimated evaporation rates from a shallow, fresh reservoir lake in Tunisia to be between 4 and 5 mm/d, depending on the calculation method and year. Vardavas and Fountoulakis (1996) found that for a small shallow reservoir in a tropical semi-arid climate evaporation was on average 5 mm/d. Finally, Oroud (1995) used several methods to determine evaporation rates from shallow, highly saline ponds near the Dead Sea. He found evaporation rates of 10 mm/d for a fresh lake, but rates of 6 and 4 mm/d for ponds with salt concentrations of 260 and 340 g/l, respectively, for the month of June (for which temperatures are comparable with Lac Goto).

Comparison of these figures to the measurements of evaporation in the present study (2.61 mm/d on average) suggests that measurements in the present study might have been at least a factor two too low. This was already assumed based on calculations using the equations proposed by Calder and Neal (1984) (which also takes salinity into account, appendix II) and results presented in figure 4.6. Therefore, daily evaporation sums as used in the present study were in accordance with literature rather than with observations. The importance of a good estimate of evaporation for the water balance of Lac Goto was shown by the sensitivity analysis of the model (chapter 6). In order to improve estimates in a follow up study, several causes for this discrepancy between the calculations and measurements have been identified, related to (a combination of) errors in the measurement setup, the meteorological input or the calculation procedure. Given the presented literature, it was expected that largest errors originated from the first factor, as calculated evaporation did not deviate much from literature. Possible causes, which should be considered in future water balance studies, are given in the paragraphs below.

Regarding the measurement setup, four factors have been identified. Firstly, spatters of water originating from the lake could have entered the evaporation pan, thereby decreasing cumulative evaporation. This was observed at the start of the field study and for that reason, the wooden dam (figure 3.1 A) was constructed. However, after construction occasional spatters of lake water were still observed. Assuming that evaporation must have been twice as high as measured and that this mechanism was the only mechanism influencing measurements, 2.61 mm of water must have entered each day to account for the difference. This equals 0.87 l/d (2.61×10^{-2} dm times the area, pi x $(6.5 / 2)^2$

dm^2). This requires one drop of 4 mm in diameter to enter the pan every 3.3 seconds, or one drop of 1 cm in diameter to enter the pan every minute. This was not observed to happen in this frequency during the field survey.

Secondly, a reduction in wind speed and a decrease in surface roughness (less waves) over the pan could have had an effect as well, especially considering the presence of the yellow casket on the side of the pan (figure 3.1 B). Calculated daily evaporation over the whole period for which data is available from Flamingo Airport (1980-2015) however suggests that 75% of the evaporation originates from the radiation term and only 25% of the evaporation originates from the aerodynamic term. This means that, if one would assume that the aerodynamic term was completely suppressed, the evaporation rate could have been maximally 33% higher, resulting in a daily evaporation of 3.47 mm. This is still 1.5 mm/d below the expected (based on mentioned literature) minimum evaporation.

Thirdly, the conditions inside the pan could have played a role, in two ways. An increase in salinity inside the pan could have reduced evaporation from the pan, by lowering the saturation vapor pressure deficit over the pan, allowing for less moisture to evaporate (Salhotra *et al.*, 1985 and Oroud, 1995). Measured salinity inside the evaporation pan showed a somewhat elevated salinity inside the pan (up to 124 g/l, compared to 109 g/l in the lake), which could have reduced evaporation during a part of the measurement series; decreasing the activity of water from 0.9 to 0.89 (which is an estimate; the actual change of this coefficient given the change in salinity is unknown) yields a decrease of only 0.1 mm in calculated daily evaporation over the whole period for which data is available from Flamingo Airport (1980-2015). Apart from the increased salinity, the temperature regime in the pan was different from the lake as well. Observations of water temperature (figure III.2) indicated that temperatures could deviate (at most) 1°C from the lake temperature (with the pan mostly attaining more extreme values). This increase in temperature could both be attributed to a lower albedo of the pan (which was black in color), which increases net radiation (e.g. Allen *et al.*, 1998), as well as to the higher salt concentration, which lowers the volumetric heat capacity of water (Oroud, 1995). This could either imply an increased evaporation rate as water temperatures in the pan can exceed air temperatures more often and more strongly, or could according to Oroud (1995) also reduce evaporation due to a combination of a decrease in net radiation (more outgoing long wave radiation due to higher temperatures) and a reduced saturation vapor pressure deficit.

Finally, the measurement location could have influenced cumulative evaporation. The pan was situated on the western side of the lake, with a fetch length of approximately 1 km over the lake. The vapor pressure deficit of air over the lake will have been largest on the eastern edge, as air flows from the adjacent land surface. Air traveling towards the western side of the lake, takes up evaporating water, which reduces the vapor pressure deficit, and attains the temperature of the lake, decreasing temperature contrasts which were identified to be important for evaporation. This would therefore result in a lower evaporation on the western side as compared to the eastern side; average lake evaporation would therefore be higher than measured (Weisman and Brutsaert, 1973, McJannet *et al.*, 2012). On the other hand, wind speeds on the western side will have been higher than on the eastern side due to the absence of obstructions, resulting in an increased evaporation rate on the western side due to a lower aerodynamic resistance (Granger and Hedstrom, 2011). The net effect remains uncertain.

Apart from measurement uncertainty, there were uncertain aspects in the calculation of evaporation as well. These have to do with the calculation procedure, as well as with the quality of input data. With regards to this first factor, differences between air – and water temperature have been found to be of importance for evaporation due to stability of the air. However, this factor is not taken into account in the equations proposed by Calder and Neal (1984). Furthermore, heat storage in the lake was not included in the present study (although originally present in the equations of Calder and Neal (1984)). Given the relatively constant daily average temperatures over a year and little in- and outflow of water (and therefore heat) compared to the lake volume, this factor was not expected to be of importance on a daily timescale, but this factor was certainly of importance on a smaller timescale (e.g. Granger and Hedstrom, 2011). With regards to the quality of input data, the Flamingo Airport dataset did not contain measurements of direct radiation. In the calculation procedure of radiation, several non-calibrated constants were used, including sunshine duration (fixed at 8 hours), activity of water (fixed at 0.9) and albedo (fixed at 0.05), as described in appendix II. Additionally, the resolution of e.g. temperature data of Flamingo Airport was coarse (1°C) for a part of the historical period, influencing estimated evaporation rates as well. Furthermore, the distance between weather stations and the lake might be important, as temperature and wind speed could deviate between the locations. Finally, weather station Republiek reported relatively low wind speeds, which indicated that this station might have been located in a less-open environment. This could have influenced other measurements (e.g. temperature), and therefore calculated evaporation, as well.

Water levels

Seawater level measurements have shown that the data set from Flater (2015) represented reality well (figure III.1), although it should be remarked that it remains unclear whether the reference height used here is the same as the Bonairian Reference Level, as, despite several attempts, no measurements of absolute height were available. The absence of this reference also influenced the estimates of the dam conductance and terrestrial reservoir coefficient, as these used water levels with respect to Bonairian Reference Level. This problem was also present in the water levels used for validation.

Measurements of the water level in Lac Goto revealed that fluctuations in this level were surprisingly small. Daily fluctuations were not observed visually either. This was in contrast to a previously conducted baseline study for Lac Goto and other saliñas in the northwestern part of Bonaire (Buitrago *et al.*, 2010); they estimated water level variations for most saliñas to be between 3 and 5 cm a day. The observations given in the present study suggest this large variation was not present in Lac Goto; the change measured by Buitrago *et al.* (2010) can most likely be attributed to changes in air pressure. Air pressure showed a distinct daily pattern with two peaks in pressure occurring every day at the same time (11 AM and 11 PM, figure III.2). The pressure during such a peak was generally between 3 and 5 hPa higher than pressures in between peaks. These peaks occurred approximately four hours after high seawater levels reported by Buitrago *et al.* (2010), similar as the time lag between high sea levels and high lake levels mentioned by Buitrago *et al.* (2010). As the estimate of water level variation by Buitrago *et al.* (2010) was used to determine which resolution would be sufficient for the divers recording water levels, the present study used divers with a coarse resolution for the water level variations occurring.

Surface runoff

No proper estimate of surface runoff as a function of precipitation intensity or sum could be made in the present field study, due to a lack of high-intensity precipitation events. Estimations made for rain events for which very local and very minor surface runoff was observed, seemed to be too large. Three possible causes were identified for this too high estimate. The first two causes originated from precipitation measurements; both the (possible) underestimation of precipitation discussed previously as well as the assumption that precipitation falling on the lake can be approximated by the average of PR2, PR3 and PR4 might have resulted in an underestimation of the actual precipitation falling on the lake. If the actual amount of precipitation on the lake would have been higher, the calculated surface runoff amounts for the events in table 4.1 would have been lower. A third cause was found in the diver resolution. There was a relatively large uncertainty in actual water level, as indicated by fluctuations between individual

measurements in figure 4.5. The water level increase, as estimated by calculating the water level eight hours after the precipitation event minus the water level eight hours prior to the event, was therefore subject to the time of reading. If the criteria to read the water level difference were chosen differently, the estimated water level increase could have changed by several millimeters.

In the case of a larger (several tens of millimeters) precipitation event, the relative importance of these sources of uncertainty would be smaller, as the absolute uncertainty in the timing of reading the water level recordings would not change. Underestimation of precipitation due to wind effects would increase at higher rainfall intensity, but equations proposed by Mekonnen *et al.* (2015) to account for this effect indicated that this would be a fraction of the total precipitation; therefore its relative importance would decrease as well. The method to calculate the effect of surface runoff as used in this study was therefore expected to yield better results when applied in precipitation events with larger rainfall sums.

Another possibility to measure surface runoff in future water balance studies in the catchment of Lac Goto would be to use the methodology as proposed by Hobbelt (2014). She divided a catchment in Bonaire into several sub-catchments and subsequently measured surface runoff flowing out of these catchments through gullies. These gullies are similar, but less well defined in the landscape compared to gullies in the catchment of Lac Goto, due to the less pronounced topography in that area. Therefore, it is expected that this method will yield even better results for the catchment of Lac Goto.

Tidal – and groundwater flow

Several approaches were used to determine the exchange of water through the dam in combination with groundwater interaction (using cross correlations (1), daily averaged water level development (2) and a water balance model (3)). The sensitivity analysis of the model study (chapter 6) showed that this factor was of importance in determining both the modeled water level and salt concentrations. Cross correlations (method 1) were in general very low (table III.2). The second method (results shown in figure 4.6) revealed why this was the case; despite a distinct average daily water level development, day to day variability in measured water levels was large, so that the average daily water level development was not significantly different from zero. This large variability could have originated from (a combination of) three aspects. The first aspect was measurement uncertainty, caused by the aforementioned diver inaccuracy as well as by the evaporation measurements. The second source of variability was the composition of the residual time series (after taking into account evaporation and precipitation), as this was a resultant of both tidal – and groundwater interaction. The relative contribution to the water level

development was not constant in time, due to changing differences in sea – and lake level and input of rain at certain times. Finally, day to day variations were present as a consequence of slightly different timings of low and high tide, wind effects (as clearly visible on the 2nd of December) and the possible presence of a non-linear relation between inflow through the dam and water level as a result of a changing dam conductance with water height (Rooth, 1965). It should be noted that the average water level development as shown in figure 4.6 was not caused by density variations due to changes in water temperature and salinity, as the influence of these variations on density was very small (max 0.2 mm) or atmospheric pressure fluctuations, as these were accounted for.

The third approach used a set of water balance equations which did not take the effect of an increase in surface area at higher water levels into account. The effect of this simplification was only minor given the small fluctuations in water levels in Lac Goto. The difference between the highest – and lowest recorded water level was approximately 5 cm, which would yield an increase in lake surface area of less than 5%. Correspondingly, the difference in added volume for an increase of 1 cm at low levels and an increase of 1 cm at high levels would also be less than 5%. Given the aforementioned uncertainty in e.g. evaporation, precipitation and water level measurements, this factor was relatively unimportant. Note that, if much larger water level deviations were measured during the field survey, it would have been necessary to incorporate this factor.

In the third approach, only two models were able to produce a positive value for the Nash-Sutcliffe efficiency, indicating that the other models were not good at predicting water level development (table 4.2). However, these two 'good' models (using parameters for GotoFresh with groundwater flow) performed poor over the total modeling period (1980 – 2015, figure 6.1 and table 6.1). The poor performance during the field survey (in terms of NS efficiency) of the other models (including the baseline model) was mainly caused by the last few days of the fitted dataset (figures 4.7, III.5 and III.6), for which reported evaporation was very low. If these days were omitted, values for NS efficiency were positive for most of these models. Furthermore, the low fluctuation in water levels made sure that the average of the observations was always close to the observations. Schaefli and Gupta (2007) also mention that this is an important aspect in the NS efficiency. If higher peaks in water level would have been present (and represented well by the model), the NS efficiency would automatically have been much higher. A longer measurement period with inclusion of a wetter period would therefore likely have resulted in positive NS efficiencies (when these peaks would have been modeled correctly).

Water level development as calculated with the n-layer dam model was similar as the development calculated with the 1-layer dam model for both divers, as was shown in figure 4.7. Also this could be explained by the low variation in water levels during the measurement period. If a high-intensity precipitation event, resulting in higher water levels in Lac Goto, would have occurred during the measurement period, it would have been easier to determine whether the permeability of the dam was higher for the upper parts of the dam due to an increase in relative contribution of flow through the upper parts of the dam to the total flow through the dam at high water levels. This effect was observed in modeled water levels in 2010, where water levels returned to normal faster for the n-layer models (figure 6.1). Given the limited range over which water levels varied, the n-layer model could not be adopted nor excluded as a (better) alternative for the 1-layer dam model. Therefore, a longer measurement period including some large precipitation events would be required to confirm the hypothesis of Rooth (1965) that dam permeability increases with height.

Such a high-intensity shower would have improved the possibility to distinguish between groundwater – and tidal flow, and therefore between reservoir coefficient and dam conductance, as well, (probably) resulting in a smaller region with well-performing parameters (figure 4.8). It is expected that during such an event terrestrial influence would become the dominant component of the water balance of Lac Goto. During a subsequent dry period, a gradual transition towards tidal influence as the most dominant factor was expected, as groundwater flow would diminish and lake water levels would return to normal. The presence of this band of equally well performing parameters in figure 4.8 showed a nearly vertical dependence at higher terrestrial reservoir coefficients, indicating that the model was insensitive for this parameter, so that the inclusion of high intensity showers would help in identifying this parameter.

The distinctly different values for the groundwater reservoir coefficient found for the two divers might be related to the different measurement period; GotoSalt1 included a relatively dry period in which water levels in Lac Goto declined steadily which was not included in the measurements of GotoFresh (which relates to the previous paragraph). Furthermore, differences could have originated from differences in precision and accuracy of the divers as well as from wind effects, as the divers were located on opposite sides of Lac Goto. Apart from this, figure 4.8 showed that the differences in parameters found for the best fit (table 4.2) seemed larger than they were; for GotoSalt1, values for the sum of squared differences were only slightly higher using the best fit parameter combinations for GotoFresh. The same was true for GotoFresh.

With regard to the absolute value of these parameters, it should be noted that they relied on the value of several fixed parameters, such as the evaporation coefficients, dam height and size of the terrestrial reservoir, as well as on the initial conditions. The dependence on the initial conditions could be reduced by using a longer measurement period; estimates of some of the other parameters might be improved by additional field work or calibration after the reservoir coefficient and dam conductance have been determined with more precision. However, note that the sensitivity analysis of the model (chapter 6) showed that the model was less sensitive for these parameters, so a proper estimate was less urgent. Apart from this, parameter values for the best fit were dependent on the water height of Lac Goto relative to the height of the sea during the study period. As this height could not be measured during the field study, only a simple approximation was made which increased uncertainty in parameter estimates.

In the second approach, the permeability of the dam as used in the original Darcy equations (appendix III) could be estimated from figure 4.6 when assuming that all inflow (4 mm times the area of Lac Goto, which is roughly 1.5 x 10^6 m^2) between 9 AM and 3 PM originated from flow through the dam. Using equation 5.4a, the conductance could be calculated and translated to permeability using the numbers given below. The permeable area of the dam perpendicular to the flow direction through the wall was estimated at 150 m (width) times 10 + 0.4 m (assumed depth of the dam (d_{dam}) plus the average of the lake – and sea water level during this time), with a thickness of 100 m and it was estimated that the average water level difference between Lac Goto and the sea was 0.2 m over this period. This yielded a permeability of 6,000 m/d, which is in the order of coarse gravel (Freeze and Cherry, 1979 and Turner and Masselink, 2012). This was consistent with the materials of which the dam is build up (figure 2.1 B). A similar approach was used for the values for the conductance obtained in the third approach. This yielded estimates for the permeability ranging between 2,500 and 5,000 m/d, with the lowest values using parameters as determined for GotoFresh. These estimates were lower than the estimates made in the second approach, but still in the order of coarse gravel.

Salt balance

The estimate of salt precipitation was a very rough estimate. In reality, precipitation of salts is a complicated process, depending on (amongst others) the ionic content and composition, temperature and humidity (Schreiber and Tabakh, 2000). Also the type of salt crystals formed, as well as impurities and water incorporated therein were could have affected the calculated deposition per day. Apart from this, rates were estimated using only one soil pit, which was assumed to be representative for the whole area, which was not the case in reality. This particular location is not always under water; therefore salt

precipitation cannot occur continuously. On the other hand, it is likely that more salt precipitates here than in the middle of the lake, as salinity can increase more rapidly in a shallow area (Schreiber and Tabakh, 2000).

Apart from salt precipitation, other mechanisms of salt deposition or removal might be present. Salt deposition was included in the model of Obrador *et al.* (2008). Using the same calculations he made, salt deposition over Lac Goto was expected to be smaller than salt precipitation. As the sensitivity analysis revealed that the influence of salt precipitation was relatively small, it was expected that errors introduced by not incorporating other mechanisms of salt deposition or removal were also small.

Halotolerant abundance and distribution

Abundance of brine shrimp as measured in the present study revealed densities similar in order of magnitude (when also accounting for the small brine shrimp) as found by Rooth (1965). He found similar, unexplained, density changes over time as seen in the present study. Rooth (1965) mentioned that differences between two samples taken at the same location right after each other mostly resulted in similar numbers. He noticed that only at 'very high' densities, the distribution of brine shrimp might not have been homogeneous due to clustering of brine shrimp.

The density variations in brine shrimp as observed in the present study (figures III.7 and III.8) were most likely not a consequence of the chosen measurement technique (assuming that the distribution was indeed homogeneous, as suggested by Rooth (1965). As there were five observations on the same location on each day, averages could be constructed. The numbers of brine shrimp as found for these five observations were (mostly) similar, and different between observation days (table III.3). Furthermore, there was no decreasing trend in brine shrimp per sample with sample number (table III.3), indicating that 'overfishing' did not occur. However, note that as a result of the chosen measurement technique, the estimate of whether a brine shrimp belonged to the small – or large category was sometimes not very clear, which could have had an influence on reported numbers.

Abundance of brine shrimp for the deeper areas of Lac Goto was only measured two times. These measurements were done during a period for which densities were high at the measurement locations close to shore (figure III.7). More information on densities for deeper areas during periods for which densities in the shallow areas are lower might provide insights on whether brine shrimp migrate through the lake. The fact that brine shrimp density was higher in shallow areas and that there were no small

brine shrimp found in deeper areas (close to the surface), suggests that some regions of the lake were more important for maturing brine shrimp, after which larger brine shrimp spread out over the lake. Nevertheless, also large brine shrimp seemed to prefer areas with shallow water close to the shore as their density was still larger in these locations. A possible explanation was found in food availability for brine shrimp; benthic algae were closer to the surface in shallow areas. Here they receive more light as compared to deeper locations, which could increase their growth rate and might therefore result in increased food availability for brine shrimp. However, no information was present on (the density of) algae floating in the water column in Lac Goto, which were of importance as source of food as well.

The estimated amounts of brine shrimp in the lake were based on the assumption that they live all over the lake, in the same density. It is however unknown whether they are also present (in the same densities) at depths below one meter, as no observations could be made here in the present study. Additionally, brine shrimp at these depths are not readily available for consumption by flamingos, so the actual available amounts for flamingos will have been lower than estimated. However, given the mobility of brine shrimp, this was a potential source of food for flamingos, in contrast to the less mobile brine fly larvae on sediments deeper than 60 cm. The model used to determine whether the population of brine shrimp was large enough to be sustainable incorporated a few assumptions. The most important assumption was that values regarding population dynamics as reported by Browne and Wanigasekera (2000) also apply to the population in Lac Goto. Naceur *et al.* (2013) illustrated that these dynamics differ between different populations of the same species.

Given the materials used in this study, the estimation of density of brine fly larvae was more difficult than for brine shrimp. Due to dispersion of the larvae into the water column and due to the fact that some larvae remained present in the sediments after loosening the sediments, larvae counts underestimated real amounts. This was also illustrated by the fact that in a second measurement at the same locations, additional brine fly larvae were caught. Also, no chrysalids were sampled, although they were reported to be commonly used as food source (e.g. Rooth, 1965 and Esté and Cassler, 2000). Densities could have been higher than reported and therefore it was expected that Lac Goto actually held a larger reserve of brine fly larvae than calculated. Given the substantial changes in brine fly density on the shore within a few days, brine fly were thought to reproduce fast (Rooth, 1965), but no literature is available on this matter so that no estimate could be made regarding sustainable amounts of brine fly.

Rooth (1965) suggested that density variations in halotolerants over time might be related to the availability of food (algae). Observations of flamingos in Lac Goto suggest the same. After having been absent for four years after the rainy season of 2010, flamingos returned in numbers up to 1,200 individuals. According to historical data (figure 1.3 and appendix VI), such a high peak in flamingos had not been observed in the 35 years prior to 2015. This behavior might be related to a very high food abundance for flamingos; turbid waters during that time would not pose a food limitation for brine shrimp (and brine fly larvae), allowing for a fast expansion (given the high reproduction rates presented by Browne and Wanigasekera, 2000 and Naceur *et al.*, 2013) of the number of brine shrimp. As the water became clear, flamingo abundance was reduced. This could be related to a reduction in halotolerants (and thus their density, resulting in a spread of flamingos towards other areas as observed by e.g. Baldassarre and Arengo (2000)) due to a reduced food availability for halotolerants. A similar observation can be made after the reduction in flamingos in 1985; flamingo counts reached up to 900 individuals after their absence (figure 1.3). However, it is unknown whether the lake was turbid at that time as well.

Salinity tolerance

Results of the salt tolerance experiment showed a large scatter in life duration for (mainly small) brine shrimp. Additionally, the probability of survival at salt concentrations similar as found in Lac Goto was only 20% after five days for small brine shrimp, which indicated that conditions in this experiment for brine shrimp might not have been optimal. Reasons for this might be found in how these individuals were collected, transported and put into the water sample. A more careful handling of the brine shrimp might have resulted in less mortality. Mortality could also have been caused by e.g. not supplying food or aeration to the water samples (as done by Browne and Wanigasekera, 2000), or by (harmful) substances in tap – or seawater (such as copper from water pipes). Finally, it is also possible that these survival rates were accurate. Browne and Wanigasekera (2000) reported survival rates of 51% of small brine fly after 21 days for a salinity of 120 g/l. The lower salinity in Lac Goto and the use of another population could be an explanation of the lower survival chances.

In this experiment, a distinction was made between small and large individuals. However, it was unknown whether this distinction reflected age, as individuals were taken out of Lac Goto rather than grown in a monitored environment. Other studies used a more controlled environment with a brine shrimp population with individuals hatched at the same day (e.g. Browne and Wanigasekera, 2000 and Naceur *et al.*, 2013). In these studies, food for brine shrimp was added and the salinity was kept constant by replacing evaporated water. In the present study however, environmental factors in water samples

were not monitored. Therefore, differences other than salinity were likely present between different treatments. For example, food availability will have been lower for samples with a larger portion of tap water, but algae growth could have been faster for these samples due to the lower salinity.

No definite conclusions could be drawn in this experiment regarding the exact reaction to salinity of the total population of brine shrimp and brine fly due to the low number of replicates (as compared to regular population dynamics studies as e.g. Browne and Wanigasekera, 2000) and other outlined uncertainties. Results of this experiment should therefore be used to indicate whether a reduction is likely at a given salt concentration.

7.2 Methodology and results of model study

Model assumptions

A study by Obrador *et al.* (2008), in a coastal lagoon separated from the Mediterranean sea by sluices, used similar fluxes (precipitation, runoff, seawater inflow, evaporation and lagoon water outflow) in a similar reservoir model for a case somewhat comparable with the present study. His results fitted observations well. Therefore, it was expected that all relevant sources of in- and outflow were incorporated in the water balance (equation 5.1) used in this study as well. If groundwater flow out of the lake would also have contributed to the balance, it would have implicitly been incorporated in the flow through the dam as this would also be driven by water level differences between the lake and sea.

By representing the lake with one water balance model, it was assumed that perfect mixing would take place in the lake, similar as was done in the study by Obrador *et al.* (2008). This was chosen as a representative approach as observations suggested that no variations in salinity and temperature in depth were present during the field survey period. In this respect, two remarks should be made.

Firstly, Mackenzie *et al.* (1995) mention that for hyper-saline marine lakes (such as Lac Goto), density stratification mainly occurs during the wet season rather than the dry, as a result of a layer of fresh (precipitation) water floating on top of denser salt water. They also state that this stratification breaks down in subsequent dry periods due to evaporation and wind action. Obrador *et al.* (2008) also mention this as a point for discussion in their reservoir model. Although the current field survey was held in the wet period on Bonaire, cumulative precipitation was not large (appendix III). Therefore, it is possible that the effect of stratification would be present in Lac Goto in wetter years.

Secondly, it was noticed during this study that a layer of less saline water formed over denser, more saline water in the south of the canal, presumably originating from seawater inflow through the dam. This front was even once observed (own observations) to reach the measurement location of GotoSalt1. Savenije (2006) describes a saline front entering a fresh estuary due to tidal differences. Although this is not completely comparable to the present study, the processes are similar. Savenije (2006) states that, unless mixing occurs, water entering the system at high tides will leave the system at low tides, therefore not allowing to affect salt concentrations in the estuary itself. He distinguishes three main driving forces for mixing: wind (driving horizontal and vertical circulation), a river (providing a constant flow of fresh water resulting in density differences and gravitational circulation) and tides (providing kinetic energy for mixing). Over the main area of Lac Goto, wind will be the most important factor driving mixing. However, in the canal, wind blows perpendicular to the direction of the canal, resulting in a short fetch of 150 m. Furthermore, a river was not present to interact with the inflowing seawater and tidal variations within Lac Goto were very small. This implies that mixing might be hampered in the canal in Lac Goto.

In light of this discussion, it can be argued that the effective residence times of PFOS in the lake could have been higher than calculated in this report. Due to a limited mixing of inflowing seawater and lake water, the transport of PFOS out of the lake could have been reduced. Additionally, the salinity of water flowing out of Lac Goto could have been lower than the average salinity in Lac Goto, influencing the salt balance. The effect on residence times and salinity of the outgoing flux through the dam most likely depends on flow paths of water through the dam. If outflow occurred only through the lower parts of the dam, the less saline top layer (with a large portion of seawater which just entered the lake) would have limited influence on the concentration of salts in this flux and the residence time of PFOS. If most flow occurred through the top layer of the dam (as was proposed by the n-layer dam model), the influence of a less saline top layer would be larger. Table 6.3 showed that, especially during wet years, outflow of water and salts through the dam was large. Those years were also years for which the development of a less saline top layer might be expected (Mackenzie *et al.*, 1995), therefore possibly reducing the amounts of salts flowing out of the lake as compared to what was modeled in this study. A small change in salinity of the flow out of the lake through the dam would impact the salt balance significantly, as 94% of salts in the lake was removed through this mechanism. More information would be required on the flow through the dam and the development and disappearance of the less-saline top layer as a result of both precipitation and tidal exchange to more accurately describe the significance of this process.

The dam model in the baseline run was the simplest model proposed (1-layer), as no improvement (in terms of a better fit to the observed water levels, chapter 4) was found for more complicated models. A factor which was not taken into account in the flow through the dam was the difference in density between lake – and seawater. In the present study, a simple linear reservoir was used to capture and average all processes acting on a groundwater body and the exchange with Lac Goto. Comparing formulas in this study to those from literature, Obrador *et al.* (2008) use a more sophisticated way of calculating fresh water flow from the surrounding area, introducing a canopy storage. Also Niedda and Pirastru (2013) use a more sophisticated model, introducing an interception storage, a soil moisture storage and bedrock storage, requiring digital elevation models, soil – and landuse maps and additional parameters (with values which were unknown for the case of Lac Goto). Several other factors which might be taken into account in (groundwater) flow models, as for instance the non-linearity soil water retention curves influencing evapotranspiration and soil water flow, spatial heterogeneity of the soil and vegetation, differential wetting and – drying of the soil, density driven flow at the interface between water of Lac Goto and the groundwater, preferential flow paths and differences in travel times, were not taken into account either. All these parameters were not available in this study and therefore the use of a more sophisticated model could not be justified. The use of a spatially distributed model in which the catchment is divided into several sub-catchments with their own properties might improve results, but as Savenije (2001) demonstrates, all processes become easier to represent when averaging over larger areas. Furthermore, he mentions that distributed models are not (always) the answer; a simple linear reservoir could suffice as well, as this model averages a lot of small-scale processes. Therefore, despite the large simplifications, the terrestrial reservoir was, given the lack of other data, a good option.

Note that the use of a model with several sub-catchments (with their own linear reservoirs) could be used to resolve the effect of the large spatial variability of precipitation. If orography was of influence, a different correction factor could be assigned to each sub-catchment. Additionally, the effects of (random) spatial variation in precipitation (e.g. due to showers) could be introduced by a parameter which multiplies measured precipitation rates with a random value (in a given interval) for each sub-catchment. This parameter should then be calibrated with help of radar imagery and long term precipitation measurements throughout the catchment.

It should be kept in mind that the quality of the weather input dataset was questionable. For some years, a lot of days with missing precipitation data were present (appendix VI). Furthermore the observations by Koster (2013) and reports of MDC (2015) and Bonaire (2016) indicated that reported precipitation events did not always coincide with actual precipitation events.

The initial precipitation correction factor of 1.5 was determined based on a correlation between reported precipitation on BOPEC rainfall station (only five yearly precipitation sums, from MDC, 2015) and Flamingo Airport weather station (with some missing data). In the baseline model, a correction factor of 1.0 was used instead. This choice was mainly based on the too strong salinity reduction in 2010 (section 6.1.1). It was however possible that precipitation amounts were on average 1.5 times higher at the BOPEC rainfall station, but were not 1.5 times higher during the 15% wettest years. The precipitation correction factor should then be a function of the total yearly precipitation amounts, with a lower factor for higher yearly sums. This would reduce the impact on the salinity reduction during wet years. However, data for such a function was not available.

Additionally, it should be mentioned that the activity of water in the calculations of evaporation was kept constant throughout the modeling period, while in fact this factor would have been dependent on salt concentrations. As the modeled salinity showed a large variation, this factor would have varied as well. The results of varying this factor could be large, as illustrated by Calder and Neal (1984) for the dead sea with calculated yearly evaporation sums of 1488 and 1563 mm for an activity coefficient of 0.71 and 0.75, respectively. The activity of water would have been larger (than used in the current model) for years with low salinity, increasing evaporation rates and increasing the rate of salinization of the lake. On the other hand, evaporation would have been reduced more for years with a high salinity, so that salinity would increase less rapidly in these years.

Model results

The two factors which were found to be the largest contributors to the water balance (inflow of seawater and evaporation), were also identified by Mackenzie *et al.* (1995) as the two most important terms in a hyper-saline marine lake. The large sensitivity of the model to the evaporation correction factor, as well as to the conductance of the dam, illustrated their importance as well.

Reports suggested that in 2010 significant surface runoff events took place, resulting in a closure of Washington Slagbaai National Park (Bonaire, 2016, own correspondence with park rangers). According to park rangers, surface runoff was also occurring in the park in the rainy season of 2004. Occurrences of surface runoff was modeled in these years (figure V.3), which thus corresponds to observations.

The highest salt concentrations were modeled for the period between 1993 and 2003 (220 g/l, figure 6.2). No validation was possible regarding salinity for this whole period, so it could not be confirmed that these modeled concentrations were correct. However, there were a lot of days without any record for precipitation in the dataset for this period (on average 48 days a year, appendix VI). Therefore, it is possible that salt concentrations in Lac Goto were never this high as there was more inflow of fresh water. As years in this period had low precipitation amounts (appendix VI), the use of a precipitation correction factor as function of yearly precipitation sums could have reduced modeled salt concentrations over this period as well. Additionally, the effect of a reduction in evaporation will have been larger for this period than calculated, due to the aforementioned issue related to the fixed activity of water. If (modeled) concentrations during this period would have been lower, the impact of the rainy season of 2004 on flamingo counts (figure 6.3) might potentially be attributed to low salt concentrations as well, as a similar reduction, but starting with lower salt concentrations, would result in lower concentrations after this season as well.

Based on the correlations between modeled salt concentrations and observed flamingo abundance, a threshold (at 90 g/l) seemed to be present below which flamingos did not forage in Lac Goto. Low observed flamingo abundance occurred in 1985 and 2010, in which salt concentrations were modeled to have been around this threshold. Note that this did not hold for the low observed counts in 2004, but possible explanations have been discussed in the previous paragraph. Comparing this to the results of the salt tolerance experiment (figure 4.10), it is possible that a reduction in brine shrimp due to salt stresses occurred at these concentrations. However, for reasons explained in section 7.1, uncertainty in this estimate was large. Additionally, given the discussion on a fresh water layer forming in wet seasons, conditions in the upper water layers of Lac Goto might have been less saline than in lower layers. This could have induced mortality or migration of halotolerants to locations lower in the water column, which were inaccessible for flamingos (so that food availability for flamingos was low). This would imply that the actual threshold of halotolerant reduction would have been lower than 90 g/l, but appeared to be at this value due to averaging of salt concentrations over depth in the model. The absence of correlation

between flamingo abundance and foraging area was clear. As water levels returned to regular values within each dry season, this factor can be excluded as main driving mechanism of the flamingo population. This is in contrast to findings by Vargas *et al.* (2008) on the Galapagos islands.

Given the residence time calculated based on outflow of water through the dam only (15 years), it is possible that concentrations of PFOS were diluted after five years. This could have contributed to the reestablishment of the halotolerant – and flamingo populations. However, as mechanisms of binding to organic matter or uptake by aquatic animals were not further investigated in the present study, no conclusions can be drawn regarding this matter. Also measurements of PFOS concentrations in water or sediments were not available for comparison with results from de Zwart *et al.* (2012).

8. Conclusion

With regard to the objectives, several conclusions can be drawn, which line up to a conclusion on the hypothesis whether or not the heavy precipitation events of 2010 could have caused the disappearance of flamingos from Lac Goto.

8.1 Objectives

Water balance

Fluxes acting on the water balance have been quantified in a two-month field survey. Evaporation as measured with an evaporation pan placed inside the lake were (at least) two times lower compared to calculated values and literature, but the correlation between the difference of lake – and air temperature and evaporation, as found in other studies as well, suggested that the timing of evaporation was measured correctly in this setup. There were very little changes in water level (4 cm) during the measurement period, which, together with the uncertainty in the magnitude of the evaporation term, resulted in uncertainty in parameter estimates for tidal – and groundwater flow. The water balance model which produced a best fit for water levels measured with GotoSalt1, using the 1-layer dam model, showed that flow through the dam (87%), precipitation (10%) and groundwater flow (3%) contributed to inflow and evaporation (96%) and outflow through the dam (4%) contributed to outflow of water during the field study. Surface runoff was observed only at a small scale and did not occur according to the water balance model.

The modeling study (over the period of 1980 – 2015) revealed that in a normal year (the 85% driest years), the most important fluxes acting on the water balance are inflow of water through the dam deposits (72%) and outflow of water via evaporation (90%). The influence of the 15% wettest years was remarkable, with a smaller contribution of inflow of seawater through the dam (36%) and a larger contribution of outflow of lake water through the dam (36% as compared to 10% for normal years). The water – and salt balance models were most sensitive to parameters related to these two most important water balance terms.

Residence times of water were approximately one year. Residence times based on outflow through the dam were 15 years, which is a more relevant number for dilution of PFOS.

Salt balance

Variations in space and time in salinity were minor. Using the water balance model for GotoSalt1 with the 1-layer dam model, salt concentrations increased by 2.8 g/l over the study period, which was similar as observed. For the total modeling period, salinity decreased in the 15% wettest years and increased in all other years, due to the changing contribution of in- and outflow of water and salts through the dam. Salt concentrations were modeled to have been between 60 and 240 g/l, with the lowest concentration in 2010. For the salt balance, transport of salts resulting from in- and outflow of water through the dam was most important; other mechanisms (e.g. salt precipitation) only had a minor influence.

Halotolerants

Brine fly larvae showed no reaction to differences in salinity, whereas mortality in brine shrimp was higher at lower salt concentrations; the probability of survival for large brine shrimp was 50% after five days at a salt concentration of 60 g/l, but this number should be interpreted with caution as a result of the chosen experimental setup. Predators (fish) for halotolerants were observed at salt concentrations below 75 g/l.

The current population of brine shrimp was sustainable and could provide enough food sources for flamingos, given a predation by 500 flamingos. The population of brine fly larvae as estimated during the field survey was not sufficient. However, these larvae were sampled only once, and additional data from literature was not available.

Relation between flamingo counts and water level or salinity

A correlation between observed flamingo abundance and modeled salinity showed a threshold at a salinity of 90 g/l below which hardly any flamingos foraged in the lake (based on a period with low observed flamingo counts in Lac Goto in 1985 and 2010 – 2014). The precipitation events in 2010 could have had an influence on the flamingo population, as concentrations were below this threshold in the period of 2010 to 2014. Comparison of this threshold concentration with the salt tolerance experiment showed that the probability of survival for large brine shrimp was 70% after five days for this salinity, but given the setup of this experiment this could neither exclude nor confirm a causal relation between this threshold and halotolerant abundance.

There was no correlation between observed flamingo abundance and foraging area, as lake levels always returned to normal (for a dry season) heights during a dry season.

8.2 Hypotheses

Based on modeled salt concentrations and the results of the salt tolerance experiment, it was likely that the precipitation events of 2010 were of influence on the halotolerants, and thus on (the food supply of) flamingos, but a direct (causal) relation could not be confirmed. The alternative hypothesis could not be confirmed or rejected either. The residence time of water based on outflow through the dam was 15 years. It is therefore possible that concentrations of PFOS were diluted within the five years after the fire, so that these were below toxic levels. Therefore, neither one of the hypotheses posed can be confirmed or rejected. The cause of the disappearance of flamingos from Lac Goto was therefore most likely a combination of both contamination with PFOS due to the fires at the BOPEC oil facility and the extreme precipitation amount in the rainy season of 2010.

8.3 Recommendations

In order to reduce uncertainties related to the water balance, a longer measurement period (including high-intensity precipitation events) would enable a better distinction between groundwater flow and tidal flow. Also a measurement of reference water levels would aid to this purpose. For such a measurement period, it would be useful to (at least) install one diver with a water temperature sensor and a thermometer for air temperatures and a tipping bucket rain gauge to continuously measure water level development and precipitation and to determine evaporation (using the correlation between water – and air temperature differences and evaporation) of the lake. Precipitation measurements should be combined with radar images of the weather institute of Curaçao (MDC, 2015) to account for spatial variability. Additionally, evaporation could be measured with a more accurate device (e.g. eddy covariance) for a short period of time (e.g. a week) to relate observed temperature differences between the air and lake to the actual magnitude of evaporation. Measurements of salinity should be carried out once every month at the location of the diver as an additional way of fitting the water and salt balances to observations, improving the possibility to discriminate between seawater inflow and terrestrial inflow.

To be able to confirm that indeed both hypotheses were valid, measurements of PFOS concentrations in water and sediments should be carried out and used together with an improved estimate of residence times from the extended measurement period. Furthermore, a more thorough study (using a larger number of replicates and reducing other sources of uncertainty) of the effects of salinity on halotolerants is advised.

References

Alazard, M., Leduc, C., Travi, Y., Boulet, G. & Salem, A. B. (2015). Estimating evaporation in semi-arid areas facing data scarcity: Example of the El Haouareb dam (Merguellil catchment, Central Tunisia). *Journal of Hydrology: Regional Studies*, *3*, 265-284.

Alexander, C. S. (1961). The marine terraces of Aruba, Bonaire, and Curaçao, Netherlands Antilles. *Annals of the Association of American Geographers, 51(1)*, 102-123.

Allen, R.G., Pereira, L.S., Raes, D. & Smith, M. (1998). Crop evapotranspiration – Guidelines for computing crop water requirements. *FAO Irrigation and drainage paper no. 56*.

Arengo, F. & Baldassarre, G. A. (1995). Effects of food density on the behavior and distribution of nonbreeding American Flamingos in Yucatan, Mexico. *Condor, 97(2),* 325-334.

Baldassarre, G. A. & Arengo, F. (2000). A review of the ecology and conservation of Caribbean Flamingos in Yucatan, Mexico. *Waterbirds, 23(1),* 70-79.

Beets, D., Mac Gillavry, H.J. & Klaver, G. (1977). Geology of the Cretaceous and early Tertiary of Bonaire. Guide to the field excursions on Curaçao, Bonaire and Aruba, Netherlands Antilles. *GUA Papers of Geology, 1(10),* 18-28.

Boekschoten, B. & Westermann, J.H. (1982). *Geology*. In: Field Guide National Park Washington-Slagbaai, Bonaire. STINAPA 23, pp. 22-27.

Bonaire, 2016. Local newspaper and blog 'reporting on everything concerning Bonaire'. Data retrieved on 16-01-2016 from http://bonaire.nu.

Browne, R. A. & Wanigasekera, G. (2000). Combined effects of salinity and temperature on survival and reproduction of five species of Artemia. *Journal of experimental marine biology and ecology*, *244(1)*, 29-44.

de Buisonje, P. H. (1974). *Neogene and Quaternary geology of Aruba, Curaçao, and Bonaire (Netherlands Antilles).* Uitgaven Natuurwetenschappelijke Studiekring voor Suriname en de Nederlandse Antillen 78, 291pp.

Buitrago, J., M. Rada, M. E. Barroeta, E. Fajardo, E. Rada, F. Simal, J. Monente, J. Capelo, J. & Narváez, J. (2010). *Physico-Chemical Indicators Monitoring for Water Quality in the Salinas of Northwest Bonaire, N.A.. A base line study. A technical report.* Estación de Investigaciones Marinas de Margarita to STINAPA. 23 tables, 237 Figures. 214 pp.

Calder, I.R. & Neal, C. (1984). Evaporation from saline lakes: a combination equation approach. *Hydrological Sciences Journal, 29(1),* 89-97.

Casler, C. L. & Esté, E. E. (2000). Caribbean Flamingos feeding at a new solar saltworks in western Venezuela. *Waterbirds*, *23(1),* 95-102.

DCBD (2015). Dutch Caribbean Biodiversity Database. Data retrieved on 2-10-2015 from http://dcbd.nl.

Duchon, C. E. & Essenberg, G. R. (2001). Comparative rainfall observations from pit and aboveground rain gauges with and without wind shields. *Water Resources Research*, *37*(12), 3253-3263.

Engel, M., Brückner, H., Messenzehl, K., Frenzel, P., May, S. M., Scheffers, A., Scheffers, S., Wennrich, V. & Kelletat, D. (2012). Shoreline changes and high-energy wave impacts at the leeward coast of Bonaire (Netherlands Antilles). *Earth, planets and space*, *64(10),* 905-921.

Espinoza, F., Parra, L., Aranguren, J., Martino, A., Quijada, M., Pirela, D., Rivero, R., Gutierrez, T., Jimenez, N., Leal, S. & Leon, E. (2000). Numbers and distribution of the Caribbean Flamingo in Venezuela. *Waterbirds, 23(1),* 80-86.

Esté, E. E. & Casler, C. L. (2000). Abundance of benthic macroinvertebrates in Caribbean Flamingo feeding areas at Los Olivitos Wildlife Refuge, western Venezuela. *Waterbirds, 23(1),* 87-94.

Flater, D. (2015). Mobile Geographic LCC. Tidal data Kralendijk, Bonaire. Retrieved on 7-9-2015 from http://tides.mobilegeographics.com/locations/3169.html.

Freeze, R. A., & Cherry, J. A. (1979). *Groundwater*, 604 pp.

de Freitas, J. A., Nijhof, B. S. J., Rojer, A. C. & Debrot, A. O. (2005). *Landscape ecological vegetation map of the island of Bonaire (Southern Caribbean).* Royal Netherlands Academy of Arts and Science.

Google Earth (2016). Historical satellite imagery Bonaire. 12°15'42N and -68°22'38E. Retrieved on 24-02-2015.

Granger, R. J. & Hedstrom, N. (2011). Modelling hourly rates of evaporation from small lakes. *Hydrology and Earth System Sciences*, *15*(1), 267-277.

Henley, W. J., Major, K. M. & Hironaka, J. L. (2002). Response to salinity and heat stress in two halotolerant chlorophyte algae. *Journal of Phycology*, *38*(4), 757-766.

Hobbelt, L. (2014). *Fresh water and sediment dynamics in the cathcment of Lac at Bonaire.* MSc Thesis. Wageningen University, the Netherlands.

McJannet, D. L., Webster, I. T. & Cook, F. J. (2012). An area-dependent wind function for estimating open water evaporation using land-based meteorological data. *Environmental Modelling & Software*, *31*, 76-83.

Koster, G. (2013). *Mapping runoff and erosion to reduce urban flooding and sediment flow towards sea.* MSc Thesis. Wageningen University, the Netherlands.

Krajewski, W. F., Ciach, G. J. & Habib, E. (2003). An analysis of small-scale rainfall variability in different climatic regimes. *Hydrological sciences journal*, *48*(2), 151-162.

Lowe, L. D., Webb, J. A., Nathan, R. J., Etchells, T. & Malano, H. M. (2009). Evaporation from water supply reservoirs: An assessment of uncertainty. *Journal of Hydrology, 376(1)*, 261-274.

Mackenzie, F. T., Vink, S., Wollast, R. & Chou, L. (1995). *Comparative geochemistry of marine saline lakes.* In: Physics and chemistry of lakes. Springer Berlin Heidelberg, pp. 265-278

Masoner, J. R., Stannard, D. I. & Christenson, S. C. (2008). Differences in Evaporation Between a Floating Pan and Class A Pan on Land. *Journal of the American Water Resources Association, 44(3),* 552-561.

MDC (2015). Climatological summaries Netherlands Antilles, Meteorological Department Curacao. Retrieved on 21-12-2015 from http://meteo.cw/climate_reports.php?Lang=Eng&St=TNCC.

Mekonnen, G. B., Matula, S., Doležal, F. & Fišák, J. (2015). Adjustment to rainfall measurement undercatch with a tipping-bucket rain gauge using ground-level manual gauges. *Meteorology and Atmospheric Physics*, *127*(3), 241-256.

Mooij, M., van de Meent, D., Bodar, C.W.M., Boshuis, M.E., De Groot, A.C., de Zwart, D., Hoffer, S.M., Janssen, P.J.C.M., de Groot, G.M., Peijnenburg, W.J.G.M. & Verbruggen, E.M.J. (2011). *Compound depositions from the BOPEC fires on Bonaire - Measurements and risk assessment.* RIVM Letter report 609022067/2011, RIVM, Bilthoven, the Netherlands.

Naceur, H. B., Jenhani, A. B. R. & Romdhane, M. S. (2013). Reproduction characteristics, survival rate and sex-ratio of four brine shrimp Artemia salina (Linnaeus, 1758) populations from Tunisia cultured under laboratory conditions. *Invertebrate Reproduction & Development*, *57*(2), 156-164.

Nash, J. E. & Sutcliffe, J. V. (1970). River flow forecasting through conceptual models part I—A discussion of principles. *Journal of hydrology*, *10*(3), 282-290.

Niedda, M. & Pirastru, M. (2013). Hydrological processes of a closed catchment-lake system in a semi-arid Mediterranean environment. *Hydrological Processes*, *27*(25), 3617-3626.

NOAA (2015). Weather data Flamingo Airport. Retrieved on 21-12-2015 from gis.ncdc.noaa.gov/map/viewer/#app=clim&cfg=cdo&theme=daily&layers=0001&node=gis.

Obrador, B., Moreno-Ostos, E. & Pretus, J. L. (2008). A dynamic model to simulate water level and salinity in a Mediterranean coastal lagoon. *Estuaries and Coasts*, *31*(6), 1117-1129.

Oroud, I. M. (1995). Effects of salinity upon evaporation from pans and shallow lakes near the Dead Sea. *Theoretical and applied climatology*, *52*(3-4), 231-240.

Pedersen, L., Jensen, N. E., Christensen, L. E. & Madsen, H. (2010). Quantification of the spatial variability of rainfall based on a dense network of rain gauges. *Atmospheric Research*, *95*(4), 441-454.

Penman, H. L. (1948). Natural evaporation from open water, bare soil and grass. *Proceedings of the Royal Society of London A: Mathematical, Physical and Engineering Sciences, 193(1032),* 120-145.

RAMSAR. (2015). RAMSAR site information. Retrieved on 31-8-2015 from https://rsis.ramsar.org/ris/202.

Rooth, J. (1965). *The flamingos on Bonaire (Netherlands Antilles): habitat, diet and reproduction of Phoenicopterus ruber ruber.* Natuurwetenschappelijke studiekring voor Suriname en de Nederlandse Antillen, Utrecht, the Netherlands, 151 pp.

RStudio Team (2015). RStudio: Integrated Development for R. RStudio, Inc., Boston. http://www.rstudio.com/.

Salhotra, A.M., Adams, E.E. & Harleman, D.R. (1985). Effects of salinity and ionic composition on evaporation: analysis of Dead Sea evaporation pans. *Water Resources Research 21(9),* 1336-1344.

Savenije, H. H. (2001). Equifinality, a blessing in disguise?. *Hydrological processes*, *15*(14), 2835-2838.

Savenije, H. H. (2006). *Salinity and Tides in Alluvial Estuaries*. Elsevier, New York.

Schaefli, B. & Gupta, H. V. (2007). Do Nash values have value?. *Hydrological Processes*, *21*(15), 2075-2080.

Schreiber, B. C. & Tabakh, M. E. (2000). Deposition and early alteration of evaporites. *Sedimentology*, *47*(S1), 215-238.

Simal, F. (2005). *Management Plan Washington Slagbaai National Park.* STINAPA, 44 pp.

Slijkerman, D.M.E., de Vries, P., Kotterman, M.J.J., Cuperus, J., Kwadijk, C.J.A.F. & van Wijngaarden, R. (2013). *Saliña Goto and reduced flamingo abundance since 2010; Ecological and ecotoxicologial research.* Report number C211/13, IMARES, Wageningen, the Netherlands.

Stevens, J. B. & Coryell, A. (2007). Surface water quality criterion for perfluorooctane sulfonic acid. *STS Project*, *200604796, St. Paul, Minnesota, USA.*

Tanny, J., Cohen, S., Assouline, S., Lange, F., Grava, A., Berger, D., Teltch, B. & Parlange, M. B. (2008). Evaporation from a small water reservoir: Direct measurements and estimates. *Journal of Hydrology, 351(1),* 218-229.

Tanny, J., Cohen, S., Berger, D., Teltch, B., Mekhmandarov, Y., Bahar, M., Katul, G.G. & Assouline, S. (2011). Evaporation from a reservoir with fluctuating water level: Correcting for limited fetch. *Journal of Hydrology, 404(3),* 146-156.

Thom, A. S. & Oliver, H. R. (1977). On Penman's equation for estimating regional evaporation. *Quarterly Journal of the Royal Meteorological Society*, *103*(436), 345-357.

Turner, I. L. & Masselink, G. (2012). Coastal gravel barrier hydrology—Observations from a prototype-scale laboratory experiment (BARDEX). *Coastal Engineering*, *63*, 13-22.

Vallet-Coulomb, C., Legesse, D., Gasse, F., Travi, Y. & Chernet, T. (2001). Lake evaporation estimates in tropical Africa (Lake Ziway, Ethiopia). *Journal of hydrology*, *245*(1), 1-18.

Vardavas, I. M. & Fountoulakis, A. (1996). Estimation of lake evaporation from standard meteorological measurements: application to four Australian lakes in different climatic regions. *Ecological modelling*, *84*(1), 139-150.

Vargas, F. H., Barlow, S., Hart, T., Jimenez-Uzcátegui, G., Chavez, J., Naranjo, S. & Macdonald, D. W. (2008). Effects of climate variation on the abundance and distribution of flamingos in the Galápagos Islands. *Journal of Zoology, 276(3),* 252-265.

Verburg, P. & Antenucci, J. P. (2010). Persistent unstable atmospheric boundary layer enhances sensible and latent heat loss in a tropical great lake: Lake Tanganyika. *Journal of Geophysical Research: Atmospheres*, *115,* D11109.

Weisman, R. N. & Brutsaert, W. (1973). Evaporation and cooling of a lake under unstable atmospheric conditions. *Water Resources Research*, *9*(5), 1242-1257.

Wetlands International (2015). Waterbird Population Estimates. Retrieved on 13-9-2015 from wpe.wetlands.org.

Wunderground (2015). ICARIBIS2 Republiek weather station. Retrieved on 21-12-2015 from http://www.wunderground.com/personal-weather-station/dashboard?ID=ICARIBIS2.

Yang, Y. & Chen, Y.L. (2008). Effects of terrain heights and sizes on island-scale circulations and rainfall for the island of Hawaii during HaRP. *Monthly Weather Review, 136(1),* 120-146.

Zonneveld, J.I.S. (1982). *Geomorphology*. In: Field Guide National Park Washington-Slagbaai, Bonaire. STINAPA, 23, 28-33.

de Zwart, D., de Groot, A., Kotterman, M., van der Aa, M., Aalbers, T., Slijkerman, D. & Bodar, C. (2012). *Follow-up study on the chemical status of Lake Goto, Bonaire. Measurements and risk assessment.* RIVM Letter report 609224001/2012.

Zweers, G., De Jong, F., Berkhoudt, H. & Berge, J. V. (1995). Filter feeding in flamingos (Phoenicopterus ruber). *Condor*, *97(2),* 297-324.

Appendices

Appendix I Maps of the catchment and measurement locations

Overview of the catchment of Lac Goto and the measurement locations within this catchment. The coordinates of these measurement locations are listed as well. Furthermore, a map is shown of the distribution of soils and geology in the catchment.

Appendix II Additional formulae

An outline of the calculations of evaporation, as well as an explanation and example of the dam models used in the field survey.

Appendix III Supplementary data field survey

Values for some measured variables are given which were referred to in the text. Additionally, more detailed information is provided for some of the analyses performed in chapter 4.

Appendix IV Satellite imagery

Satellite imagery for seven days, used for water level estimates for model validation. Estimated water levels for the images shown are given as well.

Appendix V Supplementary material model study

Model output with extra detailed information on some aspects mentioned in chapter 6.

Appendix VI Summary of external data sources

Summary of the weather and flamingo abundance data sets.

Appendix I – Maps of the catchment and measurement locations

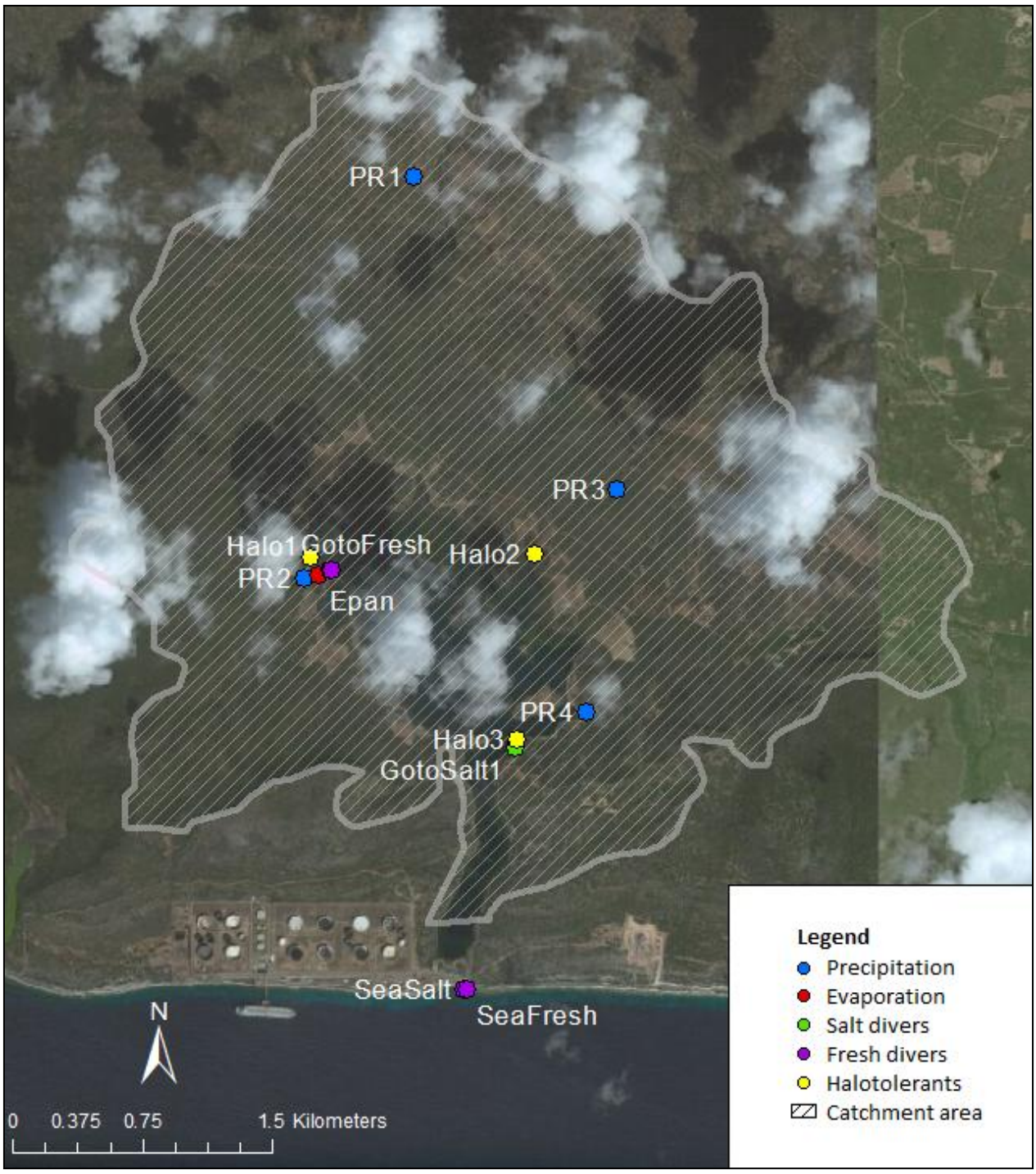

Figure I.1: Overview of measurement locations within the catchment of Lac Goto, together with the (topography based) catchment delineation (grey striped area). GotoSalt2 is not displayed on this map, but is located at the same location as GotoFresh. Adapted from Google Earth (2016).

Table I.1: Coordinates of measurement locations used in study

Location name [-]	Northing [Deg-hr-min-sec]	Easting [Deg-hr-min-sec]
PR1	12°15'42.13"	- 68°22'38.35"
PR2	12°14'30.29"	- 68°22'56.83"
PR3	12°14'45.25"	- 68°22'00.31"
PR4	12°14'04.73"	- 68°22'06.26"
Epan	12°14'30.60"	- 68°22'55.96"
SeaSalt	12°13'14.00"	- 68°22'28.36"
SeaFresh	12°13'14.00"	- 68°22'28.36"
GotoSalt1	12°13'59.89"	- 68°22'19.06"
GotoSalt2	12°14'30.81"	- 68°22'55.66"
GotoFresh	12°14'30.81"	- 68°22'55.66"
Halo1	12°14'31.29"	- 68°22'56.61"
Halo2	12°14'33.69"	- 68°22'15.92"
Halo3	12°13'59.69"	- 68°22'19.15"

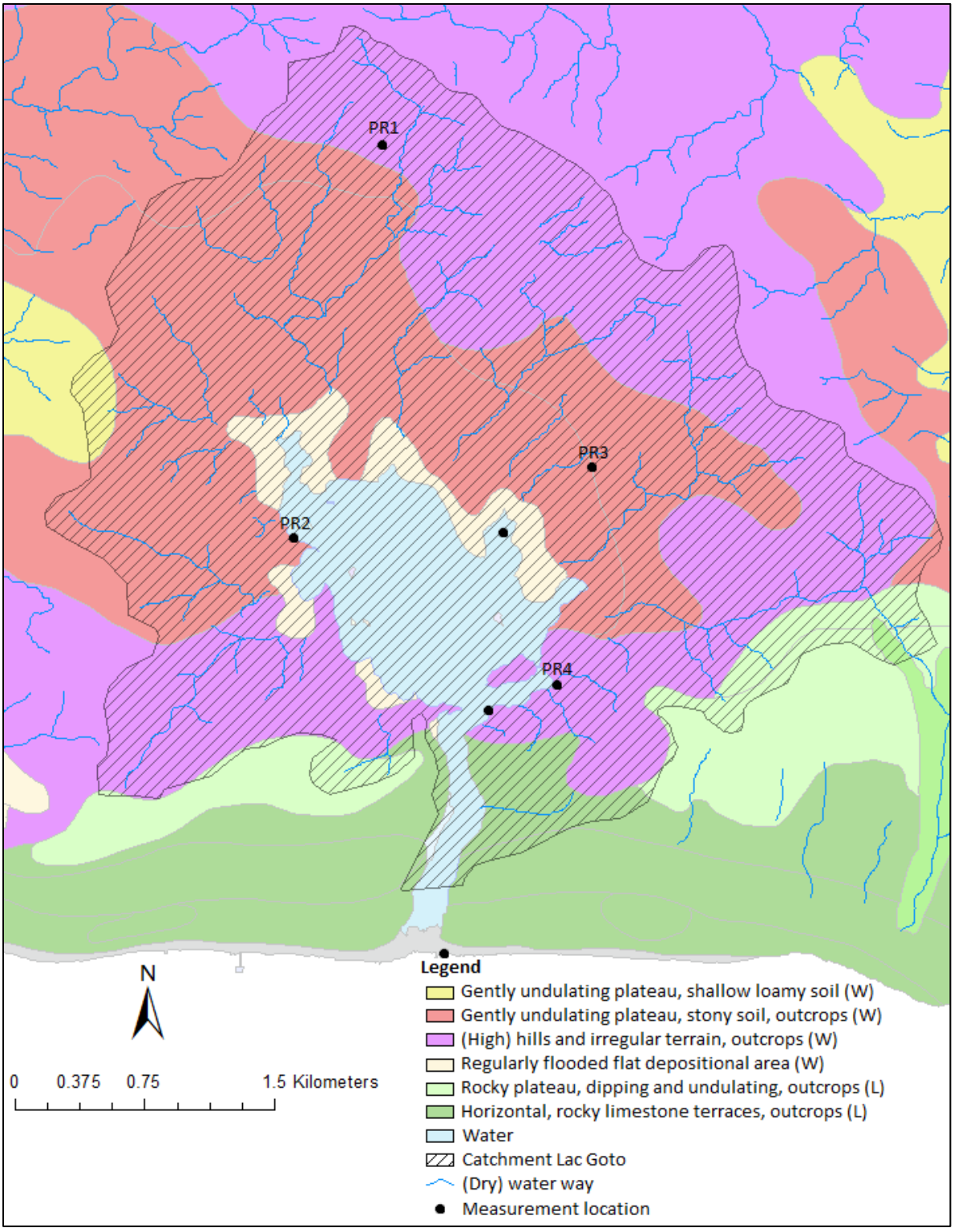

Figure I.2: Map of geology, soils and creeks, modified after DCBD (2015). Also indicated are measurement locations. The additions of (W) and (L) in the legend represent the Washikemba and Limestone formation, respectively.

Appendix II – Additional formulae

The first section of this appendix describes how evaporation was calculated for both the field survey and model study. In the second section construction of the dam models (equations 3.3a, 3.3b, 3.3c and 3.4 and equations 5.4a and 5.4b) is described.

Evaporation

The general formula used to calculate evaporation for both the field survey (e.g. figure 4.4) and model study was a modified Penman equation as proposed by Calder and Neal (1984) (equation II.1). The aerodynamic resistance was calculated using a function proposed by Thom and Oliver (1977) (equation II.2). Other parameters were calculated using the FAO guidelines, as presented by Allen *et al.* (1998). Note that some deviations from literature might be present due to unit conversions. An explanation of symbols and fixed values used for the calculation of evaporation are listed in table II.1.

Note that for the conversion of units in equation II.1 from the right hand side to the left hand side, the right hand side was divided by density of water (1000 kg m^{-3}) and the unit was changed from m d^{-1} to mm d^{-1} by multiplication with 1000. For the calculation on a five-minute timescale the measured temperature at each time step rather than an average of the vapor pressure for minimum and maximum temperature was used in equation II.4.

$$\text{Eq. II. 1} \quad : \quad E = \frac{\Delta * R_{net}}{\lambda * (\Delta + \frac{\gamma}{a_w})} + \frac{86400 * \rho_{air} * c_p * \frac{e_s - {e_a}/{a_w}}{r_a}}{\lambda * (\Delta + \frac{\gamma}{a_w})} \quad [\frac{mm}{d}]$$

$$\text{Eq. II. 2} \quad : \quad r_a = \frac{250}{0.536 * u_2 + 1} \quad [\frac{s}{m}]$$

$$\text{Eq. II. 3} \quad : \quad e^0 = 0.6108 * e^{\left(\frac{17.27*T}{T+237.3}\right)} \quad [kPa]$$

$$\text{Eq. II. 4} \quad : \quad e_s = \frac{e^0(T_{\max}) + e^0(T_{\min})}{2} \quad [kPa]$$

$$\text{Eq. II. 5} \quad : \quad e_a = e^0(T_{\text{dew}}) \quad [kPa]$$

$$\text{Eq. II. 6} \quad : \quad \Delta = \frac{4098 * e^0}{(T + 237.3)^2} \quad [\frac{kPa}{°C}]$$

Eq. II. 7 : $\gamma = \frac{c_p * p_{air}}{\varepsilon * \lambda} = 0.665 * p_{air} \quad [\frac{kPa}{°C}]$

Net radiation (R_{net}) was calculated using equations II.8 to II.17. For the five-minute interval calculations, incoming shortwave radiation was measured rather than calculated. Therefore, calculation of net radiation only required the use of equations II.15 to II.17. Furthermore, in equation II.15, the measured temperature for each interval was used rather than the minimum and maximum temperature, similar as for equation II.4.

Eq. II. 8 : $R_a = \frac{G_{sc}}{\pi} * d_r * (\omega_s * \sin(\varphi) * \sin(\delta) + \cos(\varphi) * \sin(\omega_s) \quad [\frac{MJ}{m^2 °C}]$

Eq. II. 9 : $d_r = 1 + 0.33 * \cos\left(\frac{2 * \pi}{365} * DOY\right) \quad [-]$

Eq. II. 10 : $\delta = 0.409 * \sin\left(\frac{2 * \pi}{365} * DOY - 1.39\right) \quad [rad]$

Eq. II. 11 : $\omega_s = \arccos(-\tan(\varphi) * \tan(\delta)) \quad [rad]$

Eq. II. 12 : $N = \frac{24}{\pi}\omega_s \quad [\frac{hour}{d}]$

Eq. II. 13 : $R_{so} = (a_s + b_s) * R_a \quad [\frac{MJ}{m^2 °C}]$

Eq. II. 14 : $R_s = \left(a_s + b_s * \frac{n}{N}\right) * R_a = \frac{n}{N} * R_{so} \quad [\frac{MJ}{m^2 °C}]$

Eq. II. 15 : $R_{ns} = (1 - \alpha) * R_s \quad [\frac{MJ}{m^2 °C}]$

Eq. II. 16 : $R_{nl} = \sigma * \frac{{T_{max,K}}^4 + {T_{min,K}}^4}{2} * \left(0.34 - 0.14 * \sqrt{e_a}\right) * \left(1.35 * \frac{R_s}{R_{so}} - 0.35\right) \quad [\frac{MJ}{m^2 °C}]$

Eq. II. 17 : $R_{net} = R_{ns} - R_{nl} \quad [\frac{MJ}{m^2 °C}]$

Table II.1: Explanation and value of symbols used in equations II.1 to II.17. This table is only valid for this appendix. Note that some symbols are similar as used in the main report, but this table only applies to this appendix. Table continues on next page.

Symbol	Unit	Description	Value (if constant)	Used in equations [a]
a_s	-	Empirical constant; fraction of extraterrestrial radiation reaching the earth on clear-sky days	0.25	13, 14
a_w	-	Activity of water	0.9	1
b_s	-	Empirical constant; fraction of extraterrestrial radiation reaching the earth on clear-sky days	0.50	13, 14
c_p	MJ kg^{-1} °C^{-1}	Specific heat at constant pressure	1.013 x 10^{-3}	1, 7
d_r	-	Inverse relative distance Earth-Sun		8, 9
DOY	-	Day of year		9, 10
e^0	kPa	Vapor pressure		3, 4, 5, 6
e_a	kPa	Actual vapor pressure		1, 5, 16
e_s	kPa	Saturation vapor pressure		1, 4
E	mm d^{-1}	Evaporation		1
G_{sc}	MJ m^{-2} d^{-1}	Solar constant	118.08	8
n	Hours d^{-1}	Sunshine duration per day	8	14
N	Hours d^{-1}	Maximum possible sunshine duration		12, 14
p_{air}	kPa	Atmospheric pressure		7
r_a	s m^{-1}	Aerodynamic resistance		1, 2
R_a	MJ m^{-2} d^{-1}	Extraterrestrial solar radiation		8, 13, 14
R_{net}	MJ m^{-2} d^{-1}	Net radiation		1
R_{nl}	MJ m^{-2} d^{-1}	Net longwave radiation		16, 17
R_{ns}	MJ m^{-2} d^{-1}	Net shortwave radiation		15, 17
R_s	MJ m^{-2} d^{-1}	Incoming solar radiation		14, 15, 16
R_{so}	MJ m^{-2} d^{-1}	Clear-sky solar radiation		13, 14, 16
T_{dew}	°C	Dewpoint temperature		5
T_{max}	°C	Daily maximum temperature		4
T_{min}	°C	Daily minimum temperature		4
$T_{max,K}$	K	Daily maximum temperature		16
$T_{min,K}$	K	Daily minimum temperature		16
u_2	m s^{-1}	Wind speed at 2 meters height		2
α	-	Albedo of water	0.05	15
γ	kPa °C^{-1}	Psychrometric constant		1, 7
δ	rad	Solar declination		8, 10, 11
Δ	kPa °C^{-1}	Slope of saturation vapor pressure deficit curve		1, 6
ε	-	Ratio molecular weight of water vapor / dry air	0.622	7
λ	MJ kg^{-1}	Latent heat of vaporization	2.45	1, 7
φ	rad	Latitude	0.213	8, 11
ρ_{air}	kg m^{-3}	Mean air density at constant pressure	1.15	1

Symbol	Unit	Description	Value (if constant)	Used in equations [a]
σ	MJ K^{-4} m^{-2} d^{-1}	Stefan-Boltzmann constant	4.903 x 10^{-9}	16
ω_s	rad	Sunset hour angle		8, 11, 12

[a] All equation numbers have prefix II. as they refer to equations used in this appendix.

Dam conductance

The simplest dam model, given by equation 3.3a, assumed one constant conductance over the whole dam (1-layer dam model). This is illustrated in figure II.1 A by the dashed line. The solid line in this figure is the total flux through the dam as function of (the average of sea and lake) level. This equation originated from the Darcy equation for flow through porous media, which states (in one dimension):

$$\text{Eq. II. 18} \quad : \quad Q = k * A * \frac{\Delta H}{L} \quad [\frac{m^3}{d}]$$

where: *Q* is the flux through a porous medium [m^3 d^{-1}]
k is the permeability of the porous material [m d^{-1}]
A is the area perpendicular to the flow direction [m^2]
ΔH is the head difference between the two sides of the porous medium [m]
L is the distance between the two sides of the porous medium (thickness) [m].

In equation 3.3a, *ΔH* was the difference in water level between Lac Goto and the sea. Equation II.18 was translated into a one dimensional flux *q*, by dividing through the area of Lac Goto (A_{Goto}). Furthermore, rewriting the area of the porous medium perpendicular to the flow direction, which is the area of the dam, in width (*W*) times height ($\bar{H}$), where it is assumed that the dam is cubic, yields:

$$q * A_{Goto} = k * A * \frac{\Delta H}{L} \leftrightarrow q = \frac{k * A}{A_{Goto} * L} * \Delta H \leftrightarrow q = \frac{k * W}{A_{Goto} * L} * \bar{H} * \Delta H$$

Introducing the dam conductance, *c*, as the combination of permeability, dam width and – thickness and the area of Lac Goto, finally yields equation II.19, which is similar as equation 3.3a:

$$\text{Eq. II. 19} \quad : \quad q = c * \bar{H} * \Delta H \quad [\frac{m}{d}]$$

where: *q* is the flux through the dam [m d^{-1}]
c is the conductance of the dam [m^{-1} d^{-1}], calculated as $(k * W) / (A_{Goto} * L)$
$\bar{H}$ is the height of the dam through which water flows [m], defined as $d_{dam} + (H_{Goto} + H_{sea}) / 2$
d_{dam} is the lowest point of the dam, fixed at -10 [m +BRL]
H_{Goto} is the height of the water level of Lac Goto [m +BRL]
H_{sea} is the height of the water level of the sea [m +BRL].

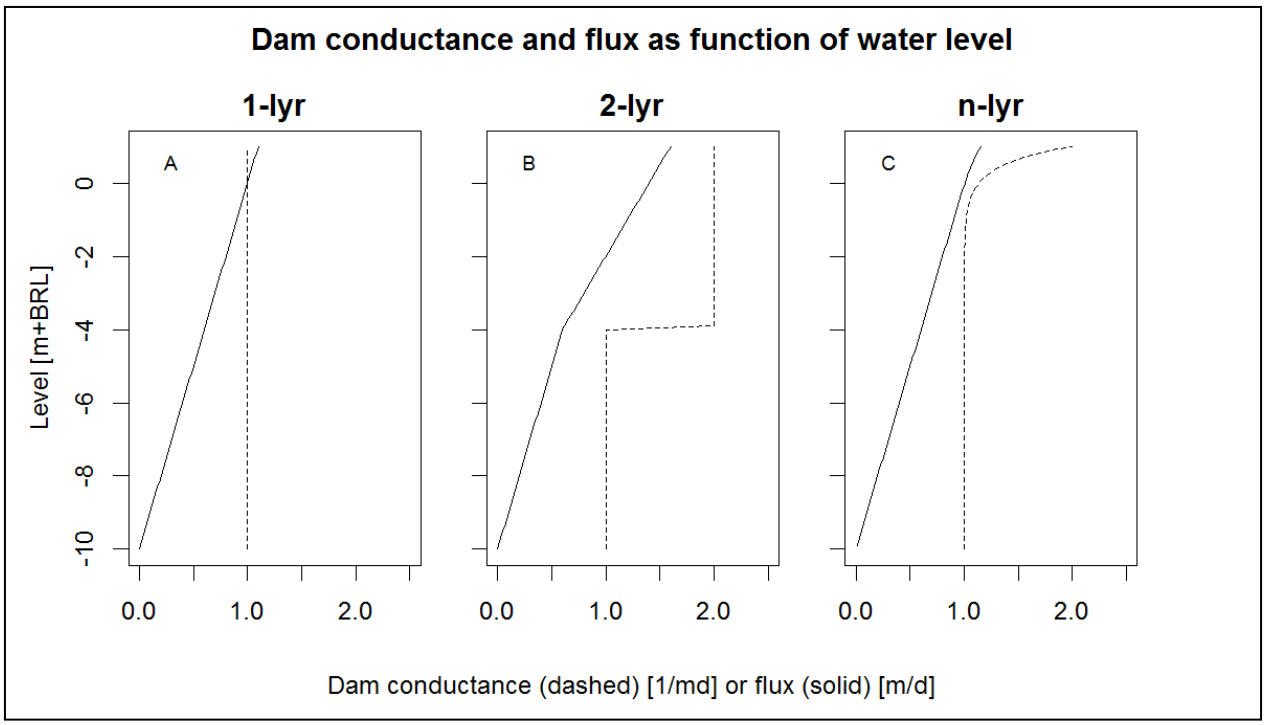

Figure II.1: Dam conductance (dotted line) and total flux through the dam (solid line) as function of the average water height of sea and lake, using $c = c1 = c_{min}$ = 1 $m^{-1}d^{-1}$, $c2 = c_{max}$ = 2 $m^{-1}d^{-1}$, ΔH = 0.1 m and γ = 2 d^{-1}. Panel A shows the situation for the 1-layer dam model (with a constant conductance), panel B for the 2-layer dam model (where a transition of the layers is located at -4 m +BRL) and panel C for the n-layer dam model, where the conductance is higher at the top of the dam.

The 2-layer dam model, using two layers with a different conductance, is shown in panel B in figure II.1. The equation describing this function calculated whether the water level at a certain moment in time was high enough to permit flow through both layers (which was the case when the average water level of the sea and Lac Goto was above a threshold, h_{trans}). If water could only flow through the lower layer, an equation similar as for the 1-layer model was used. However, if flow through both layers occurred, the flow was calculated as the sum of fluxes through both layers, shown in equation III.20.

$$\text{Eq. II. 20} \quad : \quad q = \begin{cases} if\ \overline{H} > h_{trans} & : c_1 * h_{trans} * \Delta H + c_2 * (\overline{H} - h_{trans}) * \Delta H \\ if\ \overline{H} \leq h_{trans} & : c_1 * \overline{H} * \Delta H \end{cases} \quad [\frac{m}{d}]$$

where: c_1 is the conductance of the lower layer of the dam [$m^{-1}\,d^{-1}$]
c_2 is the conductance of the upper layer of the dam [$m^{-1}\,d^{-1}$]
h_{trans} is the height of transition between the first and second layer above the bottom of the dam [m].

The n-layer dam model was defined similarly as equation II.19, albeit that here the conductance was a function of the average level of Lac Goto and the sea ($\overline{H}$):

$$\text{Eq. II. 21} \quad : \quad q = c(\overline{H}) * \overline{H} * \Delta H \quad [\frac{m}{d}]$$

Conductance as function of height was calculated using equation 3.4. This equation was derived from equation II.22, which calculates the conductance at a certain height of the dam over a smooth continuous function. For *h=0*, the conductance equals c_{min}, for $h=h_{max}$, the conductance equals c_{max}. Note that, even if water levels rise above h_{max}, this function still produces results. An example of this function is shown in figure II.1 C.

$$\text{Eq. II. 22} \quad : \quad c(h) = c_{min} + (c_{max} - c_{min}) * e^{\gamma(h-h_{max})} \quad [\frac{1}{md}]$$

where:
- c_{min} is the conductance at the bottom of the dam [$m^{-1}\ d^{-1}$]
- c_{max} is the conductance at the top of the dam [$m^{-1}\ d^{-1}$]
- γ is the shape factor of the curve, defining how gradual the transition from c_{min} to c_{max} is [d^{-1}]
- h is the height of the water level, above the bottom of the dam [m]
- h_{max} is the maximum height above the bottom of the dam for which this function is defined [m].

For this function to be of use for the model, an average of the conductance between *h=0* and $h=\overline{H}$ was required, as given by equation II.23.

$$\text{Eq. II. 23} \quad : \quad c(\overline{H}) = \frac{1}{\overline{H}} * \int_{h=0}^{h=\overline{H}} c_{min} + (c_{max} - c_{min}) * e^{\gamma(h-h_{max})} \quad [\frac{1}{md}]$$

To arrive at equation 3.4, the integral was calculated

$$\frac{1}{\overline{H}} * \int_{h=0}^{h=\overline{H}} c_{min} + (c_{max} - c_{min}) * e^{\gamma(h-h_{max})} =$$

$$\frac{1}{\overline{H}} \left[c_{min} * h + (c_{max} - c_{min}) * e^{\gamma(h-h_{max})} * \frac{1}{\gamma} \right]_{h=0}^{h=\overline{H}} =$$

$$\frac{1}{\overline{H}} * c_{min} * \overline{H} + \frac{(c_{max} - c_{min})}{\overline{H} * \gamma} * e^{\gamma(\overline{H}-h_{max})} - \frac{1}{\overline{H}} * c_{min} * 0 - \frac{(c_{max} - c_{min})}{\overline{H} * \gamma} * e^{\gamma(0-h_{max})} =$$

$$c_{min} + \frac{(c_{max} - c_{min})}{\overline{H} * \gamma} * e^{\gamma(\overline{H}-h_{max})} - \frac{(c_{max} - c_{min})}{\overline{H} * \gamma} * e^{\gamma(-h_{max})}$$

resulting in equation III.24, which is similar as equation 3.4.

$$\text{Eq. II. 24} \quad : \quad c(\overline{H}) = c_{min} + \frac{(c_{max} - c_{min})}{\overline{H} * \gamma} * (e^{\gamma * (\overline{H}-h_{max})} - e^{-\gamma * h_{max}}) \quad [\frac{1}{md}]$$

Appendix III – Supplementary data field survey

Water balance measurements

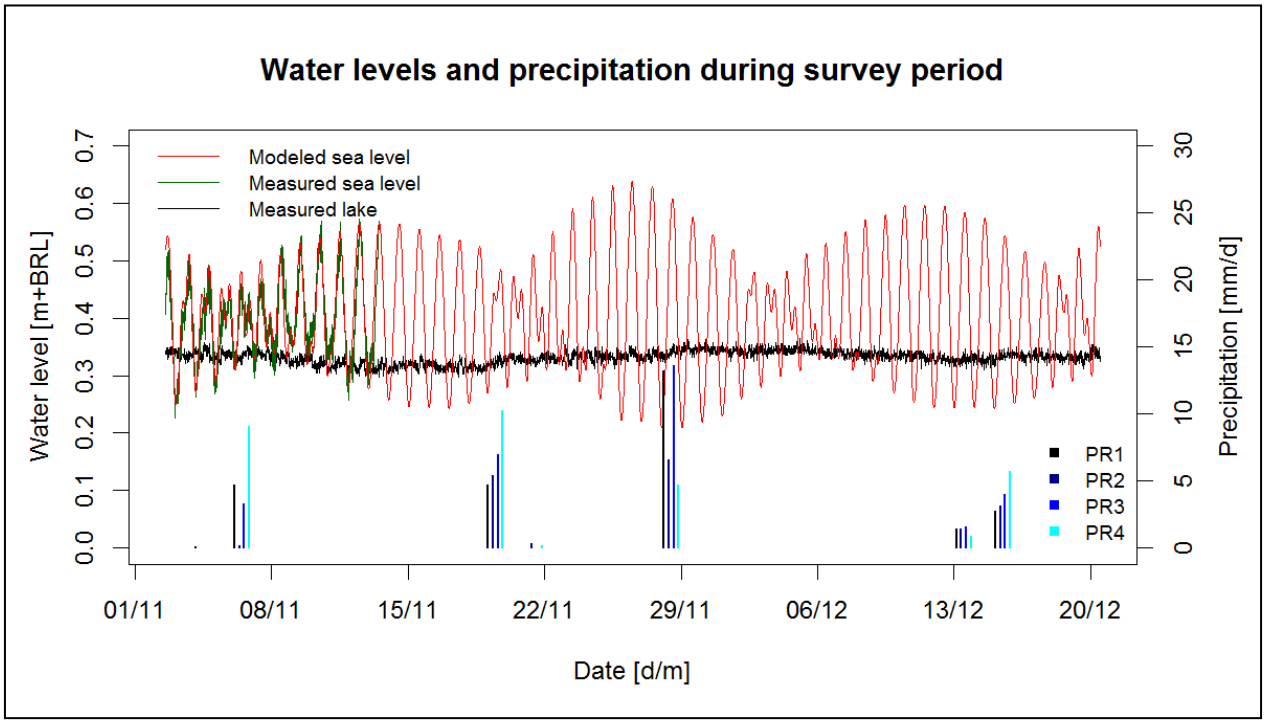

Figure III.1: Modeled (red) and measured (green, by SeaFresh) seawater levels and the water level of Lac Goto (black, by GotoSalt1). Also shown is the precipitation for all four rain gauges, on the right axis. Note that these are daily sums; the different positions of the bars in one day does therefore not indicate that precipitation occurred later on a day.

Table III.1: Measured precipitation for each rainy day, the average for all rainy days and the total precipitation sum in the field survey period for all rain gauges.

Date [d-m-y]	PR1 [mm/d]	PR2 [mm/d]	PR3 [mm/d]	PR4 [mm/d]
04-11-2015	0.1	0	0	0
06-11-2015	4.7	0.2	3.3	9.1
19-11-2015	4.7	5.4	7.0	10.3
21-11-2015	0	0.4	0	0.2
28-11-2015	13.3	6.6	13.6	4.7
13-12-2015	1.4	1.4	1.6	0.9
15-12-2015	2.8	3.1	4.0	5.8
Sum [mm]	27.0	17.1	29.5	31.0
Average [a] [mm/d]	3.9	2.4	4.2	4.4

[a] Average for days with precipitation.

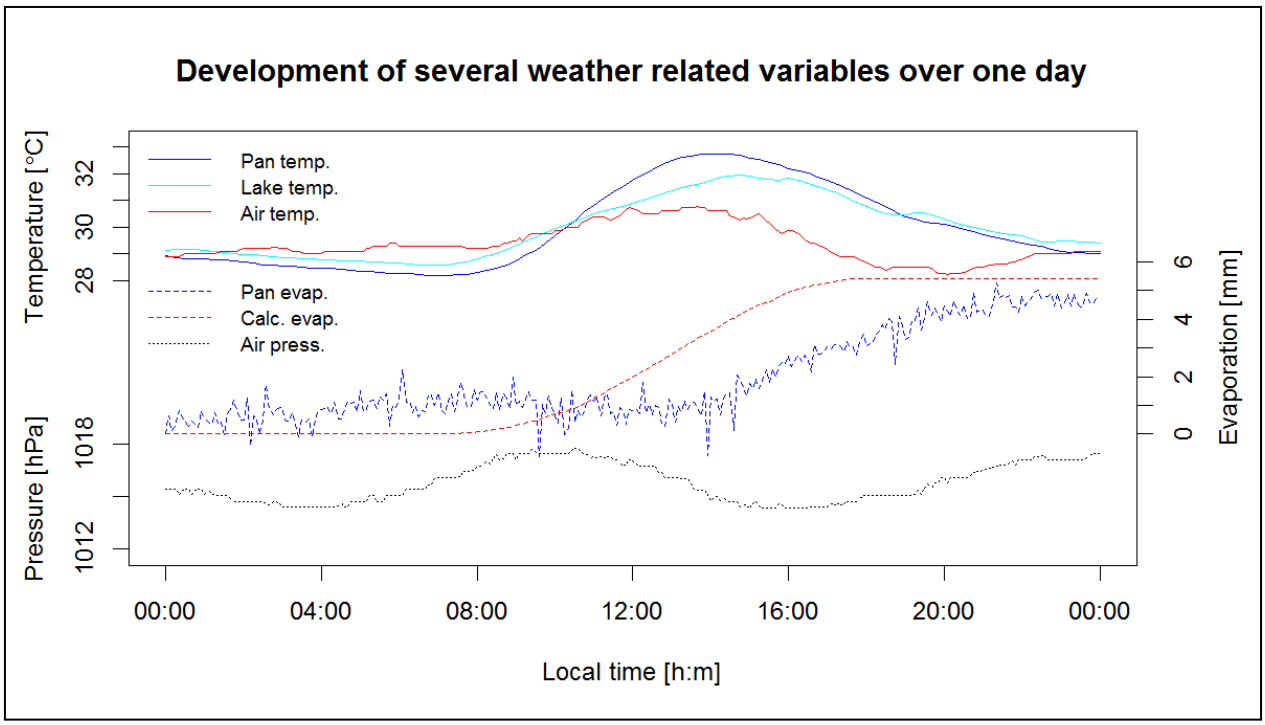

Figure III.2: Development of pan (blue), lake (cyan) and air (red) temperature over one representative day (1st of December), as well as the sum of measured (blue dashed) and calculated (red dashed) evaporation and the measured air pressure development (black dotted).

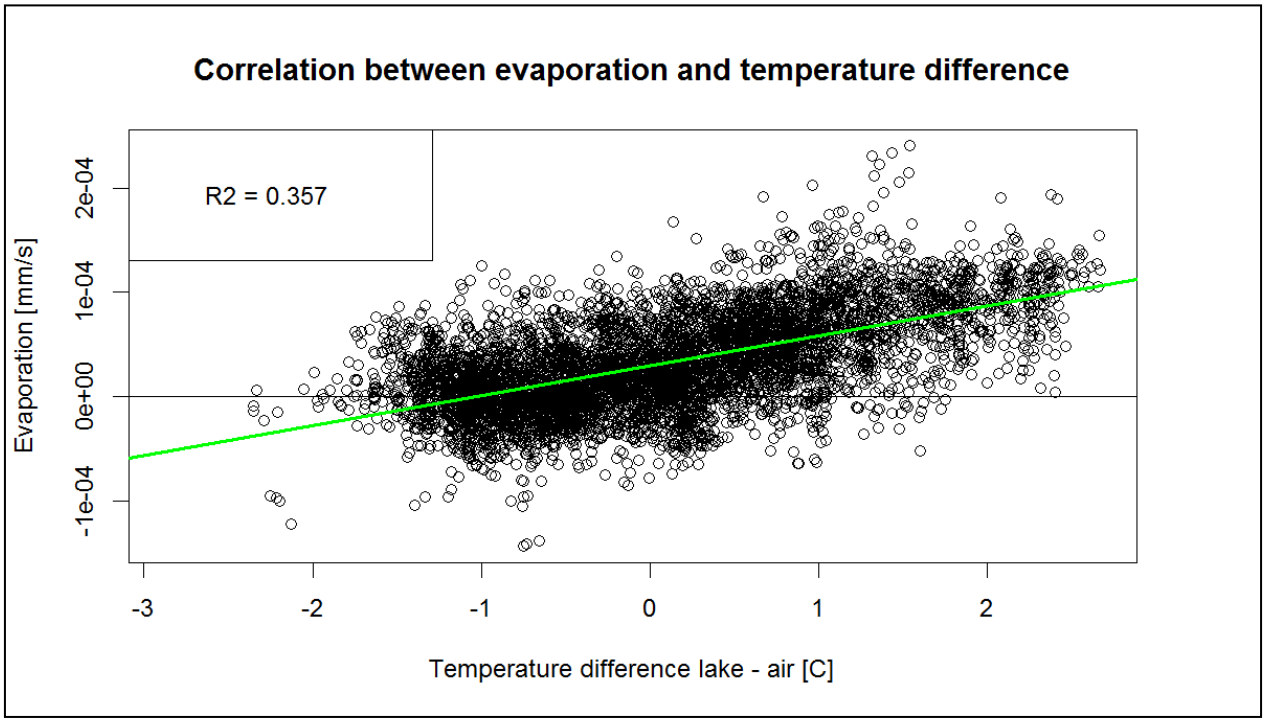

Figure III.3: Correlation between evaporation as measured with the evaporation pan and the difference in temperature between lake water and air (with positive values meaning higher lake – than air temperatures). The green line displays the linear regression, with an r^2 of 0.357.

Table III.2: Cross correlations for twelve combinations of time series, explained on page 25 and 26, for two divers. Correlation below -0.1 or above 0.1 are indicated in italic. Time lag columns indicate the time lag required for the maximum or minimum correlation, in a 48 hour time domain [-24 h : +24 h]. The meaning of the time lag is illustrated by this example: a time lag of -2 hours means that sea level [t-2] correlates with the other time series at [t].

Combinations		GotoSalt1				GotoFresh			
		Max cor. [m^2]	Time lag [h]	Min cor. [m^2]	Time lag [h]	Max cor. [m^2]	Time lag [h]	Min cor. [m^2]	Time lag [h]
Normal signal	Measured	-0.008	17.5	-0.039	-14.5	*0.062*	*-24*	*-0.160*	*-11.25*
	Residual	0.029	18.25	0.005	6.25	0.022	-22.75	-0.034	-11.25
	Measured MA	-0.009	-6.25	-0.038	-15.25	*0.051*	*-23.75*	*-0.147*	*-11.5*
	Residual MA	0.051	16	0.017	4	0.026	-24	-0.035	13.25
	Measured de-trend	0.012	-5.5	-0.043	-14.5	*0.096*	*-1.25*	*-0.230*	*-11.5*
	Residual de-trend	0.073	9	-0.074	21.25	*0.104*	*-1.75*	*-0.175*	*-12*
Derivative of signal	Measured	0.004	-7.25	-0.004	0	0.014	-3	-0.020	-11
	Residual	0.006	-7.25	-0.005	1.5	0.013	20.5	-0.016	-11
	Measured MA	0.050	-6	-0.038	-14	*0.254*	*-24*	*0.315*	*-11.25*
	Residual MA	0.068	14.5	-0.072	0.5	*0.192*	*-2.5*	*-0.250*	*-11.25*
	Measured de-trend	0.003	-8	-0.003	-12.75	0.018	-2.75	-0.018	-10.75
	Residual de-trend	0.005	9.5	-0.006	22.75	0.015	20.75	-0.013	-10.75

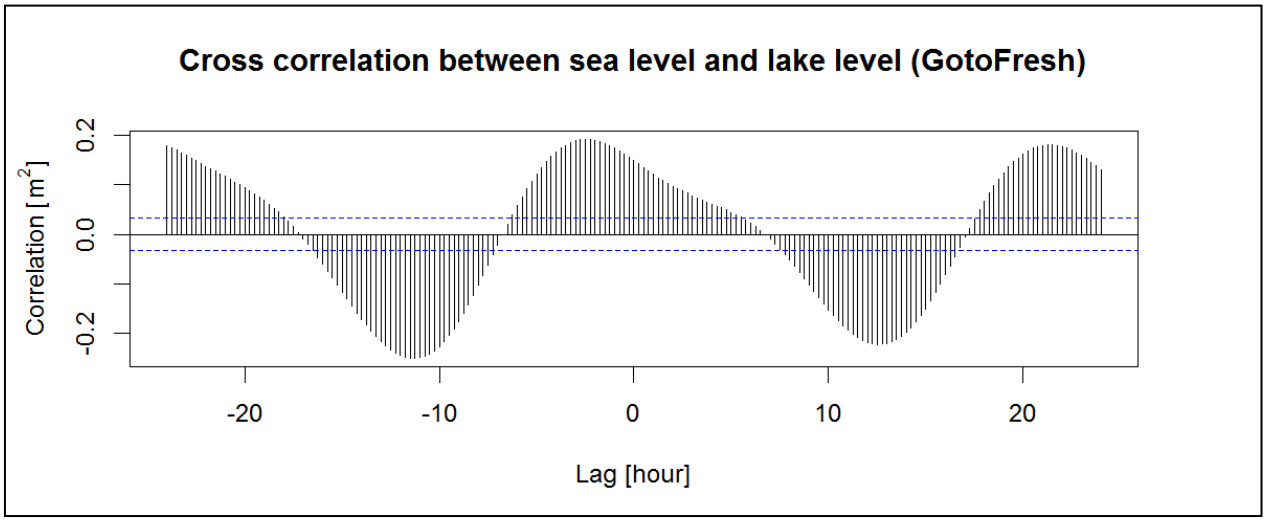

Figure III.4: Cross correlation between the derivative of the modeled sea level (Flater, 2015) and the derivative of the measured water levels in Goto (by GotoFresh). The lag (x-axis) estimates the correlation between sea[t+k] and lake[t], where k is the time lag (in hours) on the horizontal axis. Therefore, in this figure the steepest increase in lake level lags approximately one or two hours behind the steepest increase in sea level (as it is a positive correlation, with the highest value for correlation occurring at a lag of -2 hours.

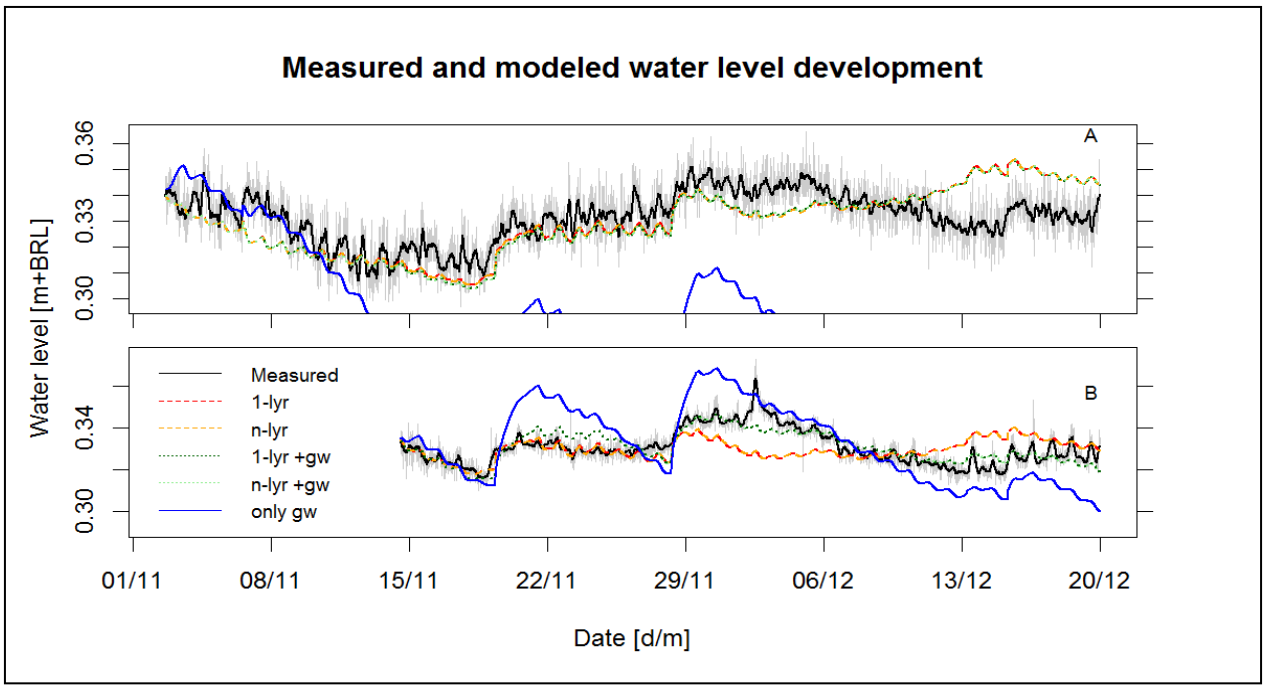

Figure III.5: Water level development as measured or modeled for GotoSalt1 (A) and GotoFresh (B). The legend given in panel B also applies for panel A. Modeled water level development was calculated using parameters as given in table 4.2. Note that for panel A, all models (except the model with only terrestrial influence) show approximately the same development, so lines are plotted over each other. For the lower panel, the models without groundwater flow show a similar behavior, as well as the models with both sea – and terrestrial influence. Measurements for GotoFresh start at the 14th of November.

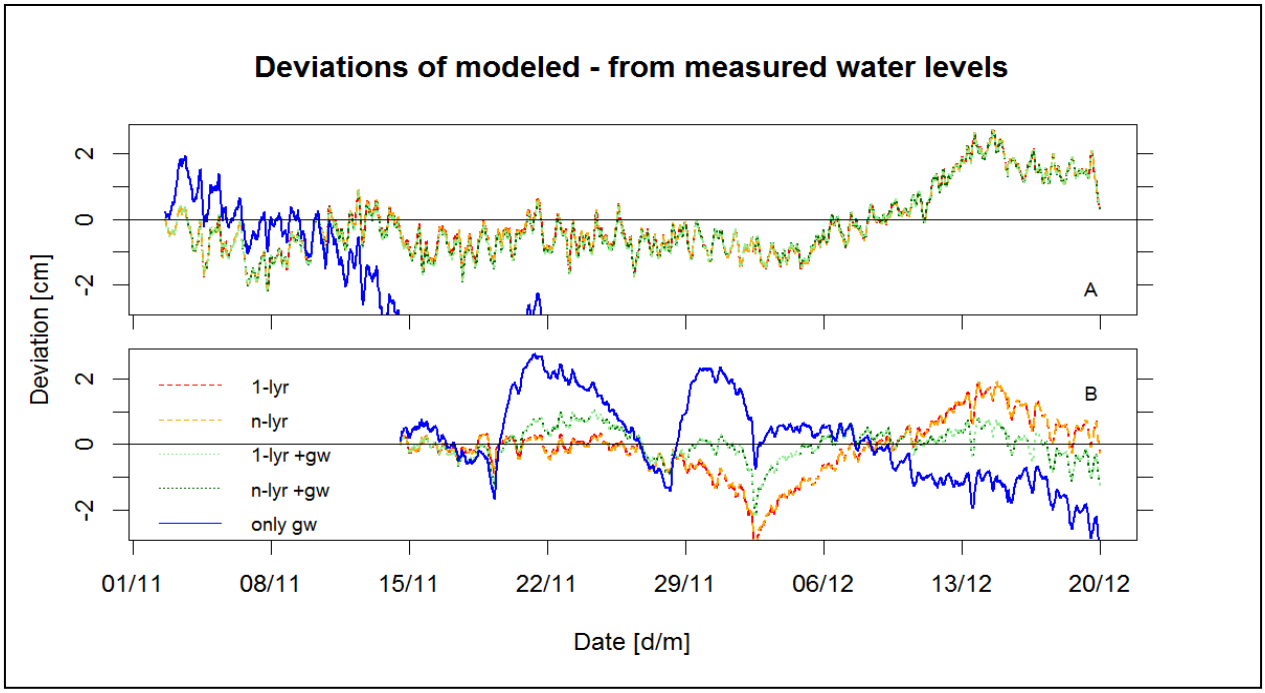

Figure III.6: Deviation (in cm) of modeled water levels from measured water levels, after applying a moving average of four hours to the measurements. Panel A shows the results for GotoSalt1, B for GotoFresh. Note that for the 1-layer and n-layer models the deviation of the modeled water levels from the measured water level shows a similar development over time; hence they are plotted over eachother. For the model without flow through the dam (for GotoSalt1), the deviation is larger than 3 cm after the 17th of November, hence it does not appear in the panel after this date.

Salinity and halotolerants

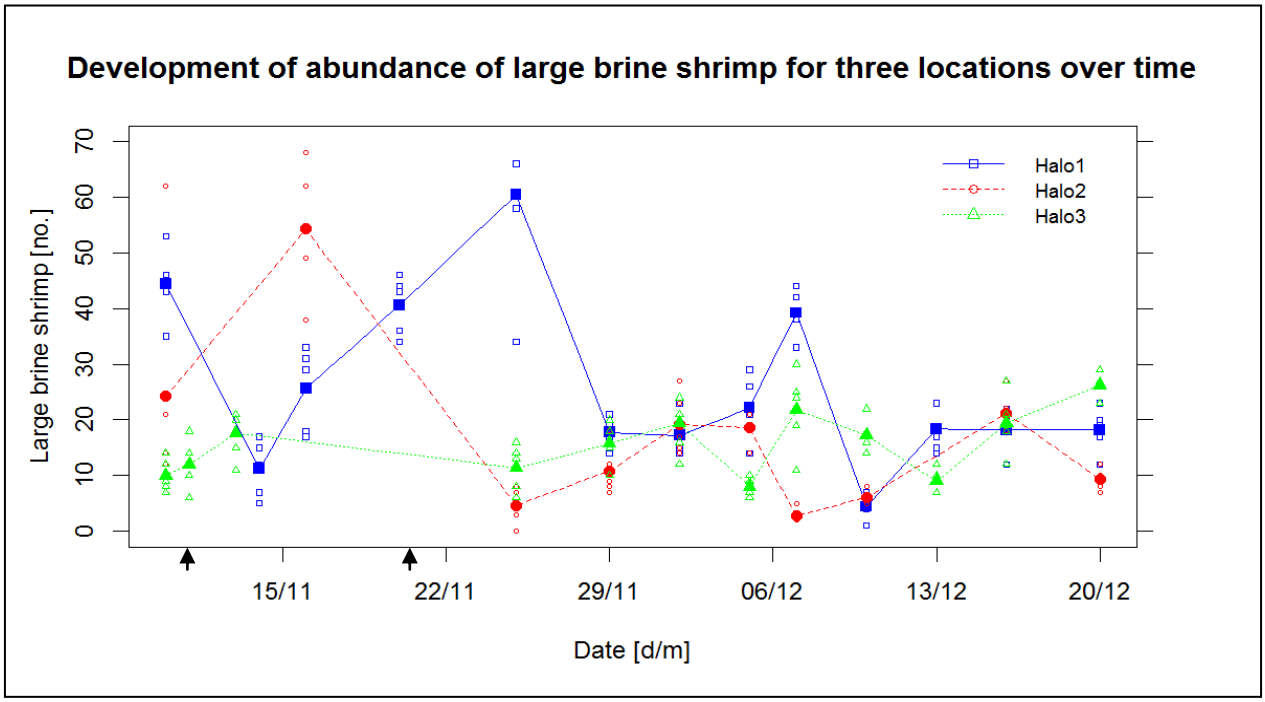

Figure III.7: Development of abundance of large brine shrimp (in 15 l samples) over time, for three locations. Filled symbols show the average of a day for which measurements were performed; empty symbols show individual measurements (5 per day). Arrows on the x-axis indicate dates when brine shrimp were sampled across the lake (11th and 20th of November).

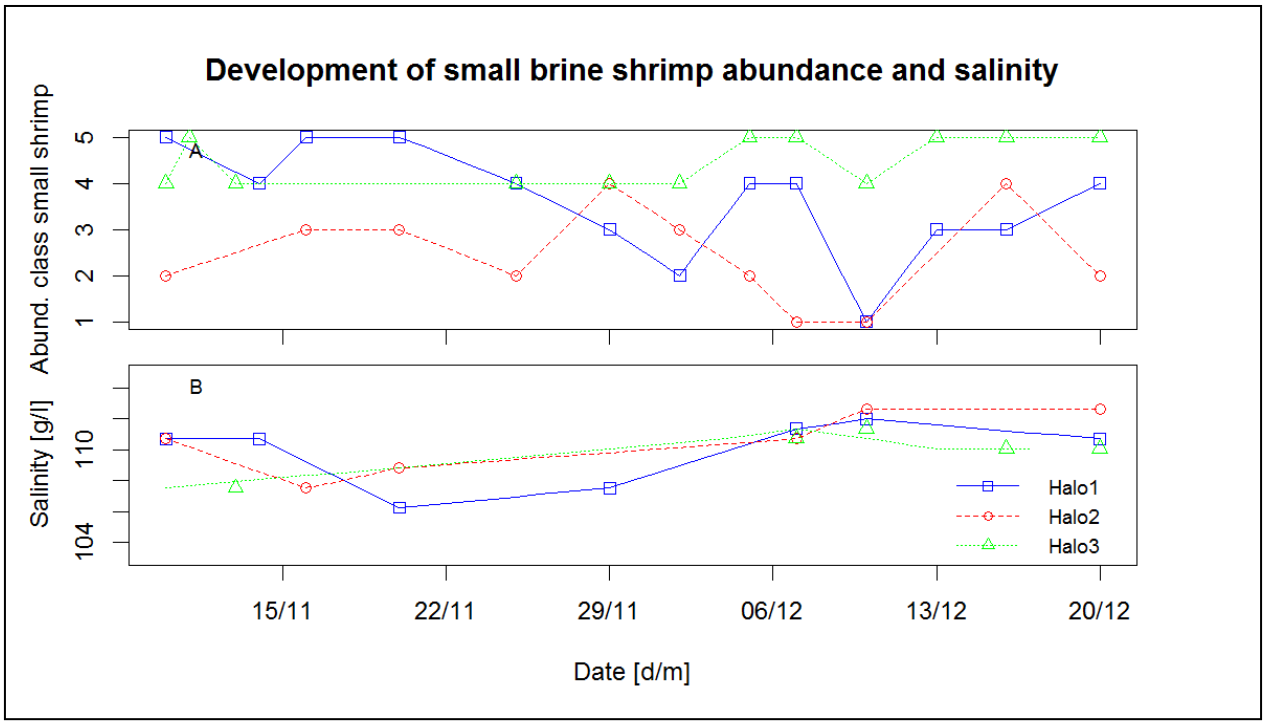

Figure III.8: Development of abundance classes for small brine shrimp (in 15 l samples) (panel A) and salinity (B) in the field survey period for three locations. Brine shrimp abundance was measured in classes: 0-5 small brine shrimp individuals (class 1), 5-20 individuals (class 2), 20-50 (3), 50-200 (4) and more than 200 (5) per sample.

Table III.3: Numbers of large brine shrimp as sampled on two days for which three locations were sampled. S. 1 to S. 5 represent the individual samples on each location, where S. 1 was the first sample taken, and S. 5 the last. Also compare with figure III.7.

Sampling date	Sample location	S. 1	S. 2	S. 3	S. 4	S. 5	Average	St.dev.
[d-m-y]	[-]	[nr]	[nr]	[nr]	[nr]	[nr]	[nr]	[nr]
10-11-2015	1	45	35	53	43	46	44	6.5
10-11-2015	2	12	62	14	21	12	24	21
10-11-2015	3	9	12	7	14	8	10	2.9
05-12-2015	1	21	14	21	26	29	22	5.7
05-12-2015	2	18	19	21	21	14	19	2.9
05-12-2015	3	8	10	9	6	7	8	1.6

Table III.4: Correlations between observed amounts of large brine shrimp (using daily averages) and small brine shrimp with daily average – and maximum temperature and wind speed (from Flamingo Airport), water temperature (using measured daily averages) and salinity (using salt concentrations measured at the corresponding locations). Significant correlations were not found.

Variable		Tmean [°C]			Tmax [°C]			Wind speed [m/s]			Tlake [°C]			Salinity [g/l]		
		Cor.	n	Sign. [a]	Cor.	n	Sign. [a]	Cor.	n	Sign. [a]	Cor.	n	Sign. [a]	Cor.	n	Sign. [a]
Large shrimp	Halo1	0.006	13	0.985	0.463	13	0.111	-0.474	13	0.102	0.058	6	0.913	-0.477	6	0.339
	Halo2	0.340	10	0.337	0.221	10	0.539	0.424	10	0.223	0.428	6	0.398	-0.907	3	0.277
	Halo3	-0.569	12	0.054	-0.540	12	0.070	-0.151	12	0.640	-0.344	6	0.504	0.290	4	0.710
Small shrimp	Halo1	0.008	13	0.979	0.456	13	0.117	-0.410	13	0.164	-0.204	6	0.699	-0.501	6	0.311
	Halo2	-0.144	11	0.672	0.117	11	0.732	-0.159	11	0.641	0.677	6	0.139	-0.907	4	0.093
	Halo3	-0.468	12	0.125	-0.577	12	0.049	0.262	12	0.410	-0.764	6	0.077	0.329	4	0.671

[a] Significance calculated as p-value. Significant results for $p < 0.05$.

Appendix IV – Satellite imagery

Figure IV.1: Satellite imagery for different dates used to estimate historical water levels for model validation. Obtained from (Google Earth, 2016).

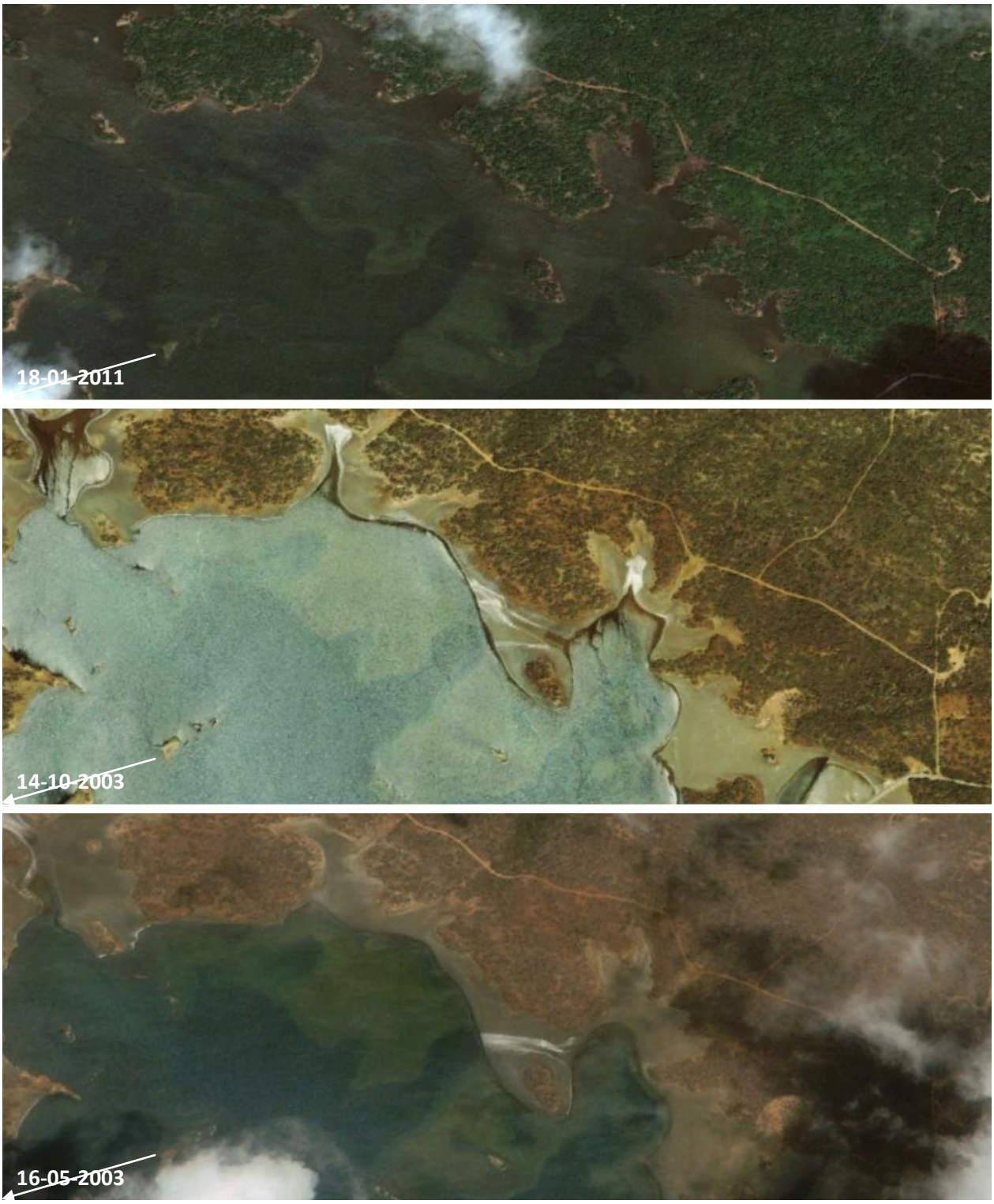

Figure IV.1: continued. The arrows indicate the location of a ridge in Lac Goto (mentioned on page 22).

Figure IV.1: continued.

Table IV.1: Water level estimates for the dates corresponding to the satellite images.

Date [d-m-y]	Estimated water level [m +BRL]
14-10-2014	0.30
23-08-2013	0.31
21-01-2012	0.40
18-01-2011	0.70
14-10-2003	0.30
16-05-2003	0.27
19-09-2002	0.26

Appendix V – Supplementary material model study

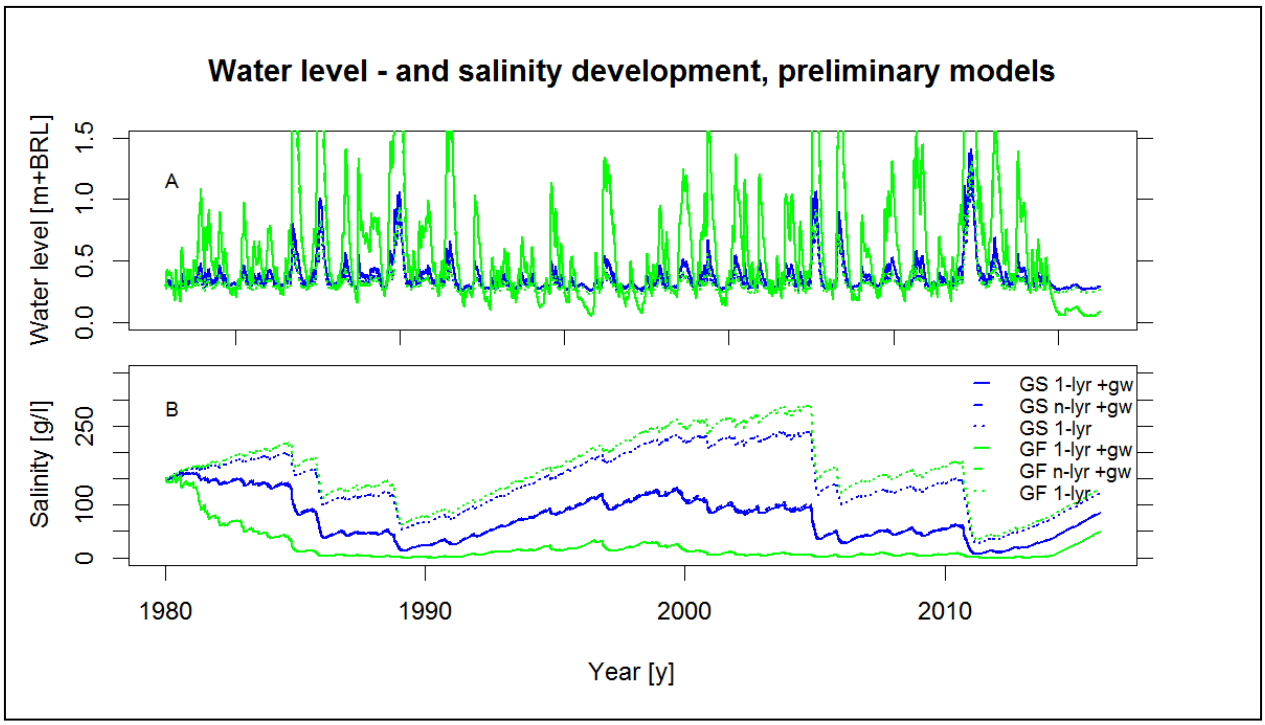

Figure V.1: Water level – and salinity development as calculated using six preliminary models for the whole modeling period. For model parameters, see table 4.2. Figure 6.1 displays a part of this modeled period in more detail.

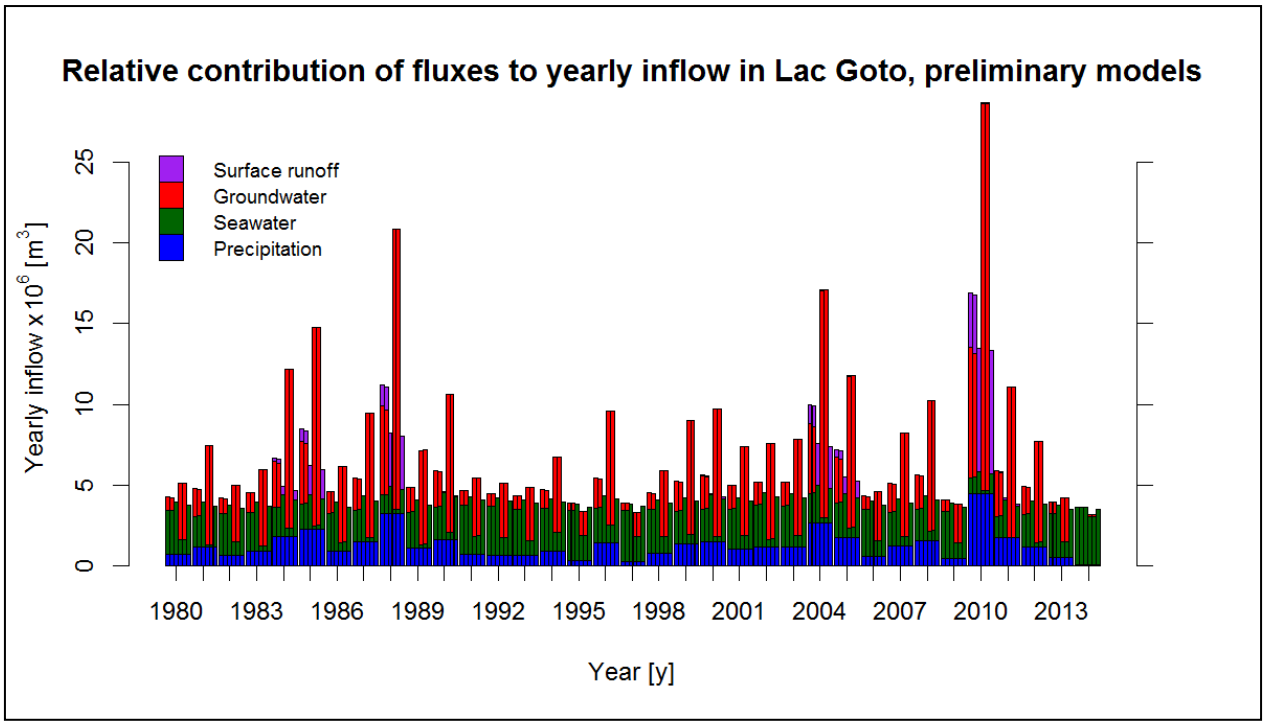

Figure V.2: Relative contribution of fluxes to yearly inflow in Lac Goto, as modeled with the preliminary models. Compare to figures 6.1 and V.1. Note that, for the last year, precipitation was not reported correctly by Flamingo Airport.

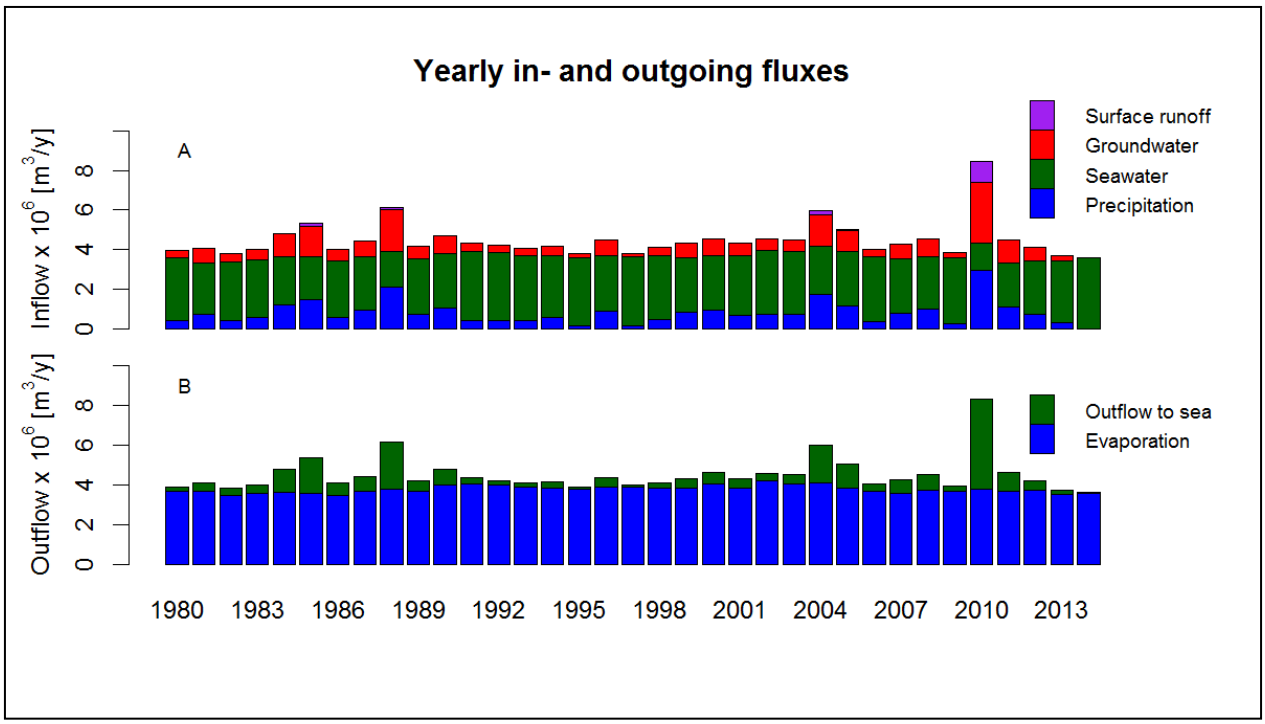

Figure V.3: Yearly total in- and outgoing fluxes (panel A and B, respectively) for the hydrological years of 1980 to 2014 and their composition, as calculated using baseline model. Note that, for the last year, precipitation was not reported correctly by Flamingo Airport.

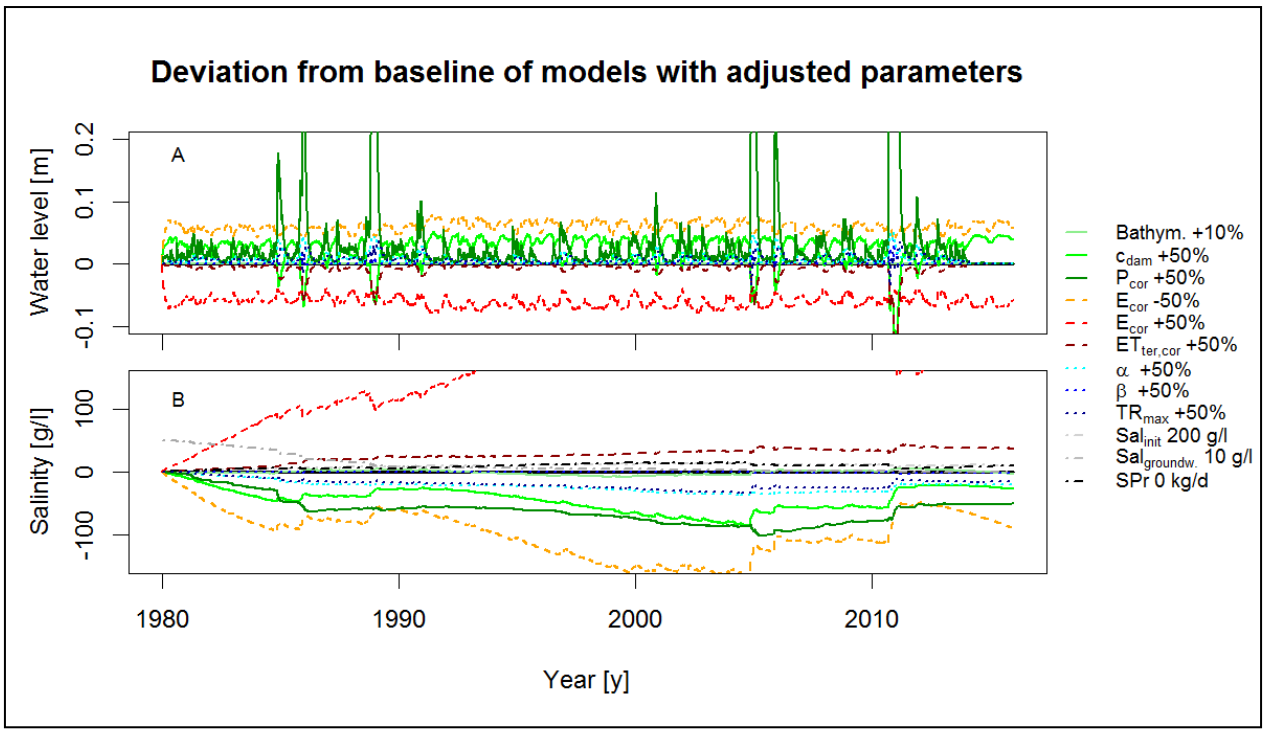

Figure V.4: Deviation from the baseline model for all models with adjusted parameters. The deviation in water levels (panel A) and salinity (B) are shown. Most model parameters influencing lake levels were increased by 50%, except for the bathymetric relations (+10%). The results of a model run with the evaporation correction factor (E_{cor}) lowered by 50% are shown as well. The lower three factors in the legend represent parameters which influence the salt balance only; they are therefore only shown in panel B.

Table V.1: Statistics of deviation in water level and percentage deviation in salinity from baseline model for model runs with adapted parameters. Bathy is short for bathymetric relations, and Sal_{init} denotes the initial salt concentration.

Parameter		Water balance				Salt balance			
		Min [cm]	Mean [cm]	Max [cm]	Sd [cm]	Min [%]	Mean [%]	Max [%]	Sd [%]
Bathy	+10%	-0.005	-0.000	0.000	0.000	-3.77	-0.216	7.31	2.40
c	+50%	-12.2	2.48	5.12	2.20	-40.3	-28.5	0	8.20
E_{cor}	+50%	-7.92	-5.98	0	0.883	0	126	240	56.0
E_{cor}	-50%	0	5.96	7.84	0.804	-76.4	-63.3	0	14.6
$ET_{ter,cor}$	+50%	-16.5	-0.762	0	1.33	0	19.2	62.8	12.7
P_{cor}	+50%	0	2.95	48.5	5.84	-84.1	-42.9	0	18.2
β	+50%	-0.452	0.029	3.93	0.241	-5.30	-0.84	0	0.96
α	+50%	0	0.789	5.14	0.856	-28.9	-16.1	0	6.54
TR_{max}	+50%	-3.50	0.744	3.73	0.657	-21.0	-13.3	0	4.87
Sal_{init}	200 g/l	.	.	.	.	0.176	6.77	33.33	8.50
C_{gw}	10 g/l	.	.	.	.	0	6.44	13.8	2.93
SPr	0 kg/d	.	.	.	.	0	5.60	7.91	1.79

Appendix VI – Summary of external data sources

This appendix shows a summary of the flamingo dataset (DCBD, 2015) and the weather dataset from Flamingo Airport (NOAA, 2015).

Table VI.1: Yearly averages of flamingo abundance observations and the number of counts for each year, from DCBD (2015).

Year [y]	Number of counts [No.]	Average flamingos [No.]	Year [y]	Number of counts [No.]	Average flamingos [No.]	Year [y]	Number of counts [No.]	Average flamingos [No.]
1981	10	308	1993	11	319	2005	12	287
1982	16	328	1994	12	354	2006	12	481
1983	8	368	1995	11	485	2007	11	513
1984	12	392	1996	1	400	2008	12	435
1985	9	376	1997	10	452	2009	9	343
1986	10	362	1998	11	432	2010	8	386
1987	9	374	1999	10	415	2011	10	43
1988	3	347	2000	12	367	2012	9	24
1989	0	.	2001	12	411	2013	10	11
1990	3	391	2002	12	353	2014	8	294
1991	6	443	2003	12	393	2015	7 [a]	859
1992	12	390	2004	11	398			

[a] Data available until August 2015.

Table VI.2: Summary of weather data for Flamingo Airport, from NOAA (2015). Column 'missing rain FA' denotes the amount of days without precipitation record. Column 'missing other' denotes the amount of days with other missing data.

Year	Rain FA [a]	Rain BOPEC [b]	Missing rain FA	Temperature	Wind speed	Evaporation [c]	Missing other
	[mm]	[mm]	[No. days]	[°C]	[m s^{-1}]	[mm d^{-1}]	[No. days]
1980	193.0	.	52	28.4	7.94	6.88	42
1981	386.3	.	83	28.5	6.74	6.45	50
1982	282.2	.	6	28.0	7.43	6.17	2
1983	281.2	.	3	28.2	7.14	6.38	2
1984	556.0	.	6	27.9	6.84	6.22	4
1985	787.4	.	1	27.8	7.44	6.11	1
1986	317.5	.	2	27.9	7.05	6.04	1
1987	388.9	.	0	29.0	6.90	6.41	0
1988	1069.3	.	15	28.3	6.66	6.11	14
1989	347.5	.	7	28.1	6.03	6.29	6
1990	597.4	.	11	28.5	6.51	6.60	10
1991	261.1	.	16	29.3	8.65	7.52	14
1992	163.6	.	37	29.6	7.98	7.32	38
1993	226.8	.	39	29.4	8.08	7.29	42
1994	258.3	.	69	28.9	7.59	6.94	69
1995	189.0	.	165	29.4	6.82	7.28	166
1996	336.8	.	65	29.2	6.83	6.91	64
1997	205.0	.	16	29.2	7.50	7.04	16
1998	201.4	.	16	29.7	7.18	7.18	17
1999	392.2 (422.2)	908.0	25	29.0	6.47	6.77	19
2000	567.4 (673.2)	.	43	28.7	6.84	6.90	35
2001	304.8 (333.8)	.	60	29.2	7.19	6.89	58
2002	436.8 (463.4)	.	9	29.5	7.53	7.47	6
2003	275.8 (368.2)	459.7	24	29.8	7.43	7.38	23
2004	761.2 (810.0)	991.0	18	29.5	6.78	7.09	19
2005	712.0 (685.2)	.	6	30.2	6.31	6.83	5
2006	247.4 (217.2)	.	8	30.2	7.26	6.69	7
2007	397.8 (404.6)	770.5	6	29.9	7.04	6.26	5
2008	388.1 (532.2)	734.5	10	29.7	6.68	6.31	9
2009	300.2	.	2	28.6	6.76	6.68	2
2010	1256.0	.	3	28.4	5.52	6.29	3
2011	720.9	.	5	28.1	5.10	6.15	5
2012	415.0	.	1	28.2	6.16	6.39	2
2013	225.8	.	29	28.4	6.92	6.48	19
2014	6.1 [d]	.	17 [d]	28.1	7.30	6.67	4
2015	0.3 [d]	.	17 [d]	28.3	7.65	6.85	2

[a] Numbers between brackets are values from MDC (2015) for the same location (Flamingo Airport). [b] Values from MDC (2015), only available for a few years. [c] Evaporation calculated using equations appendix II. [d] Precipitation values recorded for this year were mostly 0 instead of no data.